Reports of the Department of Geodetic Science
Report No. 106

COMPARISON OF ASTROMETRIC AND PHOTOGRAMMETRIC PLATE REDUCTION TECHNIQUES FOR A WILD BC-4 CAMERA

by

Daniel H. Hornbarger

Prepared for
National Aeronautics and Space Administration
Washington, D. C.

Contract No. NGR 36-008-093
OSURF Project No. 2514

The Ohio State University
Research Foundation
Columbus, Ohio 43212

March, 1968

Reports of the Department of Geodetic Science

Report No. 106

COMPARISON OF ASTROMETRIC AND PHOTOGRAMMETRIC PLATE REDUCTION TECHNIQUES FOR A WILD BC-4 CAMERA

by

Daniel H. Hornbarger

Prepared for

National Aeronautics and Space Administration
Washington, D. C.

Contract No. NGR 36-008-093
OSURF Project No. 2514

The Ohio State University
Research Foundation
Columbus, Ohio 43212

March, 1968

PREFACE

This project is under the direction of Professor Ivan I. Mueller of the Department of Geodetic Science, The Ohio State University. Project manager is Jerome D. Rosenberg, Geodetic Satellites, Code SAG, NASA Headquarters, Washington, D.C. The contract is administered by the office of University Affairs, NASA Headquarters, Washington, D.C.

Reports related to NASA Contract No. NGR 36-008-093 and published to date are the following:

The Determination and Distribution of Precise Time, Report No. 70 of the Department of Geodetic Science, The Ohio State University.

Proposed Optical Network for the National Geodetic Satellite Program, Report No. 71 of the Department of Geodetic Science, The Ohio State University.

Preprocessing Optical Satellite Observations, Report No. 82 of the Department of Geodetic Science, The Ohio State University.

Least Squares Adjustment of Satellite Observations for Simultaneous Directions or Ranges, Part 1 of 3: Formulation of Equations, Report No. 86 of the Department of Geodetic Science, The Ohio State University.

Least Squares Adjustment of Satellite Observations for Simultaneous Directions or Ranges, Part 2 of 3: Computer Programs, Report No. 87 of the Department of Geodetic Science, The Ohio State University.

Least Squares Adjustment of Satellite Observations for Simultaneous Directions or Ranges, Part 3 of 3: Subroutines, Report No. 88 of the Department of Geodetic Science, The Ohio State University.

Preprocessing Electronic Satellite Observations, Report No. 100 of the Department of Geodetic Science, The Ohio State University.

Comparison of Astrometric and Photogrammetric Plate Reduction Techniques for Short Focal Length Cameras, Report No. 106 of the Department of Geodetic Science, The Ohio State University.

ABSTRACT

Several astrometric models are tested on entire and limited plate areas to analyze their ability to remove systematic errors from interpolated satellite directions using a rigorous photogrammetric reduction as a standard. Residual plots illustrate the absence or remainder of systematic effects in measured plate coordinates after the astrometric reduction is performed using the method of least squares. Conclusions are made as to what conditions will permit the reduction by astrometric means to achieve comparable accuracies to those of a photogrammetric reduction on the short focal length camera.

TABLE OF CONTENTS

LIST OF TABLES

LIST OF ILLUSTRATIONS

1. INTRODUCTION AND BACKGROUND

In recent decades man has achieved the capability of launching objects, manned or unmanned, into the heavens for many scientific and military purposes. Regardless of the reason for launch, a knowledge of the position in space of the missile, balloon, satellite or other body is vital information whose accuracy is a function of the technique used in the determination. The observation of heavenly bodies has long been practiced in the field of geodesy. However, the advent of satellites has provided the geodesist with a well-defined object at a finite distance useful in establishing a spatial relationship between the satellite and several ground stations or in determining parameters of the earth's gravity field due to a departure of the satellite from its orbit in a central force field. Thus, the methods in classical geodesy of performing computations on some reference surface may be altered or replaced by a vectorial solution dependent on the spatial

positions of reference points and the satellite in a tri-axial Cartesian coordinate system. Obviously, the determination of the satellite's position must be done with a specified degree of accuracy in order for the results, dependent on that determination, to be useful for geodetic purposes.

This report is concerned with the method of determining a satellite's position. More specifically, it deals with the optical determination in which the satellite is photographed against a background of stars. (There are, of course, electronic means of determining position.) The report will examine the practical application of the two basic methods of "plate reduction" and will chronicle the results of the author's experimentation with these methods.

ESSA supplied data from three photographic plates in the form of measured star and satellite coordinates. The three plates were exposed simultaneously at the following stations:

Plate No. 2559 Lynn Lake, Manitoba

Plate No. 6132 Frobisher Bay, NWT

Plate No. 5205 Cambridge, NWT

The event occurred on 30 November, 1965, the satellite being Echo II. Twenty-one satellite images were selected on each plate as test points for which directions in space were determined.

Using these same three photographic plates and their accompanying data, the author investigated the application of several astrometric techniques to the reduction of the plates with a critical view to their

ability to remove systematic errors and to their comparison with the photogrammetric approach. The results of this experimentation and its implementation will be discussed in detail and conclusions drawn.

This report will not dwell on the fundamentals of spherical astronomy or attempt to give a detailed background on plate reduction techniques and related problems. Its primary concern is the results of the experimentation.

2. THE AVAILABLE DATA

In September, 1967, the Geodetic Laboratory of ESSA forwarded the vital information concerning stellar plates 2559, 5205, and 6132 to the Department of Geodetic Science. This information was contained mostly on punched cards. For each plate the following data was available:

(1) Punched cards containing the SAO catalogue positions of the stars whose images were measured on each plate. These positions were given in radians, and the star identification number was a combination of letters and numbers having a relation to the manner in which the positions were contained on magnetic tapes. There is a code available from ESSA which will relate the ESSA SAO star number to the number found in the four-volume SAO catalogue.

(2) Punched cards containing the updated apparent positions of the stars used in the reduction, in radians. As the "apparent" position connotes, the catalogue star positions had been updated for precession, nutation, proper motion, and annual aberration. The epoch used in this updating procedure was approximately a star's mean exposure time (each star appears as more than one image), sufficiently accurate for updating to an apparent place. The method of star updating is available and will not be given here [Hotter, 1967] .

(3) Punched cards containing the measured plate coordinates of each star image referred to an origin determined by four drill holes. These coordinates were free of cancelling-type errors associated with

the comparator measuring process. The plate measurements had been made on a Mann comparator, the procedure of removing operator bias and cancelling type errors being a rigorous one [Hotter, 1967, pp. 112, 113]. The coordinates furnished were the output of the ESSA "patching and matching" program which is the final step in the rigorous procedure mentioned above. Systematic errors still remaining in the coordinates on the punched cards, then, were of the non-cancelling variety (non-perpendicularity of the comparator axis, weave of the guide of the comparator axis, periodic screw error, and the secular screw error). In the reduction procedure of ESSA, the non-perpendicularity of the comparator axis, in the form of an angle, is carried as an unknown. The method of its application will be shown later. The number of images measured for a single star and the ESSA method of exposing a plate remains to be explained also. All coordinate measurements had equal weights of one.

(4) Punched cards containing plate coordinates for each satellite image. These coordinates were of the same status as the star coordinates mentioned above; i.e., the output of the "patching and matching" program. It is important to note that while other satellite coordinates were included in the forwarded data (containing various corrections that are made by ESSA after their plate reduction procedure), the satellite coordinates of interest here are to be regarded as measurements of images of "unknown stars" without corrections for phase angle, parallactic refraction, diurnal aberration and other corrections that are applied later in the reduction process to satellite images. Of the 200 or more satellite images across the plate, 21 were selected by ESSA to be used as the test

points in the agency comparison and were also used by the author in his investigations. Henceforth, any discussion of satellite images will refer to these 21 points, and the images will be regarded as those of unknown stars. Moreover, the satellite images on each plate, although numbered in the same fashion, were considered independent of each other and not on a curve resulting from a curve-fit procedure. The brush tape times of exposure for corresponding numbered images are, in fact, identical for each plate, but this was a result of the synchronization of the clocks in the ESSA tracking system and not the result of selecting 21 times and then computing corresponding coordinates from the curve of the fitting procedure of ESSA.

(5) Listings of station latitudes and longitudes, atmospheric data, and brush tape times. A correction for each plate was given to correct the brush tape times to U.T.1. Computed local apparent sidereal times of exposure were also included.

Along with this data, the Geodetic Laboratory of ESSA included the output of its "single camera orientation" program. This program performs a least squares adjustment using the photogrammetric model of Dr. Hellmut Schmid to determine the elements of interior and exterior orientation of the taking camera and other parameters considered unknown. Included also in this output were the ESSA computed directions for the 21 satellite points. As mentioned earlier, the test satellite images for each plate were regarded as those of unknown stars. The directions given were for the apparent place of these unknown stars. No corrections were made for phase angle, parallactic refraction or diurnal aberration.

A brief description of the ESSA process of exposing a stellar plate is necessary to see how the data described above was generated. A more detailed description is available in [Hotter, 1967] or [Taylor, 1963] . First of all, the taking cameras were Wild BC-4's with the Astrotar lens. The focal length of these cameras is about 300 millimeters and the field of view 33 degrees by 33 degrees. The cameras were operated in the fixed mode, equipped with shutters that were programmed to operate in the following manner: Prior to satellite pass (pre-calibration) an exterior iris-type shutter produced four star-trails for each star in the field of view with five distinct images in each trail. During satellite passage, internal rotating disks chopped the satellite trail with the external shutter reducing the exposure rate and identifying the satellite trail. After satellite passage four more star trails were produced with five images each (post-calibration). The brush tape times of exposure were recorded. These times corresponded to the beginning of each image on the plate.

In the plate reduction process, the plate was subdivided into grid squares, and a pre-calibration star trail and a post-calibration star trail were selected in each square. The beginning of each of the five images in a trail were measured. For this problem approximately 110 star trails were selected per plate with five images measured per trail (in several cases, less than five images per trail were able to be measured). This was normal procedure for ESSA. Obviously, the same star did appear in some cases in more than one trail. However, roughly 100 different stars were used per plate in the ESSA reduction.

The star images were numbered thusly: The first two digits referred to the area of the plate in which the trail appeared. The third digit referred to the trail of exposure (1-8). The last two digits indicated the number of the image in the trail. Therefore, image number 16103 would indicate the third image of star number 161 which appeared in the first trail exposed. Further, let us assume the numbers 161 and 596 referred to the same star in the sky. Since the star was exposed at different times, 161 and 596 would be treated as different stars, one appearing in the first trail, the other in the sixth. Obviously, the catalogue positions of these "two" stars would be identical, but the updated observed positions would differ.

In the author's experimentation and in the directions issued to the agencies in how to treat the data, it must be remembered that brush tape times (U.T.C.) plus the correction to U.T.1., associated with the satellite images, were regarded as imaginary times when light was emitted. (While this was not so in reality, it negated making corrections for light travel time, a process not vital to the purpose of the agency comparisons.)

As was mentioned earlier, reproductions of the available data discussed above were forwarded to the other three agencies in October, 1967, to enable them to compute directions for the 21 satellite images on each plate. Specifically, approximate parameters for the elements of interior and exterior orientation were given along with diagrams and equations that related the image space to the object space. These were taken from [Schmid, 1959, pp. 12-15]. Other data forwarded included the brush tape times of observation for each star and satellite image with the uniform

plate correction to obtain U.T.1., plots by quadrant of the plates showing star and satellite positions, and listings of all material contained on the punched cards that were sent. Approximate right ascensions (nearest 10 seconds of time) and approximate declinations (nearest 10 seconds of arc) were also given for the satellite images. Decks of punched cards that were sent contained observation times and station coordinates as well as atmospheric data, SAO catalogue positions of the stars, and star and satellite image coordinates. The agencies were instructed that times for the satellite were treated as light emission times (as already stressed). Positions of the satellite images were requested using the exact same procedure normally employed when reducing data for the Geodetic Satellite Data Center. It was requested that the reduced data be returned in the same format used by the GSDC. Finally, any changes in reduction procedure having occurred since the compilation of agency procedures in [Hotter, 1967] were requested.

3. A BRIEF HISTORICAL SKETCH

The reduction of stellar photographic plates is not a development of the space age. In fact, one of the principal methods of reduction still in practice today was first formulated in the late 1800's. For the purposes of this paper, "plate reduction" will mean the method of determining a direction in space to a satellite or star by relating its position in the image space to the positions of known stars also in the image space to which the directions are known in the object space. It implies formulating a mathematical model or relationship, be it physically interpretable or not, that will describe a dependence among object coordinates and image coordinates. Two different techniques for plate reduction have been developed which we normally refer to as the astrometric (plate constant) method and the photogrammetric method. The photogrammetric method has a physical interpretation while the astrometric method does not.

The astrometric method has been used by astronomers for decades to determine stellar positions of unknown stars and their proper motions. However, the photographic cameras that have been used differ from the ballistic satellite tracking cameras in use today, most notably by their longer focal length; and for this reason the astrometric approach is a questionable process when applied to plates from the short focal length (less than 1000 millimeters) ballistic camera. Existing in the batch

of data sent by ESSA, then, was an excellent opportunity to evaluate some astrometric techniques and to compare them with a photogrammetric reduction for a ballistic camera. But this is a matter for later discussion. Since the cameras that have been used in astrometric reductions are of a long focal length variety, they cover a relatively small portion of the sky. Obviously, the bundles of rays in this situation are close to the optical axis even at the extremes of the plate, thus minimizing the affects of certain lens distortions. For example, the focal length of the Sheepshanks Equatorial telescope of Cambridge Observatory in England was 5.89 meters, and the region of the sky photographed was $1\frac{1}{2}$ degrees by $1\frac{1}{2}$ degrees [Smart, 1962, p. 279]. Compare this to the BC-4 cameras in this investigation which had a focal length of 300 millimeters and covered a region 33 degrees by 33 degrees. (Generally, the cameras used in astrometric work have focal lengths of about 3 meters and cover an area 2 degrees by 2 degrees and the ballistic cameras have focal lengths of 1000 to 300 millimeters and fields 30 degrees by 30 degrees [Brown, 1963].)

During World War II the computation of bombing tables necessitated the accurate knowledge of the position of the bombing aircraft at the instant the bomb was released. The cameras used, later to become known as "Ballistic" cameras, were fixed (as opposed to equatorially mounted, sidereally driven) with focal lengths of about 300 millimeters, fields of 20 degrees by 30 degrees, and directional accuracies of 10 to 20 seconds of arc [Brown, 1963]. Turner's astrometric method comprised the method of plate reduction. (The next section will discuss various

astrometric methods as well as the photogrammetric method of plate reduction.)

Deficiencies in the astrometric method of plate reduction became apparent when Hellmut Schmid performed some investigations of the techniques [Brown, 1963]. He pursued a method of plate reduction based on the photogrammetric theory of Von Gruber, thereby discarding the astrometric approach. Accuracies improved immensely with the application of Schmid's findings, due in part to improved equipment, but mainly due to the more rigorous photogrammetric method of plate reduction [Brown, 1963].

Thus, the photogrammetric method of plate reduction has been improved upon taking into account lens distortions, refraction, and other physical effects which bear upon the problem. Unprecedented accuracies are now claimed using the photogrammetric approach, and the astrometric method has all but been discarded in satellite tracking with ballistic-type cameras. One agency, the Smithsonian Astrophysical Observatory, utilizes the Turner method in its data reduction today in connection with its Baker-Nunn films.

4. EXPERIMENTATION

4.1 General

We are interested in how well several astrometric reduction models remove systematic errors in the three BC-4 plates in question and how the results compare with the photogrammetric reduction used by ESSA. In the author's approach the reductions are performed using the method of least-squares, and then the residuals (adjusted coordinates less the measured coordinates) are plotted with a view to their magnitude and direction. Any systematic effects still remaining may be then observed. Also, the residual plots may be compared to the plots of the residuals as computed for the ESSA photogrammetric reduction. In all but several of the reductions, directions are computed for the 21 satellite test points to compare with the ESSA photogrammetric results. It must be remembered that while the directions computed astrometrically for these satellite points will in many cases compare to the ESSA results within a second of arc, this in itself is not a good test of the method. For if the plotted residuals show systematic effects still remaining, we must base the decision as to the usefulness of the method on this fact. The author realizes that more sophisticated methods of statistical analysis are available for evaluating a mathematical model and comparing it to another, but feels that the analysis in this report is satisfactory to accomplish the objective.

All programming, unless otherwise indicated, is the result of the author's efforts, and is in the SCATRAN language still used at The Ohio

State University. The output of every computer run is obviously not included, but the important and meaningful results are compiled. Double precision arithmetic is used in most cases except where noted.

4.2 Organization of the Data and Star Updating

As was discussed in Section 2, there is no deficiency of star images to use in the reductions on each of the plates since there are over 100 star trails per plate with, in most cases, five images in each trail. Assuming about 100 well distributed star images are sufficient for the reductions, the third image in each trail is selected and the other four images in a trail are discarded. The breakdown of stars used is as follows: Plate 2559, 111 stars; Plate 5205, 114 stars; Plate 6132, 106 stars. The distribution of the stars and the 21 satellite images on the plates is shown in Charts 1, 2, and 3. The area represented is 17 centimeters by 17 centimeters. All images are plotted by number, the lower left-hand corner of the number indicating the actual measured position of the star or satellite image. Numbers 126 through 494 running diagonally across the center of all plates are the satellite images. The origin of the plate coordinate system is at the center (determined by fiducials) with positive x to the right and politive y to the top. A reference to star 163, for example, now refers to its third image in the trail, each star being represented by only one image. It must be remembered that, for example, on plate 2559, 111 separate SAO catalogue stars are not used, but rather 111 separate trails on the plate. "Stars" 146 and 573 are actually the same star in the sky, but for purposes of the reduction they are separate stars, appearing in different plate locations because of the fixed mode of the camera

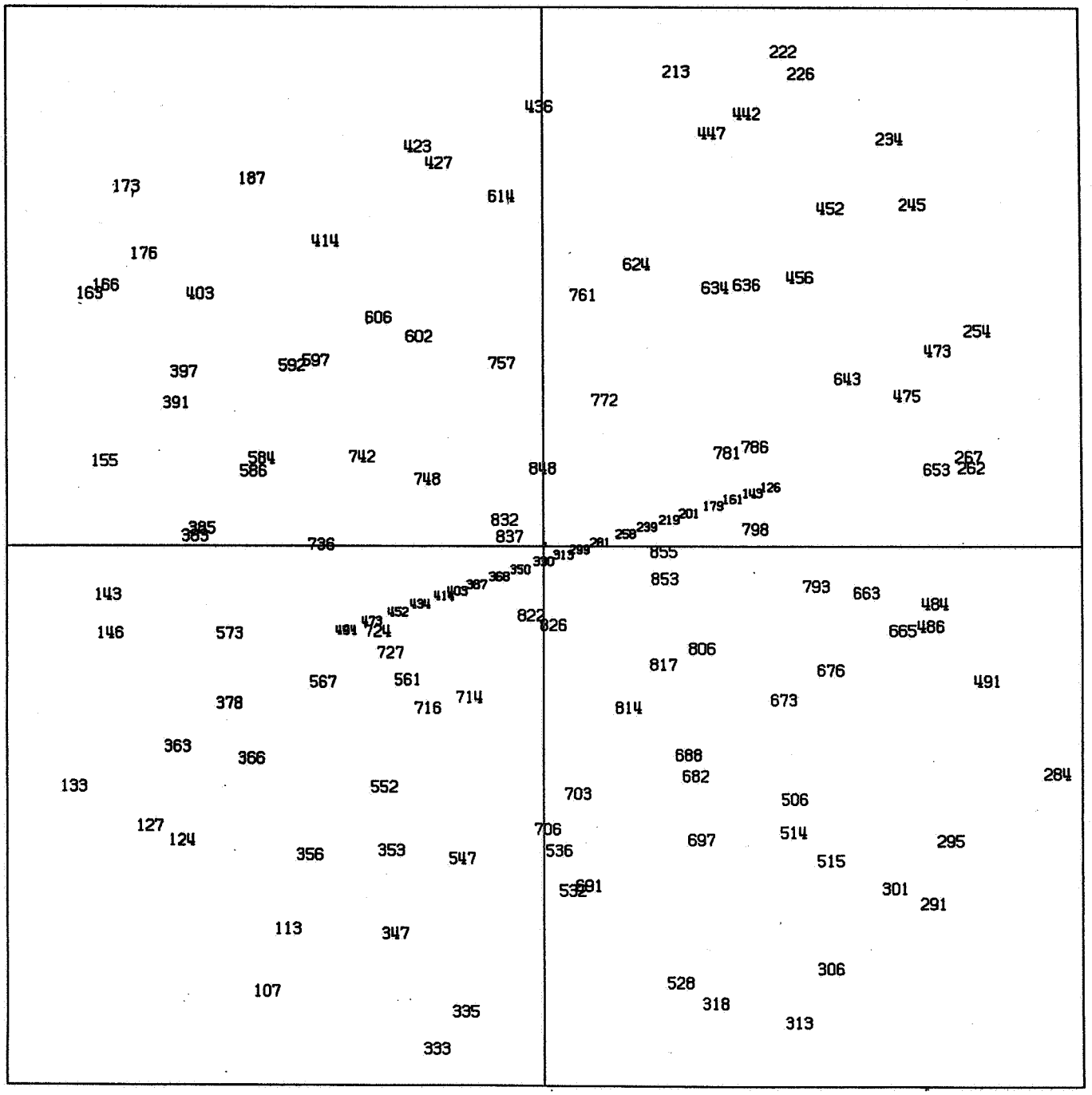

CHART 1: PLATE 2559
OBSERVED STAR AND SATELLITE LOCATIONS
Satellite Images are numbered 126-494

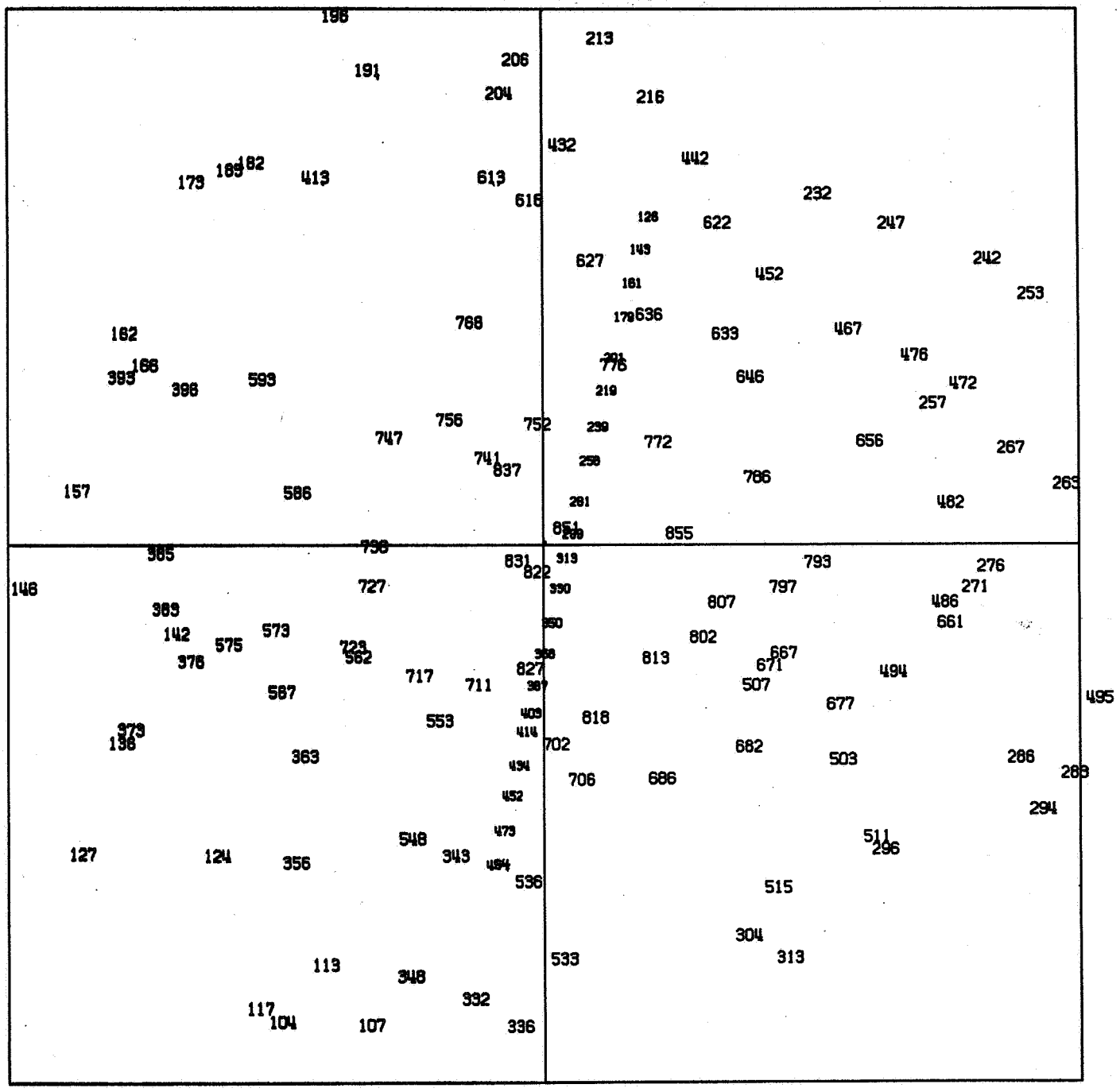

CHART 2: PLATE 5205
OBSERVED STAR AND SATELLITE LOCATIONS
Satellite Images are numbered 126-194

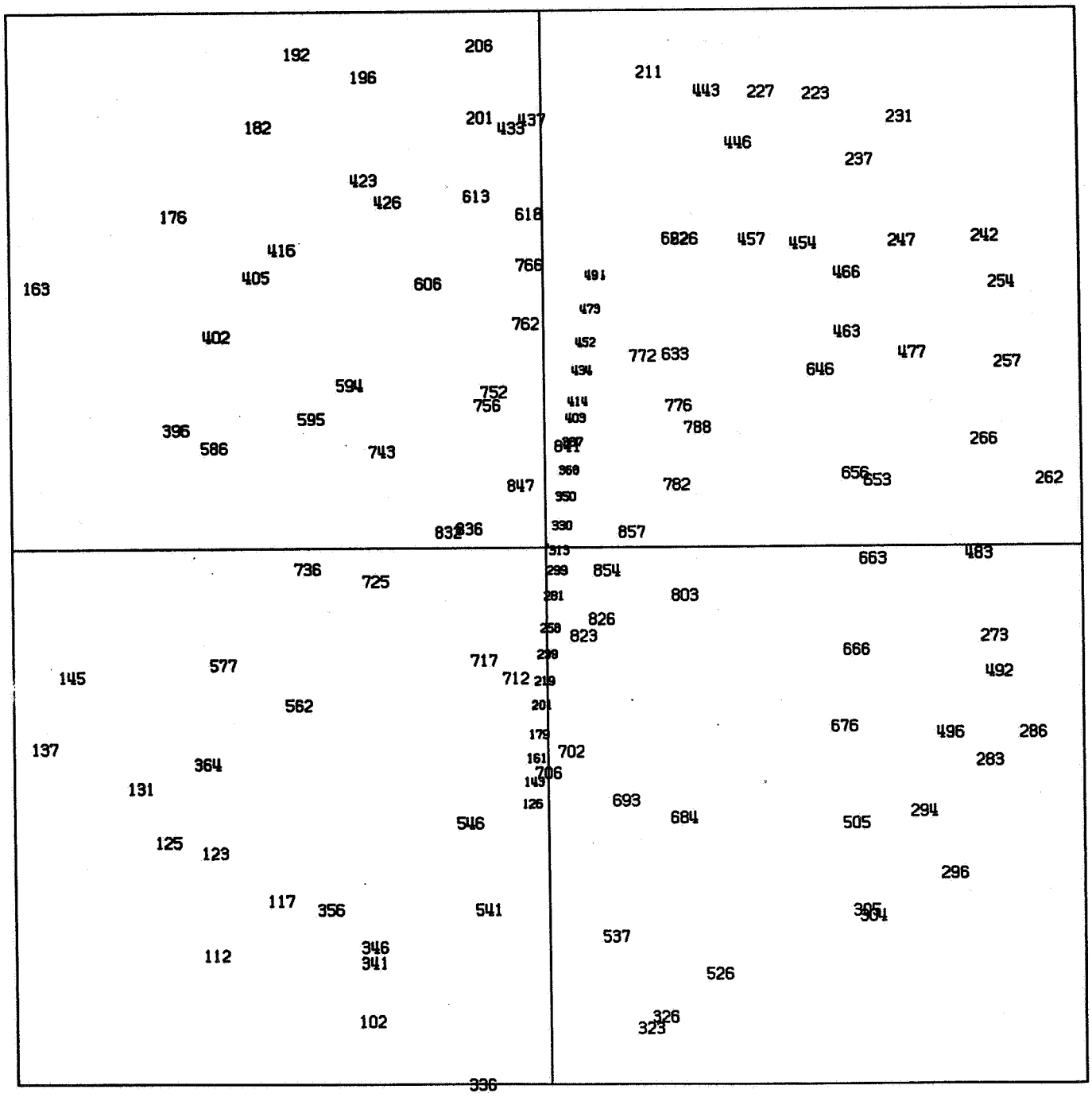

CHART 3: PLATE 6132
OBSERVED STAR AND SATELLITE LOCATIONS
Satellite Images are numbered 126-494

and a different exposure time for each. Repeating once more, all stars are in the SAO system (mean equator and equinox of 1950.0) and can be found in the SAO catalogue. As can be seen, there is a good distribution of stars on all plates, covering all areas but the farthest corners.

As the agencies did, all observed coordinates are weighted equally with weights of unity. Any other system of weighting would be difficult to handle, at best, and statistically doubtful. Obviously, the stars are of varying magnitudes, and this would undoubtedly affect their ability to be measured. But resolution and other qualities of the taking camera, very difficult to model mathematically, would have to be considered, and, thus, one can see the reason for equal weights. The standard error for a single measurement (internal consistency of comparator) is unknown to the author but probably amounts to several microns.

It might be interesting to note that the approximate altitudes and azimuths of the plate centers are: 2559, 33°15' altitude, 21°43' azimuth; 5205, 57°30' altitude, 85°36' azimuth; 6132, 41°53' altitude, 309°34' azimuth. The effects of refraction are obviously smallest for plate 5205.

The star positions in the available data are the apparent places as has been mentioned. In the computational process of the ESSA "single camera orientation" program, the stars are updated to their "observed" altitudes and azimuths (effects of refraction and diurnal aberration are added) before the photogrammetric reduction is done [Hotter, 1967, p. 111]. This is done to remove all remaining systematic effects on the object space. This task needs to be performed, therefore, at least to compute the ESSA photogrammetric residuals. However, it is an unnecessary process when

applied to the astrometric reduction. Astrometric models were designed to remove residual effects of annual aberration and refraction. In fact, the SAO uses the 1950.0 mean positions in their astrometric reduction, updating only for proper motion [Hotter, 1967, p. 101] . However, the decision is to update the stars to their "observed" positions, and to use these positions as input in the astrometric reductions. Any systematic effects of refraction remaining (diurnal aberration is an extremely small effect to begin with) should be well accommodated in the astrometric model.

The updating procedure from apparent to "observed" place is a straight-forward one. However, first a check is made on the apparent places furnished by ESSA. The star updating program of Allen, available at The Ohio State University and in modified form for SAO catalogue input (modified by J. Veach of the Department of Geodetic Science), is used to verify 23 star positions [Allen, 1966] . The largest difference in declination is 0.02 seconds of arc and in right ascension, 0.003 seconds of time. Recall the apparent position is the 1950.0 catalogue position updated to the epoch of observation for the effects of proper motion, nutation, precession, annual aberration, and annual parallax. Annual parallax has been ignored in this case because its effects are negligible for most stars.

The author's program to update to the "observed" place follows the subsequently described procedure.

The correction for diurnal aberration can be applied immediately to the apparent right ascension and declination. The correction is

given by [Explanatory Supplement, p. 49]:

$$\begin{aligned} \alpha_{new} - \alpha_{apparent} &= 0^{s}.0213 \cos\varphi \cos h \sec\delta, \\ \delta_{new} - \delta_{apparent} &= 0''.320 \cos\varphi \sin h \sin\delta, \end{aligned} \tag{4.1}$$

where h is the apparent topocentric hour angle of the star, φ is the geodetic latitude of the station, and δ is the apparent declination of the star. Implicit in equation (4.1) is the fact that the geocentric latitude of the station is approximately equal to the geodetic latitude and that the radius of the earth at the station is approximately equal to the equatorial radius. The local apparent sidereal times of observation were furnished by ESSA. These have also been checked.

The addition of astronomical refraction must be accomplished after the apparent right ascension and declination plus the effect of diurnal aberration are converted to the altitude-azimuth system (horizon). This may be accomplished using a series of matrix rotations where the end result is [Mueller, in press],

$$\begin{aligned} \cos a \cos A &= -\sin\varphi \cos\delta \cos h + \cos\varphi \sin\delta, \\ \cos a \sin A &= -\cos\delta \sin h, \\ \sin a &= \cos\varphi \cos\delta \cos h + \sin\varphi \sin\delta, \end{aligned} \tag{4.2}$$

where φ, δ, and h are the same as in the diurnal aberration correction; a is the altitude and A is the azimuth from north. Obviously the unrefracted zenith distance is $(90^{o} - a)$.

To compute the amount of refraction the United States Coast and Geodetic Survey (USC & GS) version of the Garfinkel refraction model is used and the same model employed by ESSA [Hotter, 1967, pp. 121-122].

In their reduction procedure for this event the coefficients in the refraction model were constrained. The subroutine used by the author for adding refraction was written by Marshall Stark at The Ohio State University and follows the Garfinkel model mentioned [Stark, p 80]. The formula used is [Hotter, 1967, p. 121],

$$Z_o - Z_R = T^{\frac{1}{2}} W(\eta_1 \tan\frac{B}{2} + \eta_2 \tan^3\frac{B}{2} + \eta_3 \tan^5\frac{B}{2} + \eta_4 \tan^7\frac{B}{2}), \tag{4.3}$$

where

$$W = \frac{P}{T^2},$$

$$P = \frac{P_s}{P_o},$$

$$T = \frac{T_s}{T_o},$$

$$\tan B = \frac{T^{\frac{1}{2}}}{8.7137} \tan Z_R,$$

$$\eta_1 = 1050.61030,$$

$$\eta_2 = 706.11502,$$

$$\eta_3 = 262.06086,$$

$$\eta_4 = 142.67293.$$

In the above Z_o is the unrefracted zenith distance; Z_R denotes the refracted zenith distance; T_s denotes the station temperature in degrees Kelvin; P_s is the station pressure in millimeters of mercury; and P_o and T_o are standard pressure and temperature.

Since the refracted zenith distance appears on the right side of the equation, an iterative process is used to compute the amount of refraction. Z_R is initially set equal to Z_o, and the newly computed refracted zenith distance is then inserted on the right side of the

equation until the difference in succeeding amounts of refraction is less than 0.01 seconds of arc. As we shall see later, the refracted altitude and azimuth are used to compute the photogrammetric residuals.

However, right ascension and declination are required as input to the astrometric reductions. These are obtained by using [Mueller, in press],

$$\begin{aligned} \cos\delta \cos h &= -\sin\varphi \cos a \cos A + \cos\varphi \sin a, \\ \cos\delta \sin h &= -\cos a \sin A, \\ \sin\delta &= \cos\varphi \cos a \cos A + \sin a \sin\varphi, \end{aligned} \tag{4.4}$$

and α equals LAST - h where LAST is the local apparent sidereal time.

The problem here concerns a local apparent sidereal time to use to compute an "observed" right ascension. As subsequent sections will explain, the astrometric model expresses the relationship of the measured plate coordinates of the star images to a rigorously defined rectangular ("standard") coordinate system in a plane tangent to the celestial sphere, the origin of which (also the point of tangency) is the intersection of the optical axis with the celestial sphere and is uniquely defined in right ascension and declination. The standard coordinates of a star are a function of its declination and of its right ascension minus the right ascension of the point of tangency. The key here is the fact that the right ascension of any star must refer to the same epoch in which the right ascension of the point of tangency is chosen since the camera is earth-fixed and the point of tangency constantly changes due to diurnal motion of the celestial sphere. In other words, the star images must be treated as simultaneous even though we know they are not because of

pre- and post-calibration. This is accomplished by choosing a common "fictitious" local apparent sidereal time of observation to use in computing right ascension after h is computed by equation (4.4). Henceforth, the "observed" right ascensions and declinations used in the astrometric reductions will be regarded as "fictitious" as will any interpolated satellite positions only because of this timing problem. If necessary, the actual "observed" right ascensions can be obtained by adding the true LAST of observation to the "fictitious" right ascension and subtracting 24 hours. The "fictitious observed" right ascensions and declinations, stored on punched cards along with the measured plate coordinates, are then in a usable form for the astrometric reductions.

4.3 The Photogrammetric Reduction and Residuals

The general problem of photogrammetry is well known, and the state of the art has advanced tremendously in the last decade or so. Excellent references are available in the bibliography, especially those by Brown, Hallert, and Schmid. However, this report will only deal with the specific approach used in the ESSA reduction. No original photogrammetric reduction is performed by the author. Instead, the parameters obtained by ESSA in its "single-camera orientation" program are used to compute residuals for the star images used in the astrometric investigations. Their graphical presentation provides a basis for comparison between the photogrammetric reduction and an astrometric reduction. It is assumed that the ESSA reduction is representative of the general photogrammetric approach since the mathematical model used is a physical reconstruction of the geometrical event, and the formulae and corrections employed are

representative of those in current usage by most photogrammetrists.

While systematic errors are intended to be absorbed by the plate constants in an astrometric model without regard to any specific source of systematic error, the photogrammetric approach attempts to identify the main sources of systematic error, model them mathematically, remove the errors from the measured coordinates, and then relate these "undistorted" coordinates to the object space through use of the collinearity equations. This is the application of the "central-projection" theory. Without regard to any physical influences on the emulsion, the systematic errors usually modeled in the photogrammetric reduction of stellar plates are those non-cancelling errors contributed by the comparator and errors contributed by lens distortions. Since stars provide the control, refraction is added to the star directions as described in the previous section rather than removed from the plate coordinates.

The formulae used by ESSA in its reduction and used by the author to compute the plate residuals are now given. It must be remembered that the Garfinkel model (USC & GS version) has already been applied to the stellar directions to account for astronomical refraction.

For non-perpendicularity of the comparator axis the corrections are [Hotter, 1967, p. 119] .

$$\begin{aligned} \bar{x} &= x_B + \epsilon y_B, \\ \bar{y} &= y_B \text{ (correction is negligible),} \end{aligned} \qquad (4.5)$$

where x_B and y_B are measured plate coordinates of the image and ϵ is an adjustable correction angle for the amount of non-perpendicularity. A physical description is available in [Brown, 1957, p. 80] .

The radial distortion corrections are [Slama, 1967] ,

$$
\begin{aligned}
x^* &= \bar{x} - \frac{\Delta R}{d}(x - x_s) = \bar{x} - \Delta x_{radial}, \\
y^* &= \bar{y} - \frac{\Delta R}{d}(y - y_s) = \bar{y} - \Delta y_{radial}, \\
\frac{\Delta R}{d} &= K_1 d^2 + K_2 d^4 + K_3 d^6, \\
d^2 &= (x - x_s)^2 + (y - y_s)^2.
\end{aligned}
\tag{4.6}
$$

In these equations x and y are undistorted image coordinates; x_s and y_s are adjustable coordinates of the origin of distortion in the plate coordinate system; and K_1, K_2, and K_3 are adjustable coefficients of radial distortion.

To correct for Conrady (decentering) distortion, the formulae are [Slama, 1967] ,

$$
\begin{aligned}
x^* &= \bar{x} - \Delta T\,[DC_3 \sin\varphi_T + DC_1 \cos\varphi_T] \\
&= \bar{x} - \Delta x_{conrady} \\
y^* &= \bar{y} - \Delta T\,[DC_3 \cos\varphi_T + DC_2 \sin\varphi_T] \\
&= \bar{y} - \Delta y_{conrady}, \\
DC_1 &= [2(x - x_s)^2/d^2] + 1, \\
DC_2 &= [2(y - y_s)^2/d^2] + 1, \\
DC_3 &= 2(x - x_s)(y - y_s)/d^2, \\
\Delta T &= K_4 d^2 + K_5 d^4.
\end{aligned}
\tag{4.7}
$$

Here K_4 and K_5 are adjustable coefficients of tangential distortion, and φ_T is an adjustable angle from the $\bar{y}$ axis to the axis of maximum tangential distortion.

When combining the distortion corrections, the result is

$$x^{**} = \bar{x} - \frac{\Delta R}{d}(x - x_s) - \Delta T\,[DC_3 \sin\varphi_T + DC_1 \cos\varphi_T],$$
$$y^{**} = \bar{y} - \frac{\Delta R}{d}(y - y_s) - \Delta T\,[DC_3 \cos\varphi_T + DC_2 \sin\varphi_T]. \qquad (4.8)$$

Several years ago, the thin-prism model was employed instead of the Conrady form for decentering distortion. However, Duane Brown showed that while the thin-prism model was equivalent to the Conrady form for first-order effects, it was not the same for higher-order effects, and, thus, the Conrady form is now used [Brown, 1966]. The theory is based on the work of A. E. Conrady, an English astronomer years ago [Conrady, 1919]. References to the photogrammetric theory and its development for ballistic cameras may be found in [Schmid, 1959], [Brown, 1957], [Brown, 1964], and [Brown, 1966].

Notice that in the above formulae, the undistorted coordinates are used on the right-hand side of the equations. This is theoretically correct and is the form used by the author to compute the photogrammetric residuals for the three plates, only because in this case the undistorted coordinates are available. Normally, as in the case of the ESSA reduction, the measured (observed) coordinates are initially used on the right-hand side and are being replaced by x** and y** after each computation. The solution is iterated until $\frac{\Delta R}{d}$ and ΔT converge to a prescribed tolerance [Hotter, 1967, p. 120] and [Slama, 1967].

The undistorted coordinates, x and y, are computed by the collinearity equations [Schmid, 1959, p. 13].

$$x = \frac{c_x (A_1 X + B_1 Y + C_1 Z)}{q} + x_p,$$

$$y = \frac{c_y (A_2 X + B_2 y + C_2 Z)}{q} + y_p, \qquad (4.9)$$

where $q = D X + E Y + F Z,$

$$A_1 = -\cos\alpha \cos\varkappa + \sin\alpha \sin\omega \sin\varkappa,$$
$$B_1 = -\cos\omega \sin\varkappa,$$
$$C_1 = \sin\alpha \cos\varkappa + \cos\alpha \sin\omega \sin\varkappa,$$
$$A_2 = -\cos\alpha \sin\varkappa - \sin\alpha \sin\omega \cos\varkappa,$$
$$B_2 = \cos\omega \cos\varkappa,$$
$$C_2 = \sin\alpha \sin\varkappa - \cos\alpha \sin\omega \cos\varkappa,$$
$$D = \sin\alpha \cos\omega,$$
$$E = \sin\omega,$$
$$F = \cos\alpha \cos\omega.$$

In these equations, x_p and y_p are adjustable coordinates of the principal point in the plate coordinate system; c_x and c_y are adjustable principal distances to the $\bar{x}$ and $\bar{y}$ axis from the projection center; X, Y, and Z are coordinates of the point in object space; and α, ω, $\varkappa$ are the Eulerian rotation angles which rotate the arbitrary rectangular coordinate system of object space (X, Y, Z) into the plate coordinate system (x, y, c). Diagrams and a physical interpretation of the above are available in [Schmid, 1959].

In the ESSA reduction and, therefore, in the author's computation of photogrammetric residuals, X, Y, and Z are the direction numbers of a star

in the horizon system centered at the projection center (this substitution is necessary since most stars are located practically at infinity) and computed by,

$$X = \cos a \cos A,$$
$$Y = \cos a \sin A, \qquad (4.10)$$
$$Z = \sin a,$$

in which a is the "observed" altitude and A is the "observed" azimuth. A and a are available from the author's star updating program and are stored on punched cards.

To compute the photogrammetric plate residuals the following procedure is used:

1. Given a and A for a star, compute X, Y, Z
2. Compute x and y using (4.9)
3. Compute Δx_{radial}, Δy_{radial}, $\Delta x_{conrady}$ and $\Delta y_{conrady}$, by formulae (4.6) and (4.7)
4. $x' = x + \Delta x_{radial} + \Delta x_{conrady}$

   $x_{distorted} = x' - \epsilon \bar{y}$

   $y_{distorted} = y + \Delta y_{radial} + \Delta y_{conrady}$
5. $v_x = x_{distorted} - x_B$

   $v_y = y_{distorted} - y_B$.

The unknown parameters used in the given formulae are available for plates 2559, 5205, and 6132 from the "single camera orientation" program [ESSA, 1967], and are listed in Table 1. The plotted residuals are shown in Charts 4, 5, and 6. The residual scale is 0.1 inch equals 3 microns or approximately 2 seconds of arc in stellar direction and the

method of plotting the residuals will be explained in section 4.4.1. The charts of the plotted residuals also give the corresponding standard error of unit weight for that plate reduction as quoted from the "single camera orientation" program [ESSA, 1967].

Table 1

ESSA Parameters from "Single Camera Orientation Program" for Computing Plate Residuals [ESSA, 1967]

Parameter		Plate 2559	Plate 5205	Plate 6132
α	(grads)	62.27051	2.471354	37.97947
ω	(grads)	19.28476	36.02114	-37.37786
$\varkappa$	(grads)	162.6365	245.5531	106.4265
ϵ	(grads)	.002923602	-.0001349864	.00005810139
xp	(meters)	-.000006689202	-.00007452753	-.0001134127
yp	(meters)	.00008196885	.00001125822	.00004536102
cx	(meters)	.3030345	.3034375	.3032675
cy	(meters)	.3030374	.3034346	.3032710
K_1		.2724793	.1796399	.1861981
K_2		-19.37803	2.066992	-5.094664
K_3		257.7927	-1171.724	-695.6819
K_4		-.00009683551	.0003342886	.0002751480
K_5		.01558277	.002749874	.001130124
φ_T	(grads)	133.4833	180.7971	150.2195
xs	(meters)	-.000006689202	-.00007452753	-.0001134127
ys	(meters)	.00008196885	.00001125822	.00004536102

It will be noted that the author in many places refers to 1×10^{-6} meters as a micron. This is done with the understanding that this small unit of distance should properly be referred to as a micrometer based on a decision made at the Thirteenth General Conference on Weights and Measures, October, 1967, in Paris.

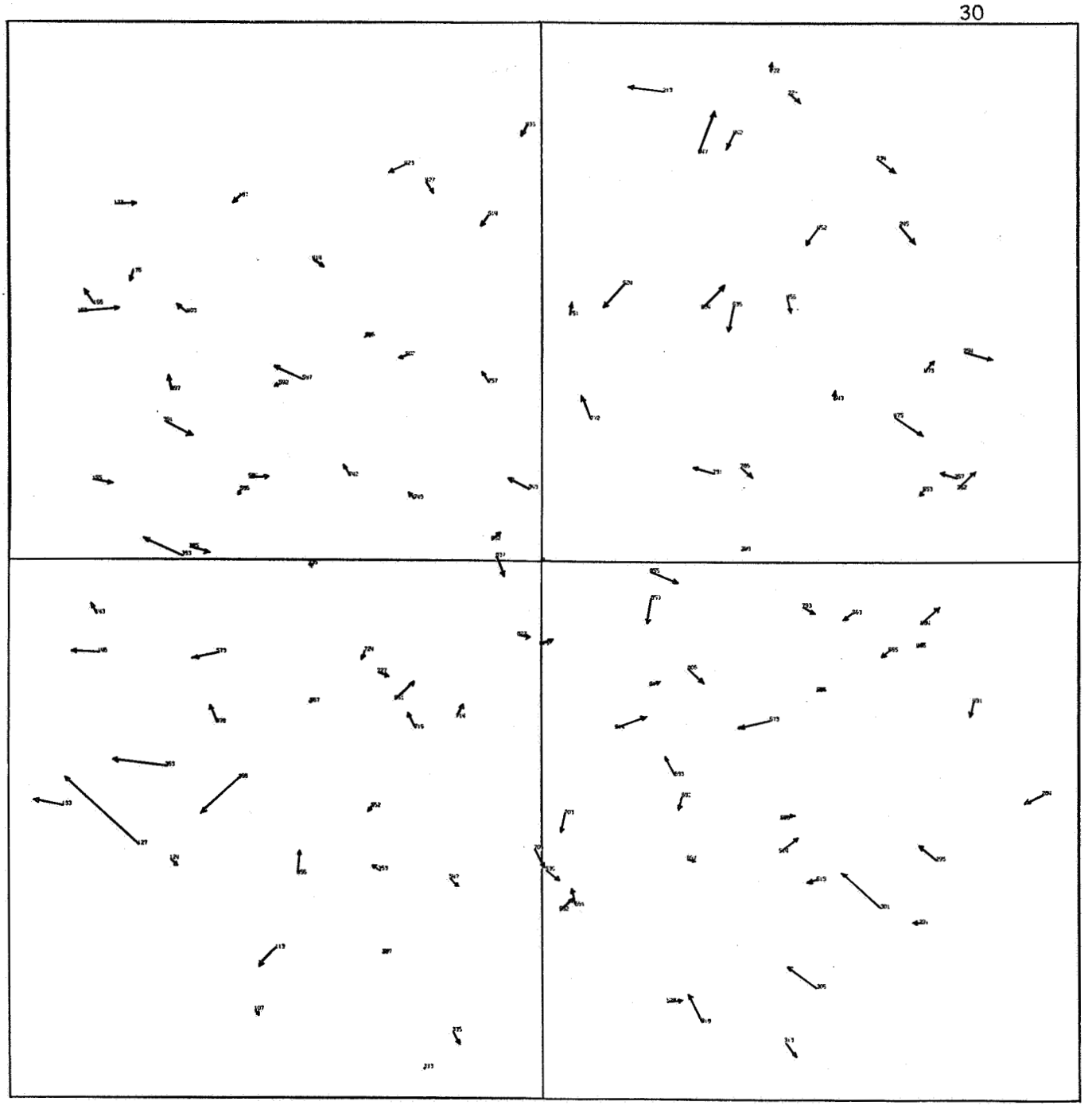

SCALE
0.1 inch = 3 microns = 2 arc seconds

CHART 4: PLATE 2559
RESIDUALS FOR ESSA PHOTOGRAMMETRIC REDUCTION

m_0 = 2.96 microns

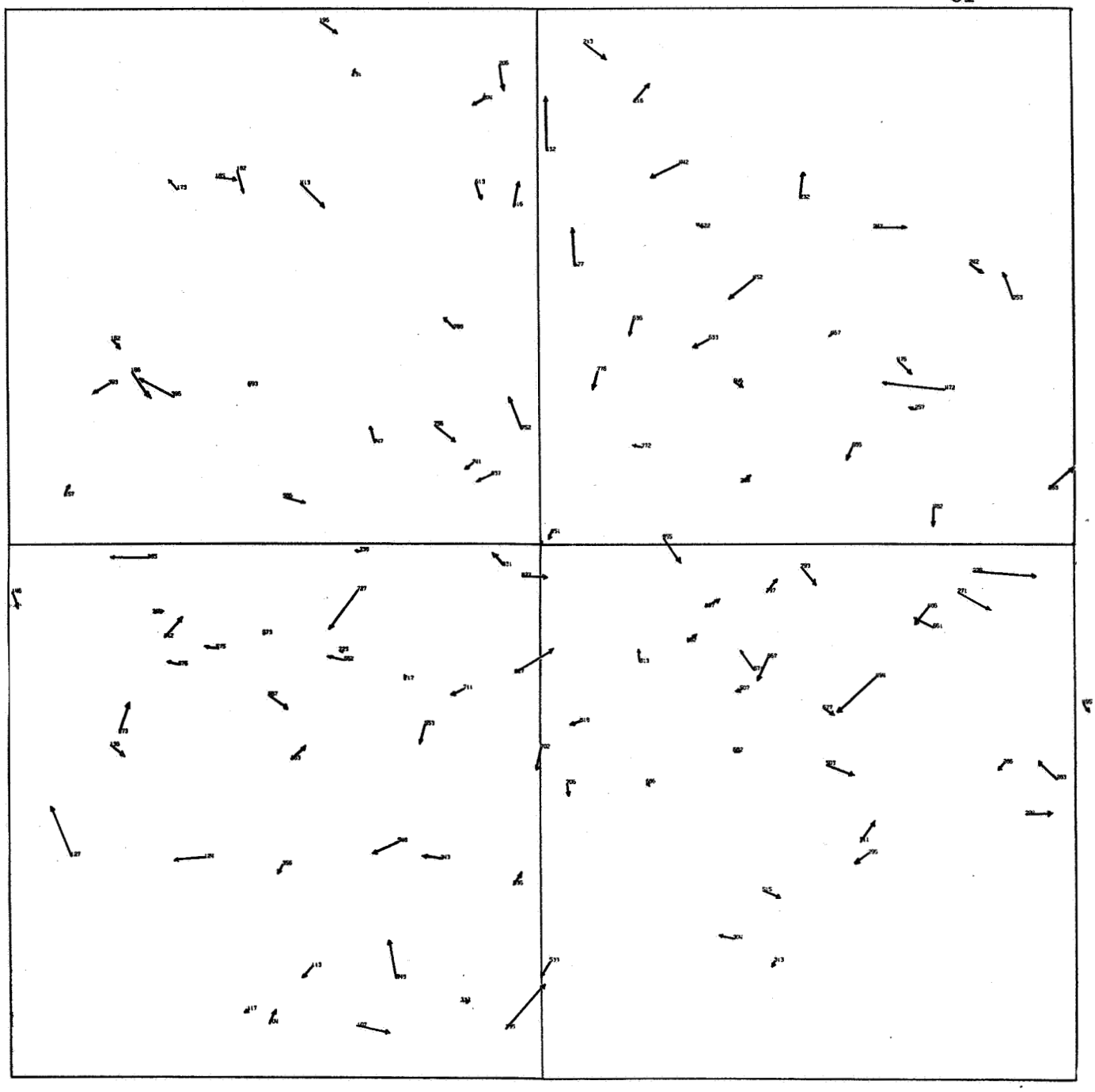

SCALE
0.1 inch = 3 microns = 2 arc seconds

CHART 5: PLATE 5205
RESIDUALS FOR ESSA PHOTOGRAMMETRIC REDUCTION

m_0 = 3.17 microns

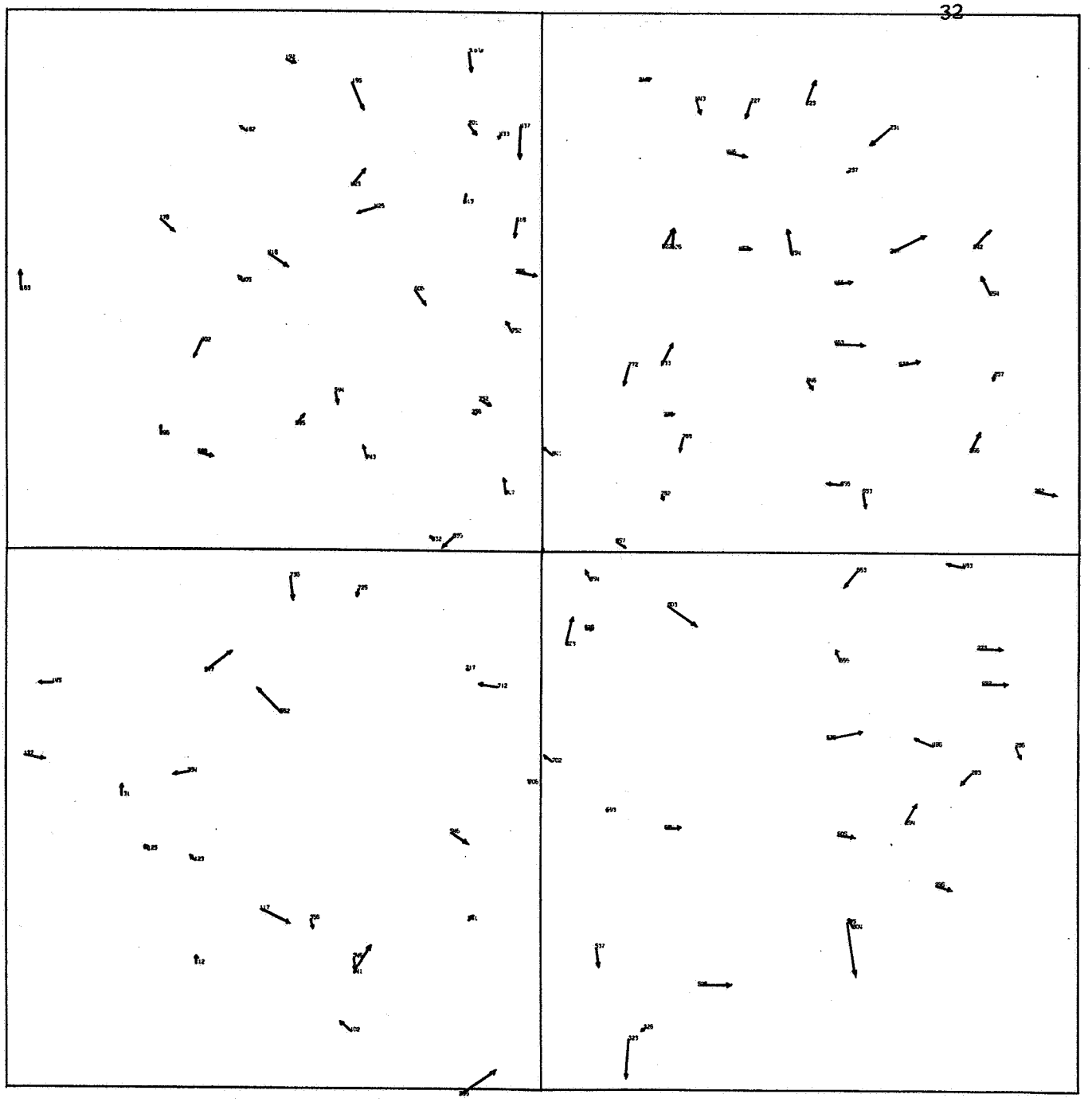

SCALE
0.1 inch = 3 microns = 2 arc seconds

CHART 6: PLATE 6132
RESIDUALS FOR ESSA PHOTOGRAMMETRIC REDUCTION

m_0 = 2.80 microns

4.4 The Astrometric Reductions

4.4.1 General.--In contrast to the photogrammetric reduction, an astrometric technique has no physical interpretation except the implicit relationship between the plane of the photograph and a plane tangent to the celestial sphere at the point of intersection of the optical axis and the celestial sphere. The models tested consist of six or more constants that are coefficients in linear or higher order equations relating object and image space. These constants are not arranged to correct a specific systematic error (except in the case of a translation term), but they are expected to absorb the combination of various systematic errors such as astronomical refraction and annual aberration (if not added to the stars before reduction),errors resulting from improper orientation of the tangent plane, and even lens distortions in some cases. Whether or not systematic errorsare removed remains to be seen. As mentioned, the astrometric techniques have been historically associated with cameras of long focal length and of narrow angular fields. Therefore, in satellite tracking they have been shunned for more advanced photogrammetric techniques. But as the reader shall see, the astrometric technique is more simple in concept and, easier to apply. If comparable accuracies could be obtained thus systematic errors removed with an astrometric reduction, its economical aspects would make it extremely appealing.

With these points in consideration, several common models will be examined. The least-squares reduction used in all cases is commonly known as the "variation of parameters" method in which for this problem, the weight matrix is equal to the identity matrix. The variation of

parameters technique uses a model of the form:

$$L = f(x) \tag{4.11}$$

where L is the observed quantity and x represents the unknown quantities. By use of a truncated Taylor series expansion, (4.11) is linearized and used to form "observation" equations, and then "normal" equations in which the unknowns are differential corrections to the assumed values of the unknowns in (4.11) (the origin about which the expansion is made). Because the method avoids higher order terms implicit in the Taylor series expansion, an iterative technique could generally be employed to get increasingly better values around the origin about which the expansion takes place. This information is well-known to physical scientists, but it is repeated here to indicate the author's approach. For example, the method of least-squares has also been developed in the form:

$$f(x, L) = 0 \tag{4.12}$$
$$G(x) = 0$$

where G (x) equal to zero implies a set of constraints on the unknowns. The computational method in this case is different and possibly the results more valid where applicable. Weighting in this latter method becomes more of a problem, and it is even sometimes feasible to weight the known quantities, thus treating them as observables [Uotila, 1967].

How does this relate to the problem at hand? The astrometric models tested are all of the form:

$$\begin{aligned} (x_B, y_B) &= f(C, \xi, \eta), \\ (\xi, \eta) &= f(C, x_B, y_B), \end{aligned} \tag{4.13}$$

where x_B and y_B are observed (measured) coordinates, ξ and η are

standard coordinates (functions of right ascension and declination as subsequent paragraphs will show), and C is a set of plate constants (the unknowns). Since all experimentation will be performed using the method of variation of parameters, all quantities on the left-hand side of (4.13) are regarded as observed quantities with weights of unity, and those on the right-hand side (except C) are regarded as "known". Since the accuracy of the catalogue star positions is immaterial to this examination (although it is extremely important in the overall question of satellite triangulation), where possible, ξ and η are kept on the right-hand side of (4.13). This procedure has to be changed in one particular model as will be seen. While it may be statistically valid to follow a model of the form (4.12) where ξ and η would be weighted on the basis of the catalogue accuracy of the stars' positions, or possibly magnitude or spectral class, this would pose more problems for this investigation than it would resolve. On the other hand, astronomers have traditionally used ξ and η on the left-hand side of (4.13) and considered the measured coordinates as known. At least for cameras of short focal length (BC-4), this is incorrect since x_B and y_B are subject to significant random errors [Brown, 1963, pp. 166-167].

While The Ohio State University has adjustment programs available, all astrometric reductions are contained in one program written by the author. Based on the model being used in the reduction appropriate subroutines generate the observation equations, the normal equations are formed and solved, and the approximate values of the plate constants are then corrected, the process being iterated until a specified maximum

number of iterations is exceeded or the corrections to the plate constants converge to a pre-set tolerance. In all the reductions this tolerance is 10^{-16}. The variance and standard error of unit weight are computed as well as the weights and variances of the unknowns and the covariance matrix. The residuals in plate coordinates are then computed, and the adjusted coordinates are punched on cards (except in Model 5). The variance of unit weight is again computed, using the actual residuals, as a check on the adjustment procedure. Finally, interpolated directions for unknown stars are computed (except in Model 2).

Generation of the observation equations implies that values of $\frac{\delta f}{\delta C}$, in terminology of (4.13), are solved for by the computer. The expressions for $\frac{\delta f}{\delta C}$ are simple derivatives and, therefore, will not be given here. Their values should be apparent when the models are discussed. Each star generates two observation equations.

The adjusted plate coordinates and the measured coordinates are then used to plot the residuals on the IBM 1627 plotter. Since the residuals are too small to appear on a reasonable size plot, they have been magnified so that 0.1 inch approximately equals 3 microns. (The originals of the plots in this report were about 3 times their size here). This same information applies to the plots of the photogrammetric residuals already exhibited.

It is assumed that the reader has a basic knowledge of astrometric theory. However, some repetition is necessary to understand the author's approach. Detailed discussions may be found in the references of Smart, Podobed, and Van de Kamp, but the origin of this theory is attributed to

Professor H. H. Turner [Turner, 1893]. Briefly, the stars are gnomonically projected onto a plane that is tangent to the celestial sphere ideally at the point of intersection of the optical axis of the taking camera with the celestial sphere. Their coordinates (ξ η) on the tangent plane are given in a rectangular coordinate system known as the standard coordinate system. Increasing values of ξ correspond to increasing values of right ascension and the η axis is directed toward the north pole. The rigorous formulae for the projection are given by [Smart, 1962, pp. 283, 284]:

$$\xi = \frac{\cot\delta \sin(\alpha - A)}{\sin D + \cos D \cot\delta \cos(\alpha - A)}$$
$$\eta = \frac{\cos D - \cot\delta \sin D \cos(\alpha - A)}{\sin D + \cot\delta \cos D \cos(\alpha - A)} \qquad (4.14)$$

where α is the star's right ascension, δ denotes the star's declination, A denotes the right ascension of the point of intersection of the optical axis with the celestial sphere, and D is the declination of the point of intersection of the optical axis with the celestial sphere. If ξ and η are known for a stellar image, the right ascension and declination may be obtained by [Smart, 1962, pp. 284, 285],

$$\cot\delta \cos(\alpha - A) = \frac{1 - \eta \tan D}{\eta + \tan D}$$
$$\cot\delta \sin(\alpha - A) = \frac{\xi \sec D}{\eta + \tan D} \qquad (4.15)$$

In the simplest case, the photographic plate is parallel to the tangent plane, and the standard coordinate system may be superimposed on the photographic plate by applying a scale factor (focal length of camera). This discussion assumes the plane of the photograph is flat. The SAO uses a Baker-Nunn camera in its optical tracking in which the film back-up is cylindrical in shape. Mueller gives formulae to get ξ and η for this case [Mueller, 1964, p. 311].

Naturally, this simple case is not achieved because of irregularities in the internal geometry of the camera and because of the impossibility of finding the true intersection of the optical axis with the celestial sphere. Discussions of the models will indicate how these problems are dealt with.

A short discussion about choosing A and D is necessary. The exact point of contact of the tangent plane with the celestial sphere is never known, so, therefore it must be approximated with the best information available. While there are various methods of doing this, the author uses one recommended method in all reductions [Mueller, 1964, pp. 311, 312]. A stellar image is chosen as close to the geometrical plate center as possible. The "fictitious" (recall the author's intended use of this word) "observed" right ascension and declination of this star are assigned as the values of A and D respectively. Because this image is then the origin of the standard coordinate system (the assumed point of tangency), the origin of the plate coordinate system is shifted from the fiducial center to this image by a simple translation so that the two origins will coincide. These origins are not changed throughout the adjustment. It is assumed that the astrometric model will adjust for the fact that the two origins do not actually coincide but differ by some differential amount [Mueller, 1964, p. 311]. On Plates 2559, and 6132, star images are initially chosen as the points of tangency by the method just described. However, because there are satellite images on both plates nearer the geometrical plate center than these star images, the satellite images are used in later reductions as the origins, their right ascensions and declinations having been computed in one of the initial reductions.

It also must be observed that the right ascension and declination of whatever image is chosen to be the origin of the coordinate systems will define the orientation of the tangent plane with respect to the photographic plane. It would be desirable to keep the two planes parallel, but because the true intersection of the optical axis with the celestial sphere is unknown, the approximation by the method described will establish a tangent plane not parallel to the plane of the photograph. The author will experiment to see just how sensitive the reduction by a particular astrometric model is to the selection of the point of tangency. Just because we make the origin of the plate coordinate system coincide with the origin of the standard coordinate system does not establish parallelism between the two planes. No matter where the origin of the plate coordinate system is, the orientation of the photographic plane remains rigid. However, each selection of a new point of tangency on the celestial sphere will define a new orientation of the tangent plane with respect to the fixed orientation of the plate. It will be shown that two of the astrometric models tested allow for some non-parallelism. The choice of the point of tangency is critical in another.

The astrometric models will now be presented as well as the results of experimentation with them. Plots of residuals will provide clues as to whether systematic errors have been removed and conclusions will be drawn in Section 6. Standard errors of unit weight will also be given for each reduction. Directions for the 21 satellite images will be computed where possible using the adjusted plate constants and the differences between the ESSA results and the author's results will be tabulated. These

differences are computed in the "fictitious observed" right ascension and declination system, the ESSA apparent satellite positions having been updated to this system with the author's updating program. Since the astrometric models are being compared to the photogrammetric reduction, the ESSA satellite positions are considered the standard in any comparison or statistical analysis.

4.4.2 Model 1; The Projective Equations.--The projective equations are given as,

$$x_B = \frac{A\xi + B\eta + C}{a\xi + b\eta + 1},$$
$$y_B = \frac{D\xi + E\eta + F}{a\xi + b\eta + 1}, \qquad (4.16)$$

where x_B and y_B are the measured plate coordinates; A, B, C, D, E, F, a and b are the plate constants to be determined; and ξ and η are the standard coordinates as given by (4.14). After adjustment, the equations used to obtain standard coordinates for an unknown star are:

$$\xi = \frac{x_B(bF - E) + y_B(B - bc) + (CE - FB)}{x_B(aE - bD) + y_B(bA - aB) + (BD - EA)},$$
$$\eta = \frac{x_B(D - aF) + y_B(aC - A) + (AF - CD)}{x_B(aE - bD) + y_B(bA - aB) + (BD - EA)}. \qquad (4.17)$$

Recall that the adjustment procedure follows the model of (4.13).

The projective equations express the projectivity between two planes, not necessarily parallel [Hallert, 1960, pp. 15, 16]. This would imply that the reduction using Model 1 is not sensitive to the choice of the origin of the standard coordinate system (point of tangency) as described in section 4.4.1.

The images tried as origins for both the plate coordinate system and the standard coordinate system are given on the residual plots. Recall the general rule in this approach is to select an image, shift the measured plate coordinate origin to it and use its "fictitious observed" right ascension and declination as A and D respectively, the equatorial coordinates of the point of tangency. However, one will notice in several tests for Plate 5205 that x_p and y_p from the ESSA photogrammetric reduction are used as the coordinates of Star 851, the selected point of tangency for that plate. This is done merely to test the sensitivity of the reduction to the choice of origins, and ordinarily x_p and y_p would not be available. In tests where a satellite image is used as an origin, the "fictitious observed" right ascension and declination of this image are taken from the results of a previous astrometric adjustment as mentioned earlier and not from an agency reduction.

Test 1

Model 1 is applied to all three plates, using all stars on the plates. Recall this allows 111 control points for Plate 2559, 114 for 5205, and 106 for 6132. Charts 7, 8, and 9 show the residual plots for these reductions. The standard errors of unit weight (m_0), quite high, are also given on the charts. The systematic effects still remaining in the residuals are quite obvious. Radial distortion appears to be the largest contributor. The effects of the remaining systematic errors are also illustrated in the differences of the computed satellite positions from the ESSA results. Nowhere are these more evident than on Plate 5205 where the satellite images extend toward the limits of the declination zone for the photograph.

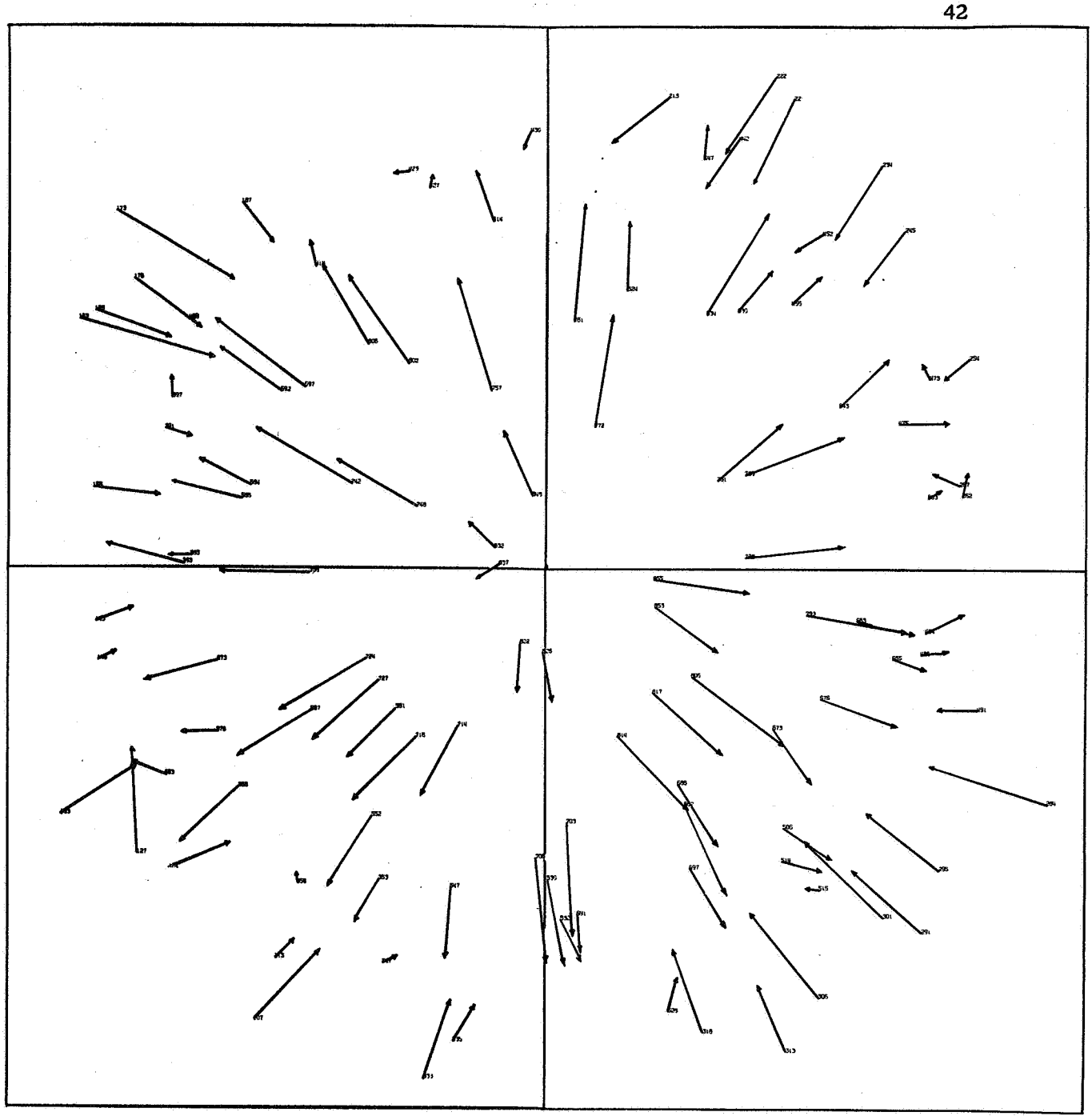

SCALE
0.1 inch = 3 microns = 2 arc seconds

CHART 7: PLATE 2559
TEST 1 RESIDUALS, PROJECTIVE EQUATIONS APPLIED TO ACTUAL MEASURED COORDINATES
Stars 837, 853 and Satellite 313 used as origins with identical results
m_0 = 10.03 microns

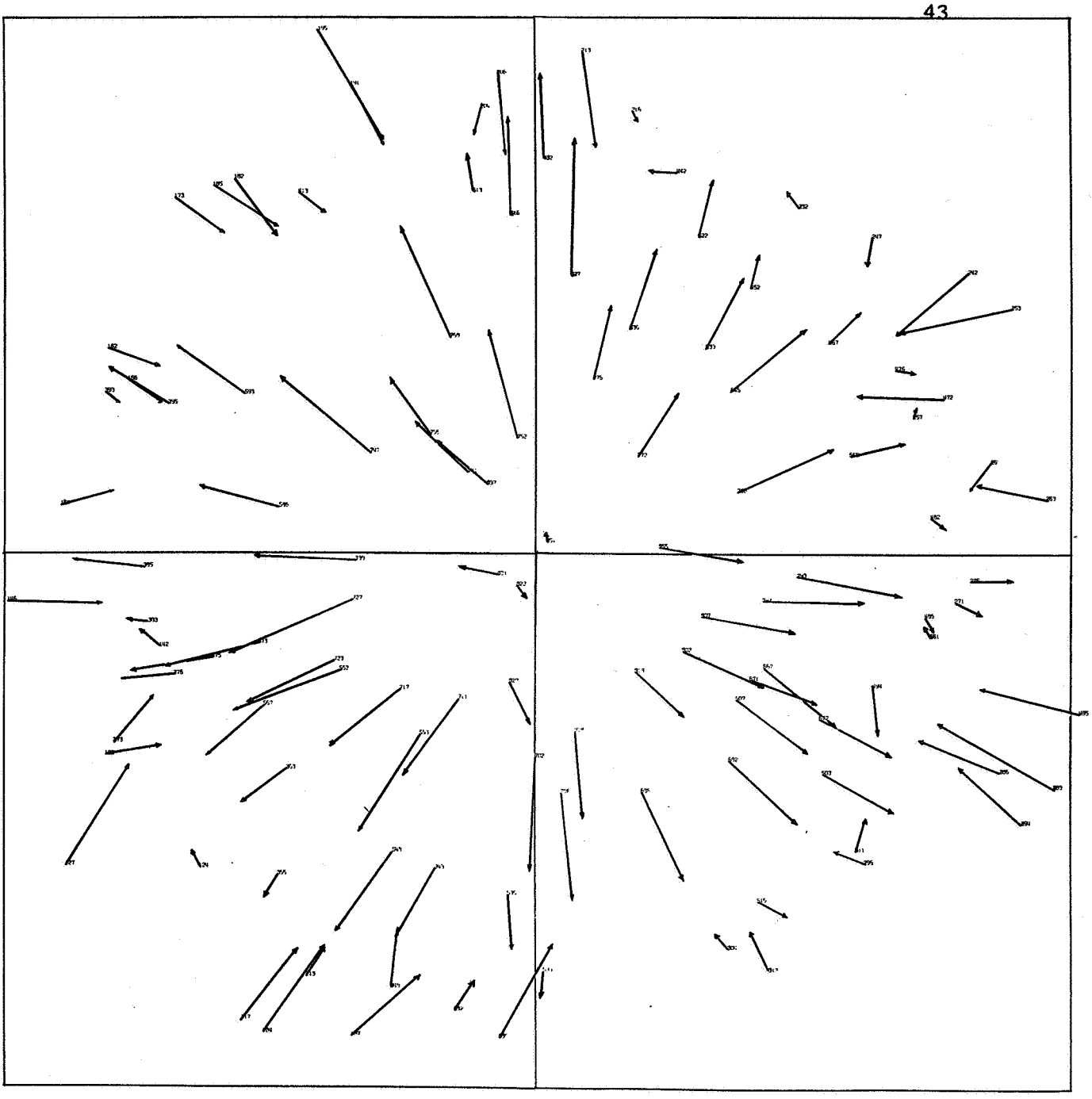

SCALE
0.1 inch = 3 microns = 2 arc seconds

CHART 8: PLATE 5205
TEST 1 RESIDUALS, PROJECTIVE EQUATIONS APPLIED TO ACTUAL MEASURED COORDINATES
Star 851 is origin
m_0 = 10.03 microns

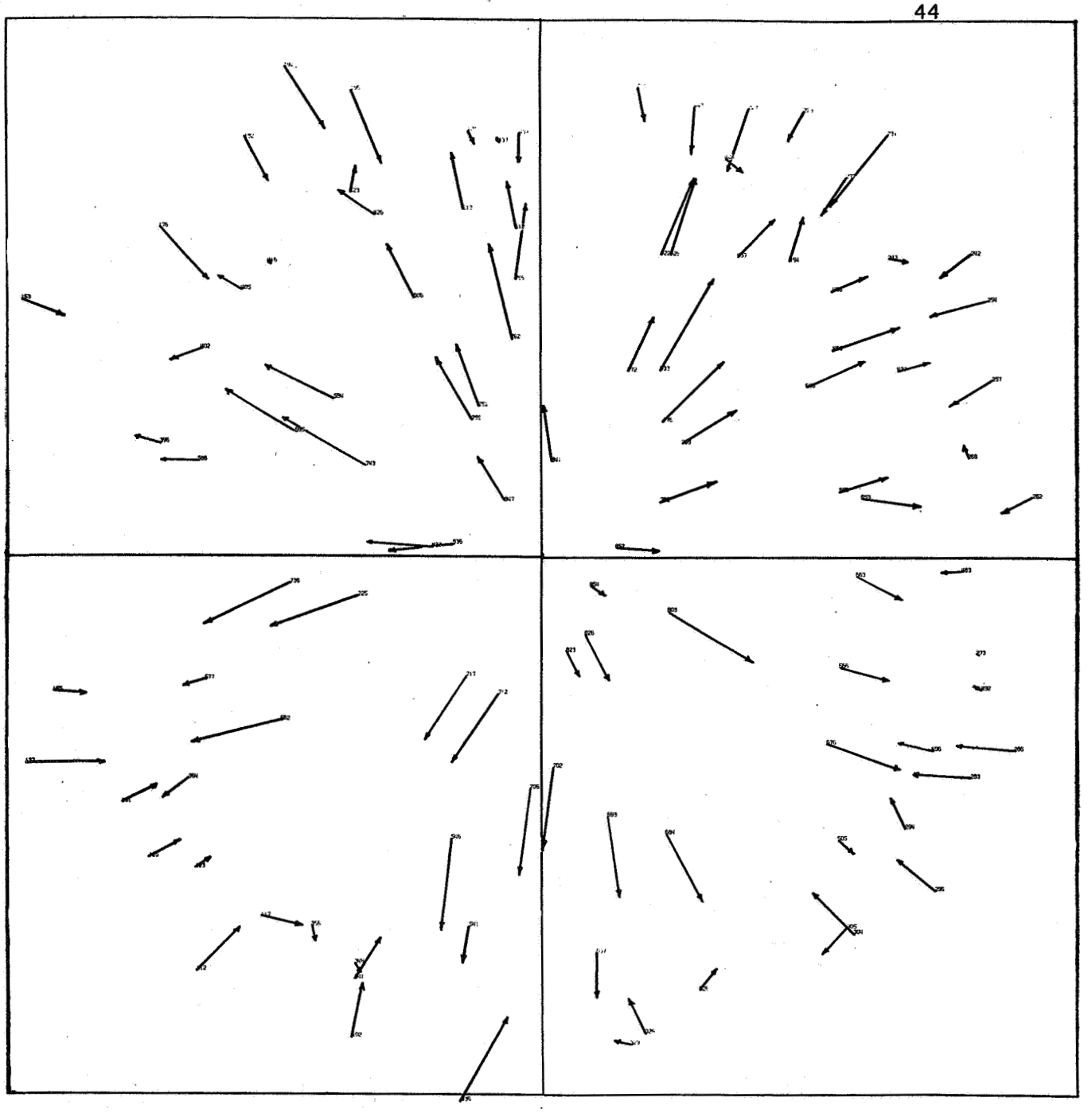

SCALE
0.1 inch = 3 microns = 2 arc seconds

CHART 9: PLATE 6132
TEST1 RESIDUALS, PROJECTIVE EQUATIONS APPLIED TO ACTUAL MEASURED COORDINATES
Star 854 is origin
m_0 = 7.81 microns

These differences are given in Tables 2, 3, and 4.

In Test 1, the origin for Plate 2559 is changed several times to test the sensitivity of the projective equations to the choice of the point of tangency. The adjusted plate constants in each case differ but all other results including the computed plate residuals and satellite directions are identical for all origins used. While one would want to choose an image as origin as close to the geometrical plate center as possible, it is apparent that any choice could be constrained during the adjustment and that no increase in accuracy could be expected by using an iteration technique to find the point of tangency that best approximates the intersection of the true optical axis with the celestial sphere.

Test 2

It is desirable to know how great the effects of decentering distortion are in regards to Model 1. The author's program for computing photogrammetric residuals is used to remove decentering distortion from the measured coordinates x_B and y_B. Still remaining, then, in the measured coordinates are radial distortion and non-perpendicularity of the comparator axis. The reductions are again performed as in Test 1. The plotted residuals are shown in Charts 10, 11, and 12. The effects of decentering distortion appear to be minimal since the results of Test 2 are almost identical to those of Test 1. Considering this fact, no satellite directions are computed in this test.

Table 2

PLATE 2559

Differences of Model 1 Interpolated Positions from ESSA Positions for 21 Satellite Images Computed in "Fictitious Observed" Equatorial System

	RA			DEC			
No.	ESSA - Test 1	ESSA - Test 4	ESSA - Test 5	ESSA - Test 1	ESSA - Test 4	ESSA - Test 3	
126	1.563		0.146	-3.05		0.99	
143	1.575		0.259	-2.97		0.64	
161	1.552	0.006	0.349	-2.82	1.07	0.36	
179	1.493	0.099	0.407	-2.62	0.73	0.16	
201	1.372	0.170	0.435	-2.31	0.44	0.02	
219	1.235	0.197	0.425	-2.04	0.26	-0.05	
239	1.044	0.192	0.380	-1.75	0.12	-0.08	
258	0.833	0.163	0.312	-1.49	0.01	-0.09	
281	0.541	0.096	0.198	-1.23	-0.09	-0.10	
299	0.292	0.027	0.094	-1.08	-0.17	-0.11	
313	0.094	-0.030	0.009	-1.00	-0.22	-0.13	
330	-0.153	-0.103	-0.099	-0.98	-0.32	-0.18	
350	-0.440	-0.184	-0.219	-1.02	-0.43	-0.26	
368	-0.689	-0.248	-0.316	-1.13	-0.55	-0.35	
387	-0.934	-0.295	-0.399	-1.32	-0.67	-0.47	
403	-1.114	-0.313	-0.445	-1.53	-0.77	-0.57	
414	-1.226	-0.312	-0.463	-1.69	-0.83	-0.64	
434	-1.393	-0.277	-0.462	-2.01	-0.91	-0.74	
452	-1.497	-0.203	-0.416	-2.29	-0.91	-0.76	
473	-1.559		-0.305	-2.61		-0.72	
494	-1.550		-0.126	-2.84		-0.51	
	1.054	0.171	0.298	1.89	0.50	0.38	*
	0.050	-0.059	-0.011	-1.89	-0.19	-0.17	**

*Mean absolute difference
**Mean difference

Table 3

PLATE 5205

Differences of Model 1 Interpolated Positions from ESSA Positions for 21 Satellite Images Computed in "Fictitious Observed" Equatorial System

No.	RA			DEC		
	ESSA - Test 1	ESSA - Test 4	ESSA - Test 5	ESSA - Test 1	ESSA - Test 4	ESSA - Test 5
126	0.633			7.47		
143	0.758			9.38		
161	0.822		-0.149	10.64		-2.12
179	0.826		-0.015	11.16	"	-0.26
201	0.772	-0.015	0.077	10.84	-0.09	1.16
219	0.690	0.030	0.105	9.91	0.65	1.73
239	0.577	0.046	0.103	8.29	0.95	1.85
258	0.455	0.039	0.080	6.29	0.87	1.58
281	0.305	0.014	0.039	3.48	0.45	0.93
299	0.189	-0.011	0.001	1.10	0.00	0.29
313	0.105	-0.029	-0.026	-0.78	-0.36	-0.21
330	0.011	-0.048	-0.055	-3.04	-0.73	-0.76
350	-0.085	-0.061	-0.079	-5.56	-0.98	-1.23
368	-0.156	-0.063	-0.091	-7.61	-0.96	-1.41
387	-0.212	-0.051	-0.089	-9.43	-0.57	-1.23
403	-0.245	-0.031	-0.075	-10.63	0.11	-0.73
414	-0.259	-0.010	-0.059	-11.26	0.78	-0.18
434	-0.267		-0.015	-11.90		1.34
452	-0.253		0.042	-11.89		3.28
473	-0.215			-11.13		
494	-0.155			-9.54		
	0.380	0.034	0.065	" 8.16	" 0.58	" 1.19 *
	0.204	-0.015	-0.012	-0.68	0.01	0.24 **

*Mean absolute difference
**Mean difference

Table 4

PLATE 6132

Differences of Model 1 Interpolated Positions from ESSA Positions for 21 Satellite Images Computed in "Fictitious Observed" Equatorial System

No.	ESSA - Test 1	ESSA - Test 4	ESSA - Test 5	ESSA - Test 1	ESSA - Test 4	ESSA - Test 5	
126	-1.251		0.065	-1.94		-0.49	
143	-1.292		-0.068	-1.83		-0.66	
161	-1.302	0.061	-0.179	-1.64	-0.07	-0.74	
179	-1.273	-0.044	-0.257	-1.40	-0.23	-0.75	
201	-1.191	-0.132	-0.311	-1.04	-0.30	-0.65	
219	-1.086	-0.172	-0.323	-0.74	-0.30	-0.53	
239	-0.932	-0.184	-0.305	-0.41	-0.25	-0.35	
258	-0.756	-0.171	-0.262	-0.20	-0.20	-0.18	
281	-0.508	-0.125	-0.182	0.14	-0.11	-0.02	
299	-0.294	-0.075	-0.105	0.27	-0.07	0.16	
313	-0.122	-0.031	-0.041	0.33	-0.03	0.25	
330	0.091	0.024	0.039	0.34	0.00	0.35	
350	0.338	0.083	0.126	0.24	-0.01	0.42	
368	0.550	0.125	0.192	0.09	-0.02	0.46	
387	0.754	0.148	0.239	-0.16	-0.04	0.48	
403	0.905	0.146	0.257	-0.42	-0.05	0.51	
414	0.994	0.130	0.254	-0.61	-0.04	0.54	
434	1.116	0.064	0.210	-0.98	0.02	0.63	
452	1.180	-0.041	0.123	-1.30	0.15	0.79	
473	1.188		-0.042	-1.63		1.29	
494	1.119		-0.282	-1.84		1.64	
	0.869	0.103	0.184	0.83	0.11	0.58	*
	-0.084	-0.011	-0.041	-0.70	-0.09	0.15	**

*Mean absolute difference
**Mean difference

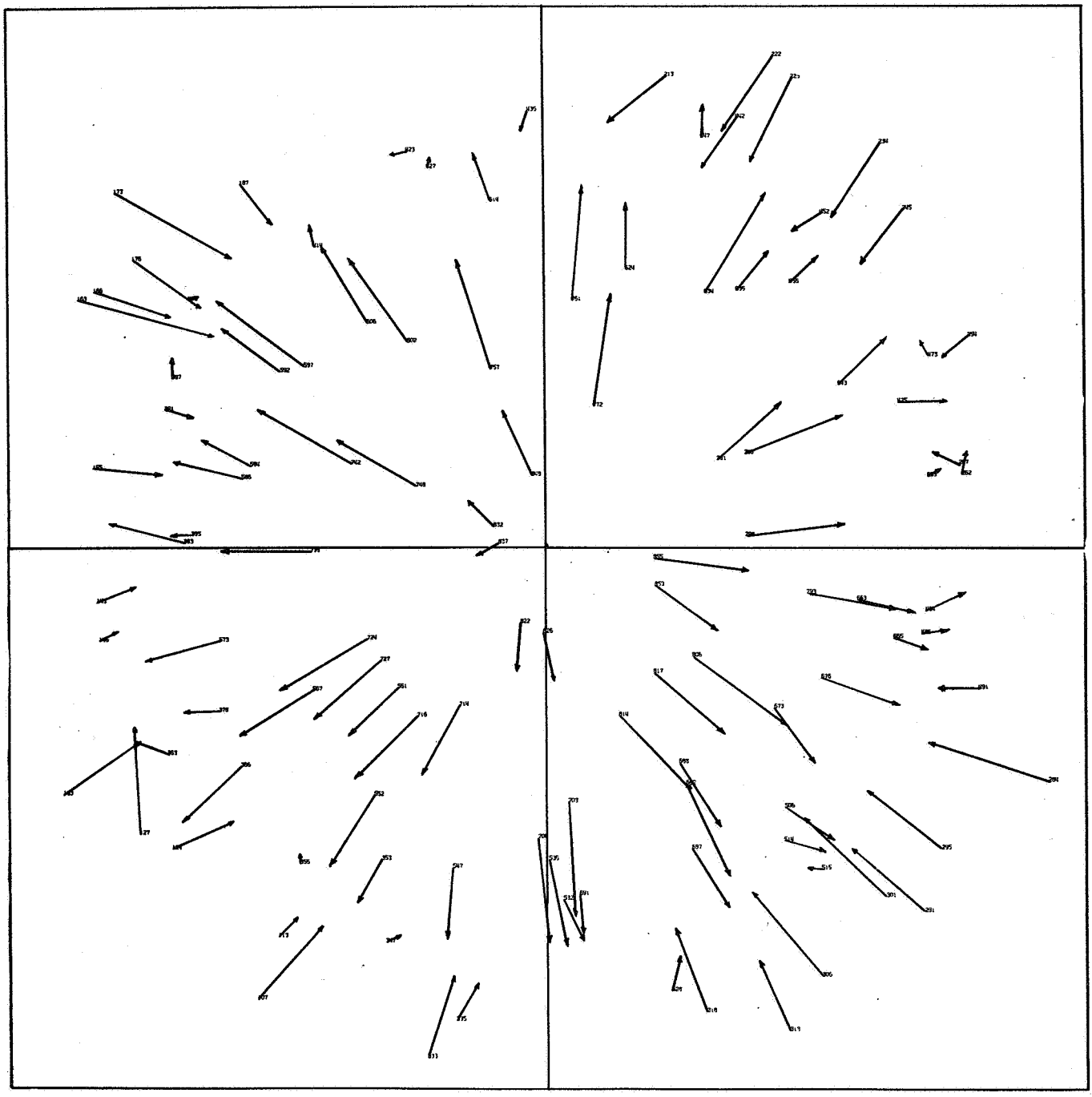

SCALE
0.1 inch = 3 microns = 2 arc seconds

CHART 10: PLATE 2559
TEST 2 RESIDUALS, PROJECTIVE EQUATIONS APPLIED AFTER DECENTERING
DISTORTION IS REMOVED FROM COORDINATES
Star 853 is origin
m_0 = 10.05 microns

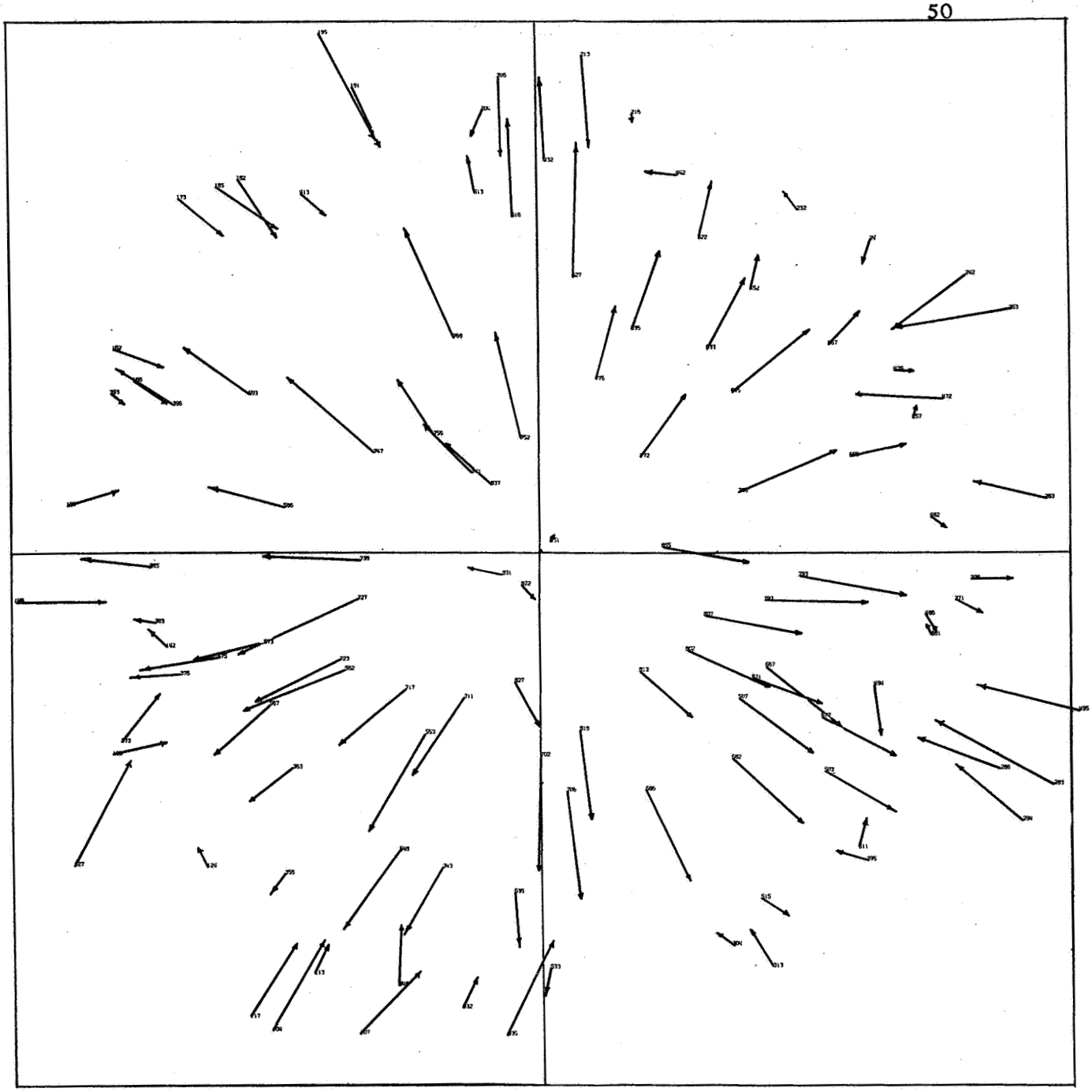

SCALE
0.1 inch = 3 microns = 2 arc seconds

CHART 11: PLATE 5205
TEST 2 RESIDUALS, PROJECTIVE EQUATIONS APPLIED AFTER DECENTERING
DISTORTION IS REMOVED FROM MEASURED COORDINATES
Star 851 is origin
m_0 = 10.35 microns

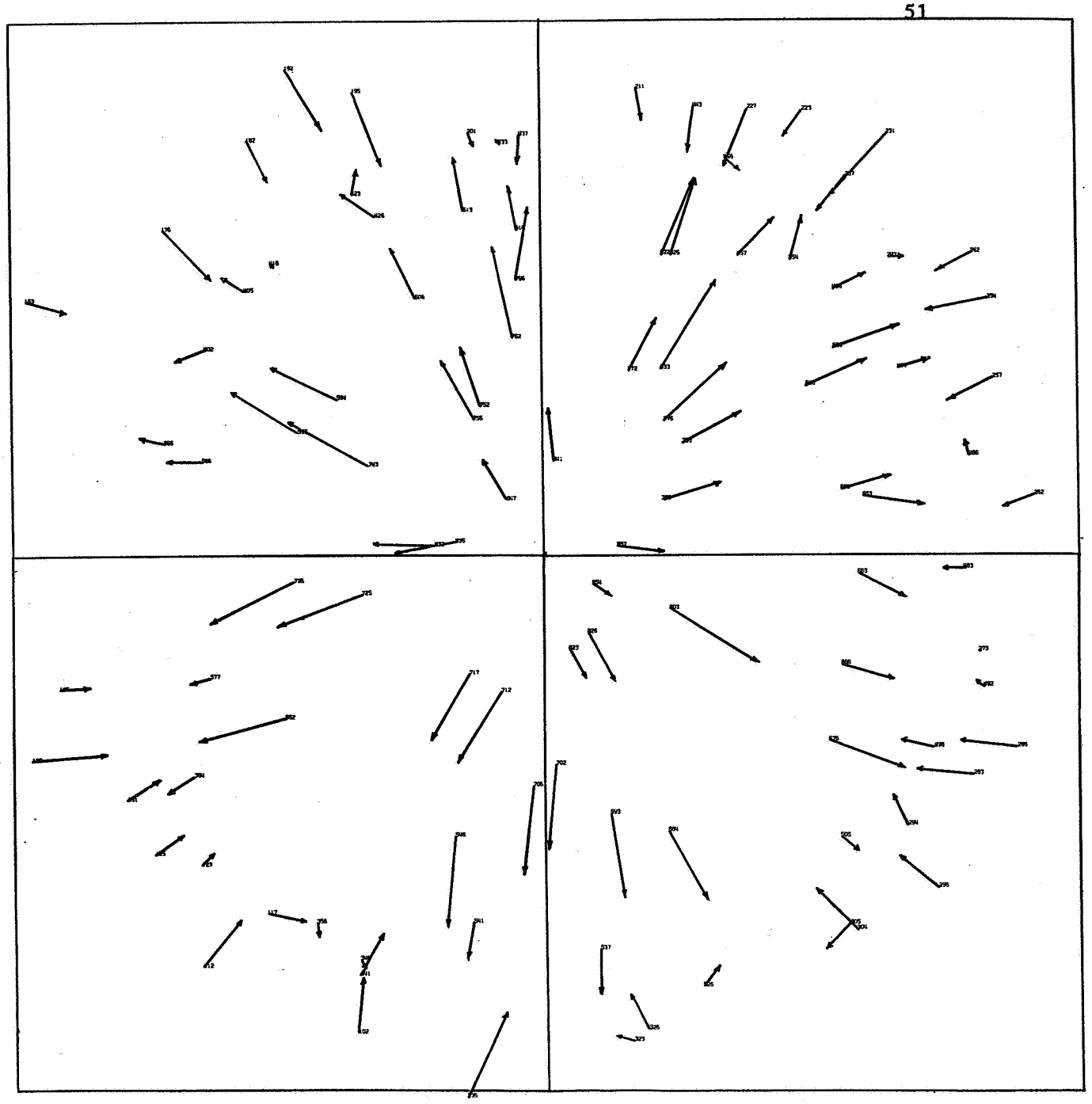

SCALE
0.1 inch = 3 microns = 2 arc seconds

CHART 12: PLATE 6132
TEST 2 RESIDUALS, PROJECTIVE EQUATIONS APPLIED AFTER DECENTERING
DISTORTION IS REMOVED FROM MEASURED COORDINATES
Star 854 is origin
m_0 = 7.77 microns

Test 3

The photogrammetric residual program is used once more with modifications, this time to remove all distortions (including non-perpendicularity, although this effect is almost negligible) from the measured coordinates. The coordinates in this form compare to the true x and y in equation (4.9). The reductions are performed as in Test 1. The residual plots are shown in Charts 13, 14, and 15. Compare these to the plotted residuals of the photogrammetric reduction. Also notice the standard errors of unit weight. No satellite directions are computed in this test since it is evident that the results will be comparable to the ESSA results and since random errors appear to be the only ones remaining after adjustment. Brown states that since only six independent parameters are required to define an undistorted central projection, the eight parameters in (4.16) must be constrained in a fashion that he specifies [Brown, 1963, pp. 165, 166]. As he observes, however, this is not done in practice and the results of Test 3 support the fact that the constraints are not necessary.

The question now arises: How far out from the origin can the reduction be performed and the results still be relatively free from the systematic effects of lens distortions? Charts 16, 17, and 18 give some indication. These are a result of plotting residuals that are computed by subtracting the actual measured coordinates from the adjusted coordinates that were obtained in Test 3. In essence, they demonstrate how lens distortions affect the central projection (mainly radial distortion). One can see radial distortion climbs to magnitudes of 80 microns or more near the outer reaches of the plate. The same picture can be presented analytically.

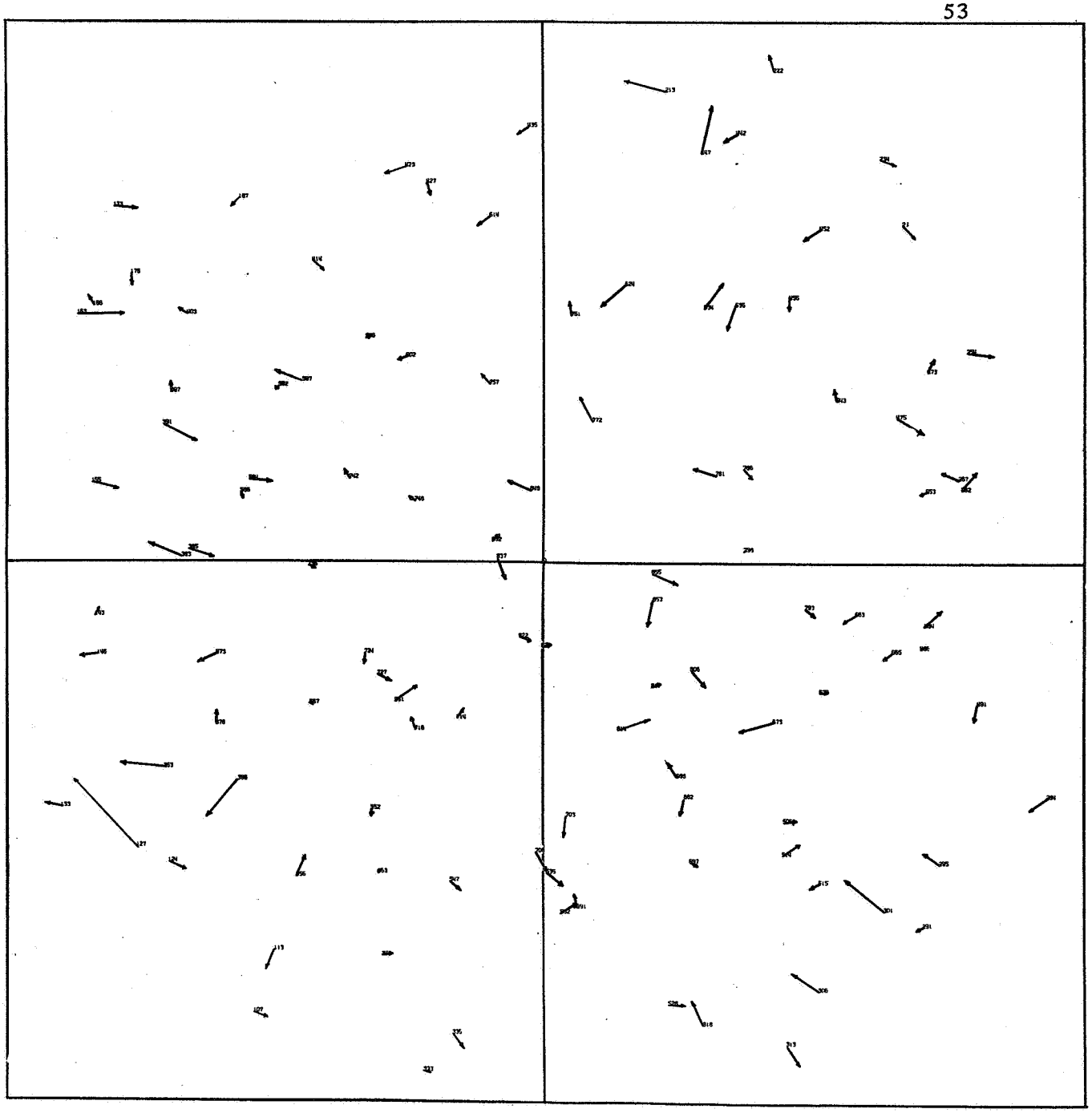

SCALE
0.1 inch = 3 microns = 2 arc seconds

CHART 13: PLATE 2559
TEST 3 RESIDUALS, PROJECTIVE EQUATIONS APPLIED AFTER ALL LENS DISTORTIONS ARE REMOVED FROM MEASURED COORDINATES
Satellite 313 is origin
m_0 = 3.06 microns

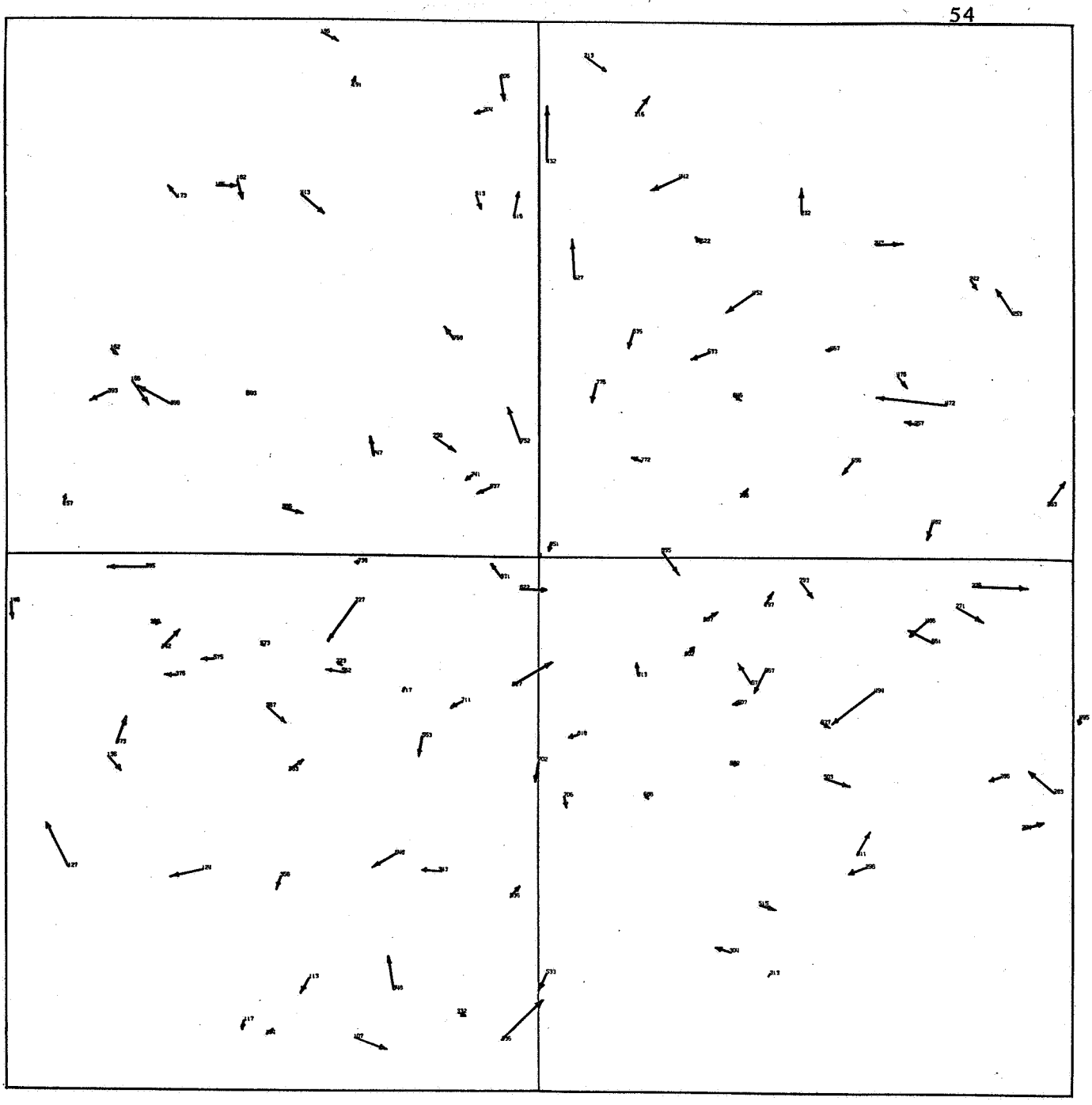

SCALE
0.1 inch = 3 microns = 2 arc seconds

CHART 14: PLATE 5205
TEST 3 RESIDUALS, PROJECTIVE EQUATIONS APPLIED AFTER ALL LENS DISTORTIONS ARE REMOVED FROM MEASURED COORDINATES
Star 851 is origin
m_0 = 3.34 microns

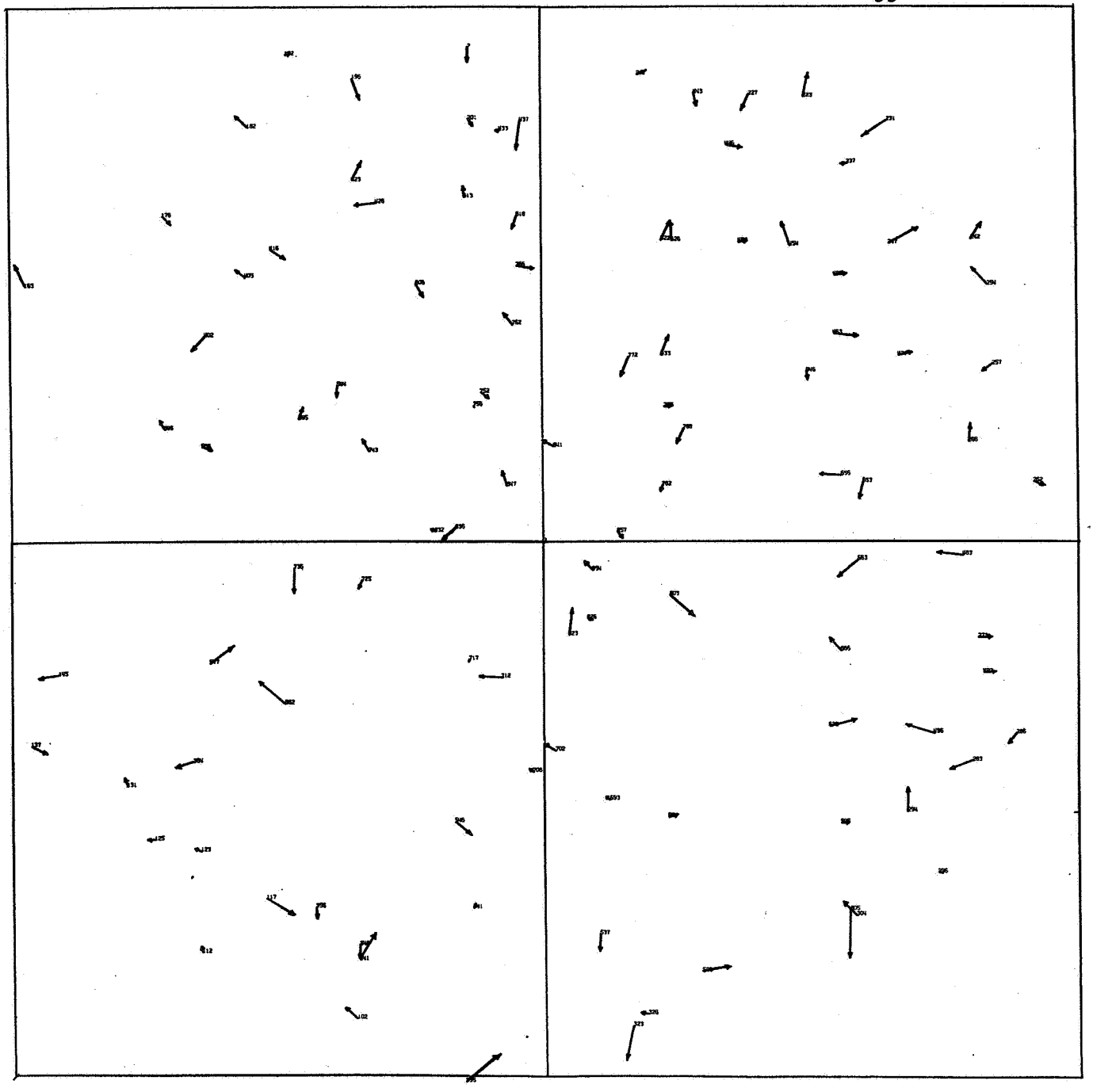

SCALE
0.1 inch = 3 microns = 2 arc seconds

CHART 15: PLATE 6132
TEST 3 RESIDUALS, PROJECTIVE EQUATIONS APPLIED AFTER ALL LENS DISTORTIONS ARE REMOVED FROM MEASURED COORDINATES
Satellite 313 is origin
m_0 = 2.62 microns

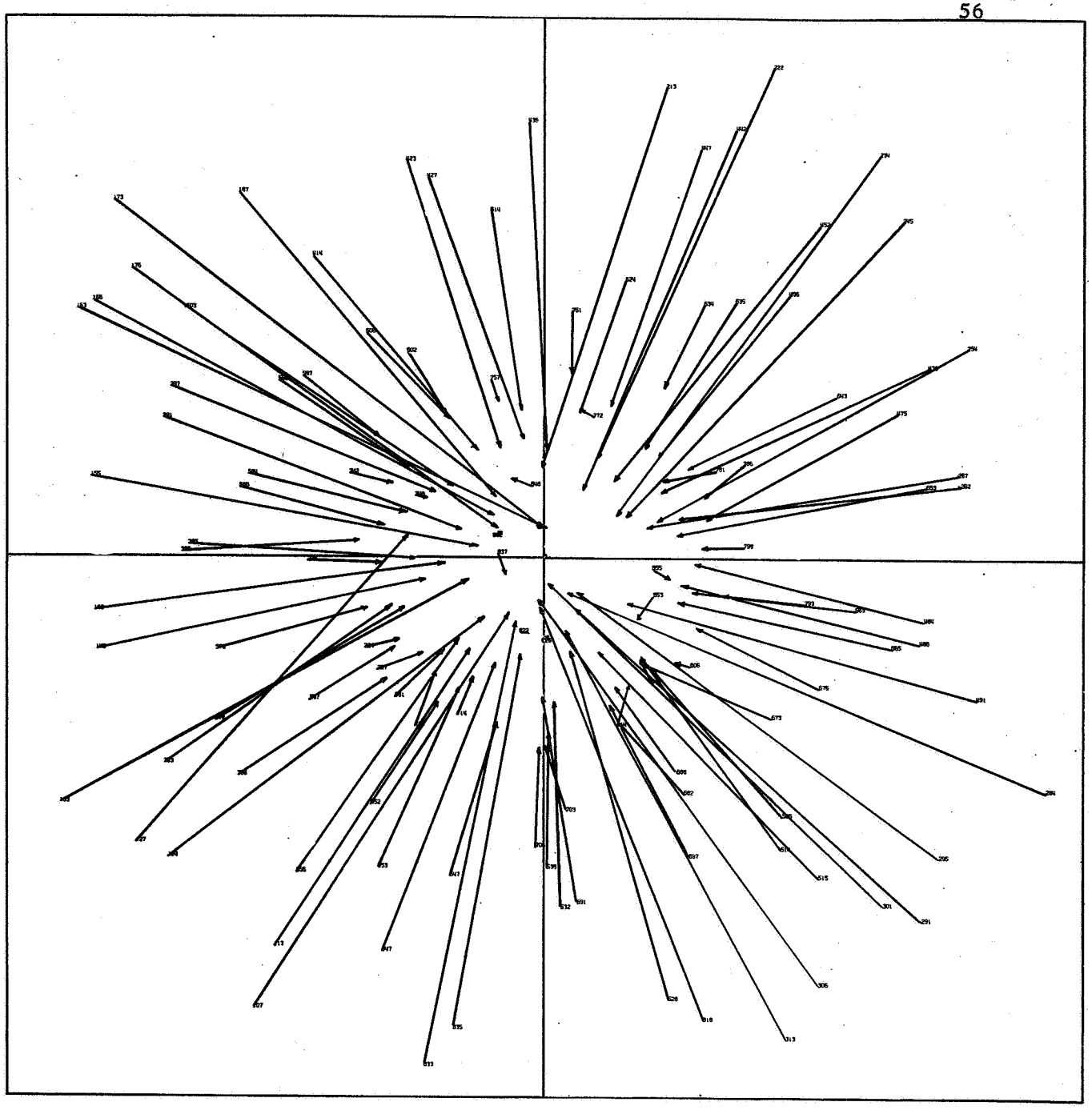

SCALE
0.1 inch = 3 microns = 2 arc seconds

CHART 16: PLATE 2559
DIFFERENCES BETWEEN UNDISTORTED STAR IMAGES AND OBSERVED IMAGES
PLOTTED AS RESIDUALS

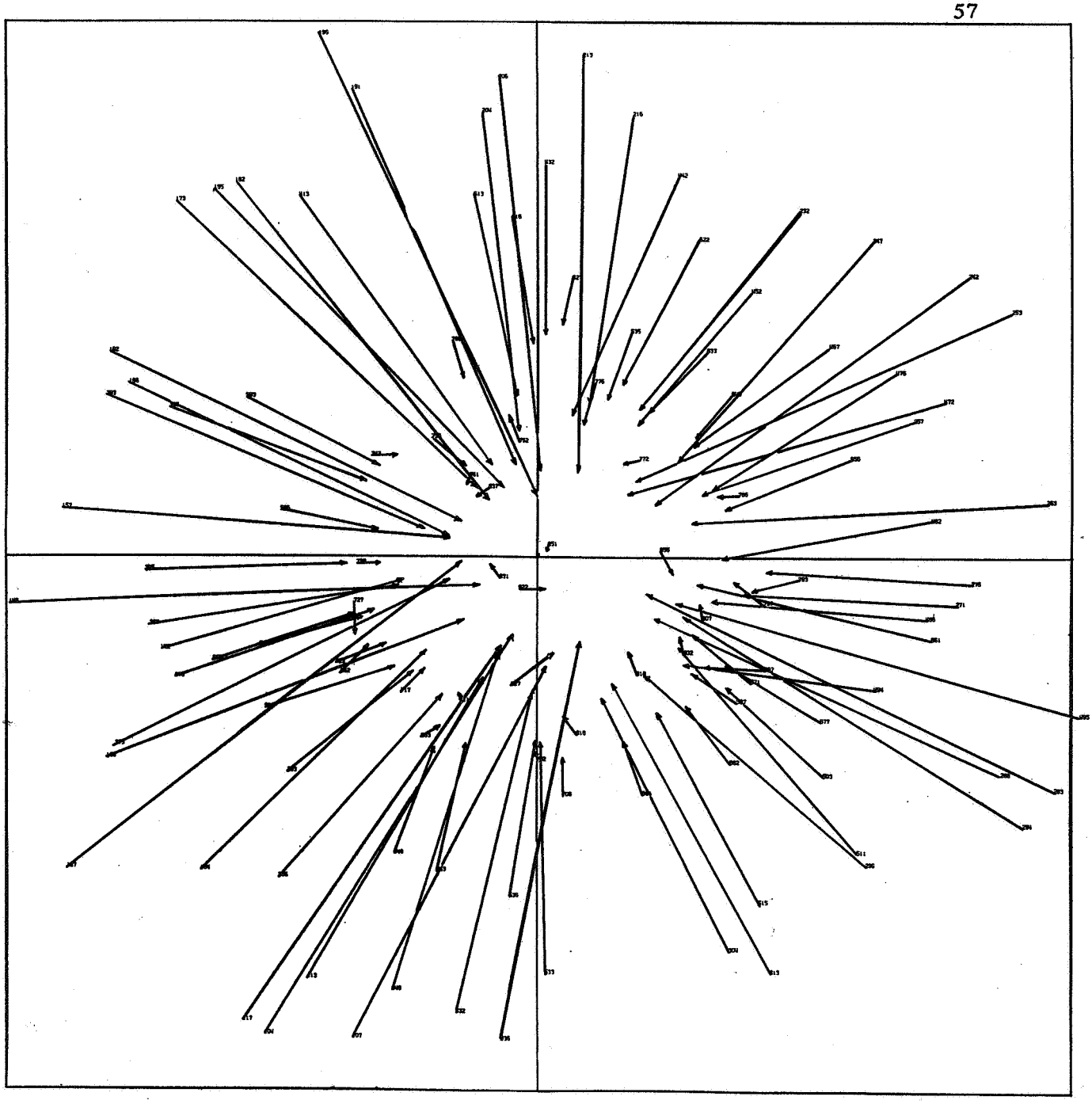

SCALE
0.1 inch = 3 microns = 2 arc seconds

CHART 17: PLATE 5205
DIFFERENCES BETWEEN UNDISTORTED STAR IMAGES
AND OBSERVED IMAGES PLOTTED AS RESIDUALS

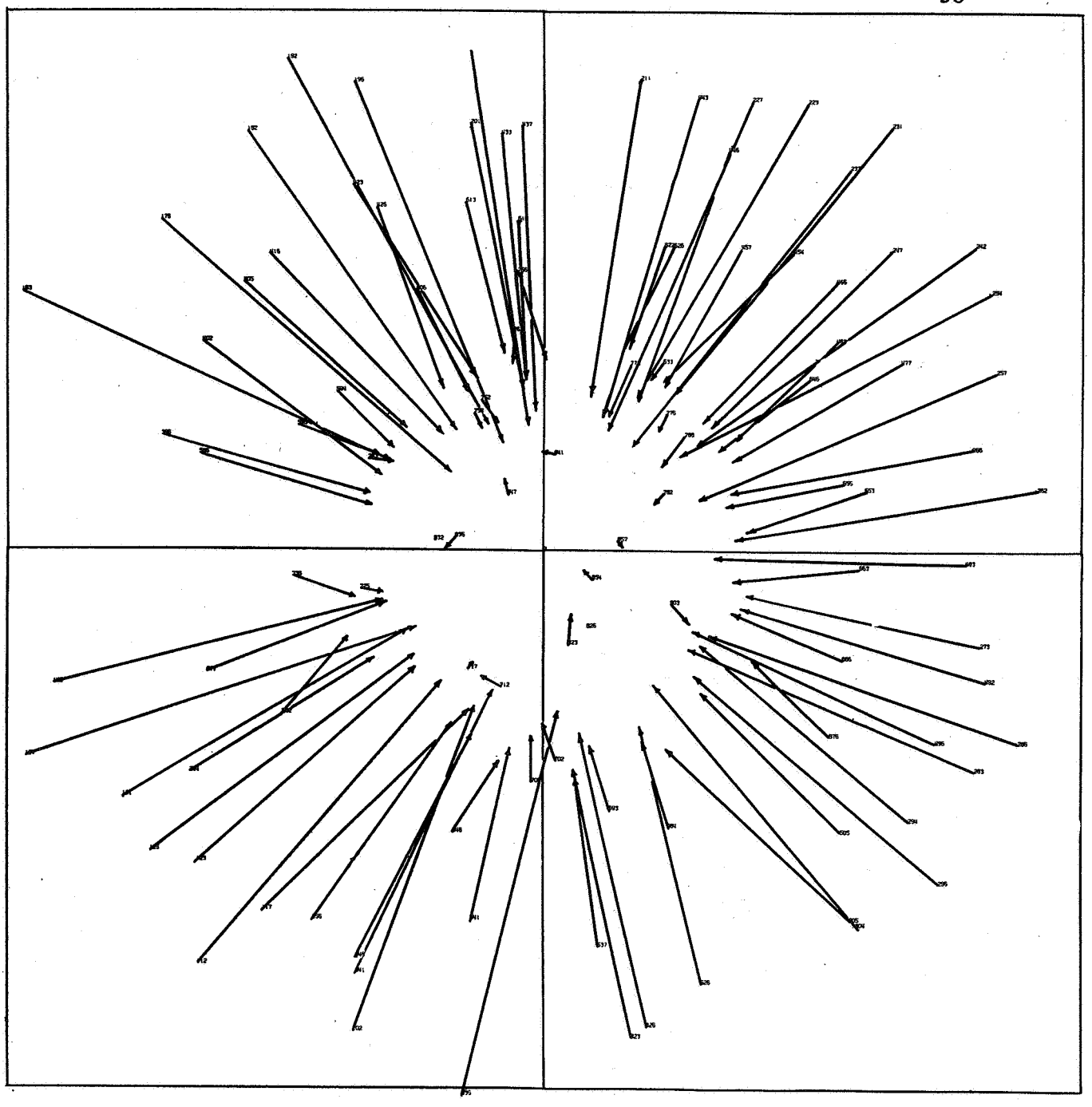

SCALE
0.1 inch = 3 microns = 2 arc seconds

CHART 18: PLATE 6132
DIFFERENCES BETWEEN UNDISTORTED STAR IMAGES
AND OBSERVED IMAGES PLOTTED AS RESIDUALS

Suppose the photogrammetric model is expanded into polynomials in x and y. The final expressions are:

$$
\begin{aligned}
x_B = {} & x - y\,(\epsilon) + x^2\,(3K_4 \cos\varphi_T) + x^3\,(K_1) + x^4\,(3K_5 \cos\varphi_T) + x^5\,(K_2) \\
& + x^7\,(K_3) + xy\,(2K_4 \sin\varphi_T) + xy^2\,(K_1) + xy^3\,(2K_5 \sin\varphi_T) \\
& + xy^4\,(K_2) + xy^6\,(K_3) + x^2y^2\,(4K_5 \cos\varphi_T) + x^3y\,(2K_5 \sin\varphi_T) \\
& + x^3y^2\,(2K_2) + x^3y^4\,(3K_3) + x^5y^2\,(3K_3) + y^2\,(K_4 \cos\varphi_T) \\
& + y^4\,(K_5 \cos\varphi_T), \\
y_B = {} & y + y^2\,(3K_4 \sin\varphi_T) + y^3\,(K_1) + y^4\,(3K_5 \sin\varphi_T) + y^5\,(K_2) + y^7\,(K_3) \\
& + yx\,(2K_4 \cos\varphi_T) + yx^2\,(K_1) + yx^3\,(2K_5 \cos\varphi_T) \\
& + yx^4\,(K_2) + yx^6\,(K_3) + y^2x^2\,(4K_5 \sin\varphi_T) + y^3x\,(2K_5 \cos\varphi_T) \\
& + y^3x^2\,(4K_5 \sin\varphi_T) + y^3x\,(2K_5 \cos\varphi_T) + y^3x^2\,(2K_2) \\
& + y^3x^4\,(3K_3) + y^5x^2\,(3K_3) + x^2\,(K_4 \sin\varphi_T) + x^4\,(K_5 \sin\varphi_T),
\end{aligned}
\tag{4.18}
$$

where x_B and y_B are the measured coordinates as usual and x and y are the undistorted coordinates as in (4.9). Assume that this model exactly describes the physical situation and as such is absolutely rigorous. We know this is not true because it represents only a hypothetical, although apparently a good one, estimate of the true situation not accounting for the multitude of causes that alter the central projection, however insignificant.

From investigation of the previous test, we conclude that equations (4.16) are rigorous (in the sense of (4.18))only so far as an undistorted central projection will permit. Therefore, x_B and y_B on the left-hand side of (4.16) actually compare to x and y in (4.18).

For ease of analysis, assume now that an image is projected, without distortions, onto the x axis. In this case the first equation in (4.18) becomes:

$$x_B = x + x^2 (3K_4 \cos \varphi_T) + x^3 (K_1) + x^4 (3K_5 \cos \varphi_T) + x^5 (K_2) + x^7 (K_3). \qquad (4.19)$$

Considering the discussion in the last paragraph, the error committed by using the projective equations is given by,

$$x^2 (3K_4 \cos \varphi_T) + x^3 (K_1) + x^4 (3K_5 \cos \varphi_T) + x^5 (K_2) + x^7 (K_3). \qquad (4.20)$$

If the parameters of Table 1 are substituted here, it becomes evident that the error is comprised mostly of the $x^3 (K_1)$ term in (4.20), this also being the largest factor in the radial distortion function. On Plate 2559, (4.20) equals roughly 16 microns at a radial distance of 4 centimeters. It is somewhat less on the other two plates. In a reduction this author assumes that maximum radial effects of about 6 or 7 microns could be "randomly" distributed using (4.16). Any residual errors remaining after the reduction would be no greater in magnitude than the expected random plate coordinate error of around 3 microns that the photogrammetric reduction indicates is to be expected (again, assuming model (4.18) is absolute). This leads to the following two tests:

Test 4

On each plate a field of stars 3.4 centimeters in radius from the geometrical center is used; 3.4 centimeters is an arbitrary choice which allows enough stars to be used to have a valid adjustment. Also, at about this distance or somewhat less, the radial distortion effects become

larger than the 6 or 7 micron limit just imposed. The residual plots are shown in Charts 19, 20, and 21. The decreased magnitude of the residuals and the low standard errors of unit weight are testimony that the projective equations are applicable in this area without pre-correcting the measured coordinates for lens distortions.

Test 5

To prove that the area used in Test 4 should not be exceeded when applying the projective equations without pre-corrections, stars out to 4 centimeters are used in the reduction. Residual plots are shown in Charts 22, 23, and 24. Four centimeters is used so that enough additional stars lying beyond 3.4 centimeters can be employed to incorporate the larger radial distortion effects that the analysis above shows exist at this distance. The plotted residuals are generally larger than in the last test and the standard errors of unit weight prove this.

It must be remembered that each camera will have its own distortion characteristics. Therefore, the projective equations cannot be applied equally well for the same areas on different plates. However, general conclusions will be given in Section 6.

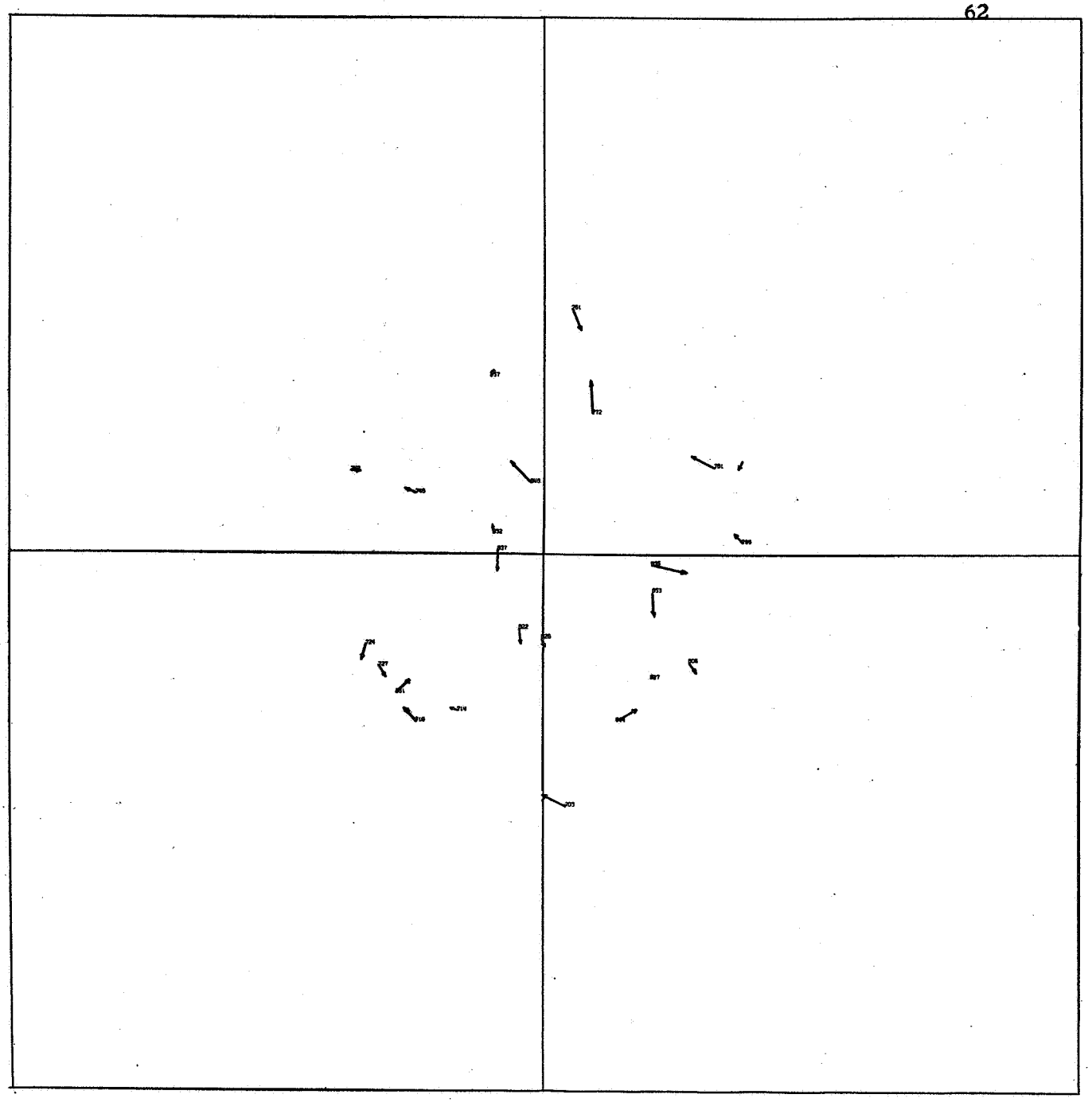

SCALE
0.1 inch = 3 microns = 2 arc seconds

CHART 19: PLATE 2559
TEST 4 RESIDUALS, PROJECTIVE EQUATIONS APPLIED TO STARS
WITHIN 3.4 CENTIMETERS OF THE PLATE CENTER
Satellite 313 is origin
m_0 = 2.82 microns

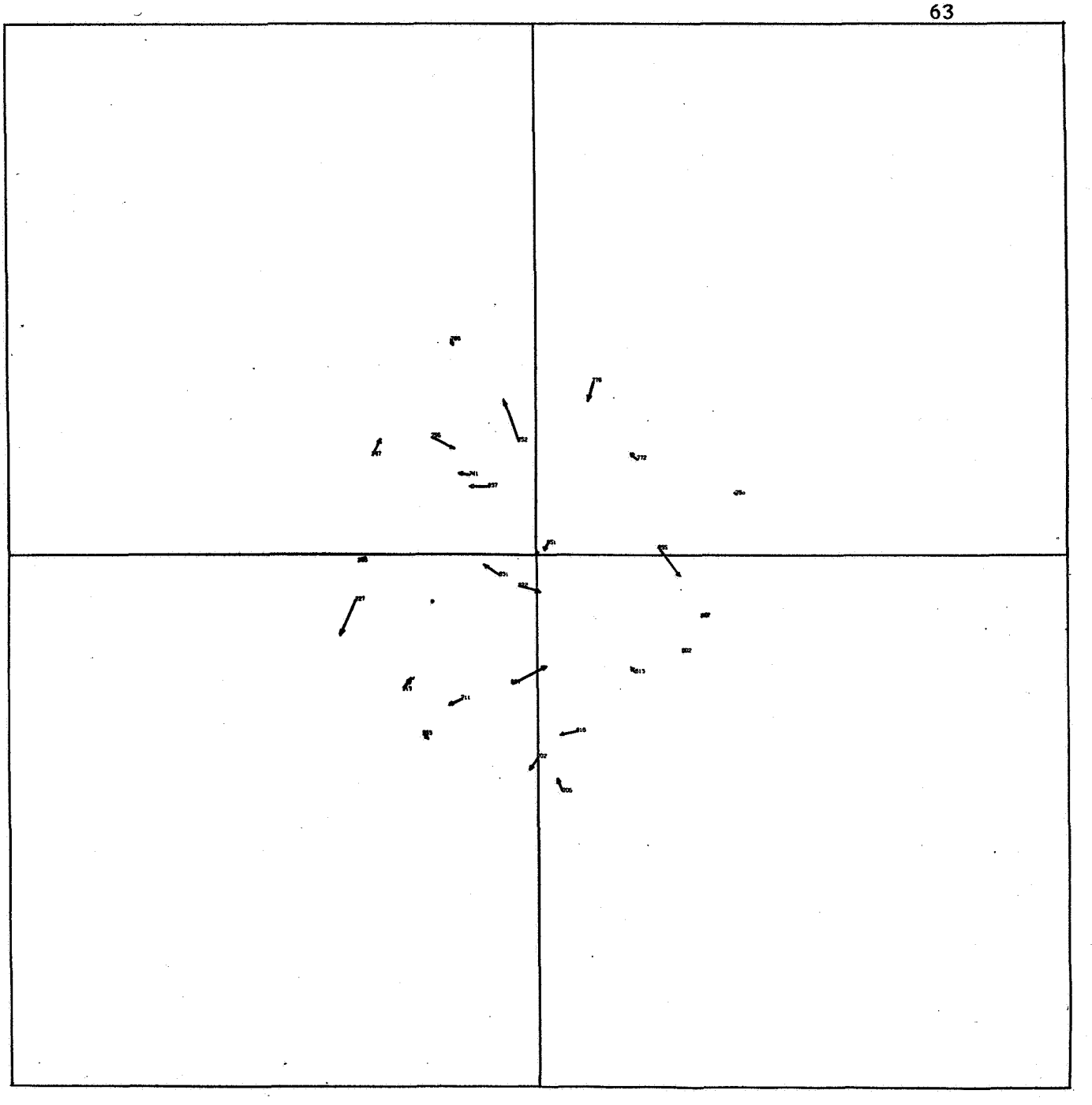

SCALE
0.1 inch = 3 microns = 2 arc seconds

CHART 20: PLATE 5205
TEST 4 RESIDUALS, PROJECTIVE EQUATIONS APPLIED TO STARS
WITHIN 3.4 CENTIMETERS OF THE PLATE CENTER
Star 851 is origin
m_0 = 2.96 microns

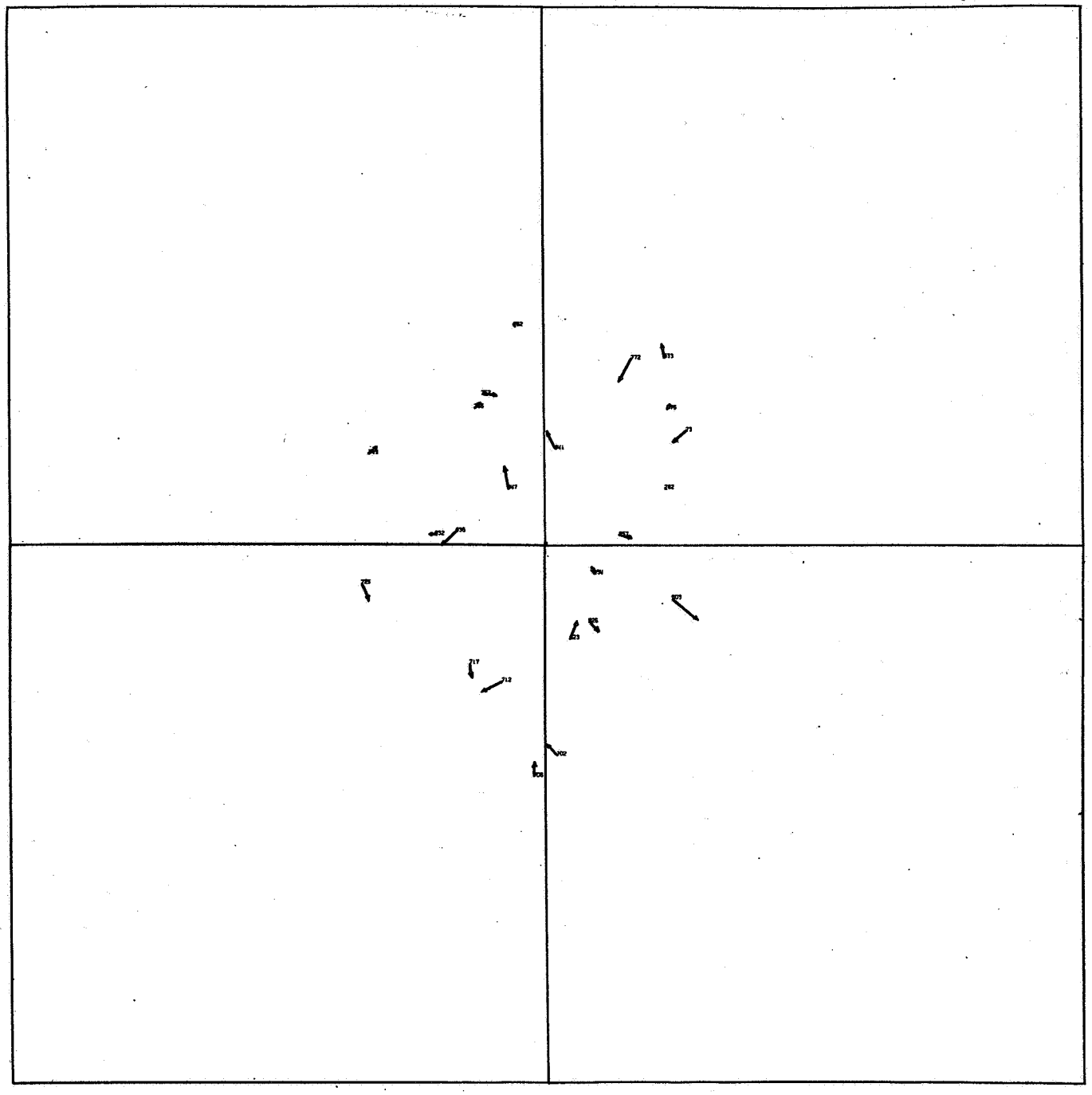

CHART 21: PLATE 6132

SCALE
0.1 inch = 3 microns = 2 arc seconds

TEST 4 RESIDUALS, PROJECTIVE EQUATIONS APPLIED TO STARS
WITHIN 3.4 CENTIMETERS OF THE PLATE CENTER
Satellite 313 is origin
m_0 = 2.37 microns

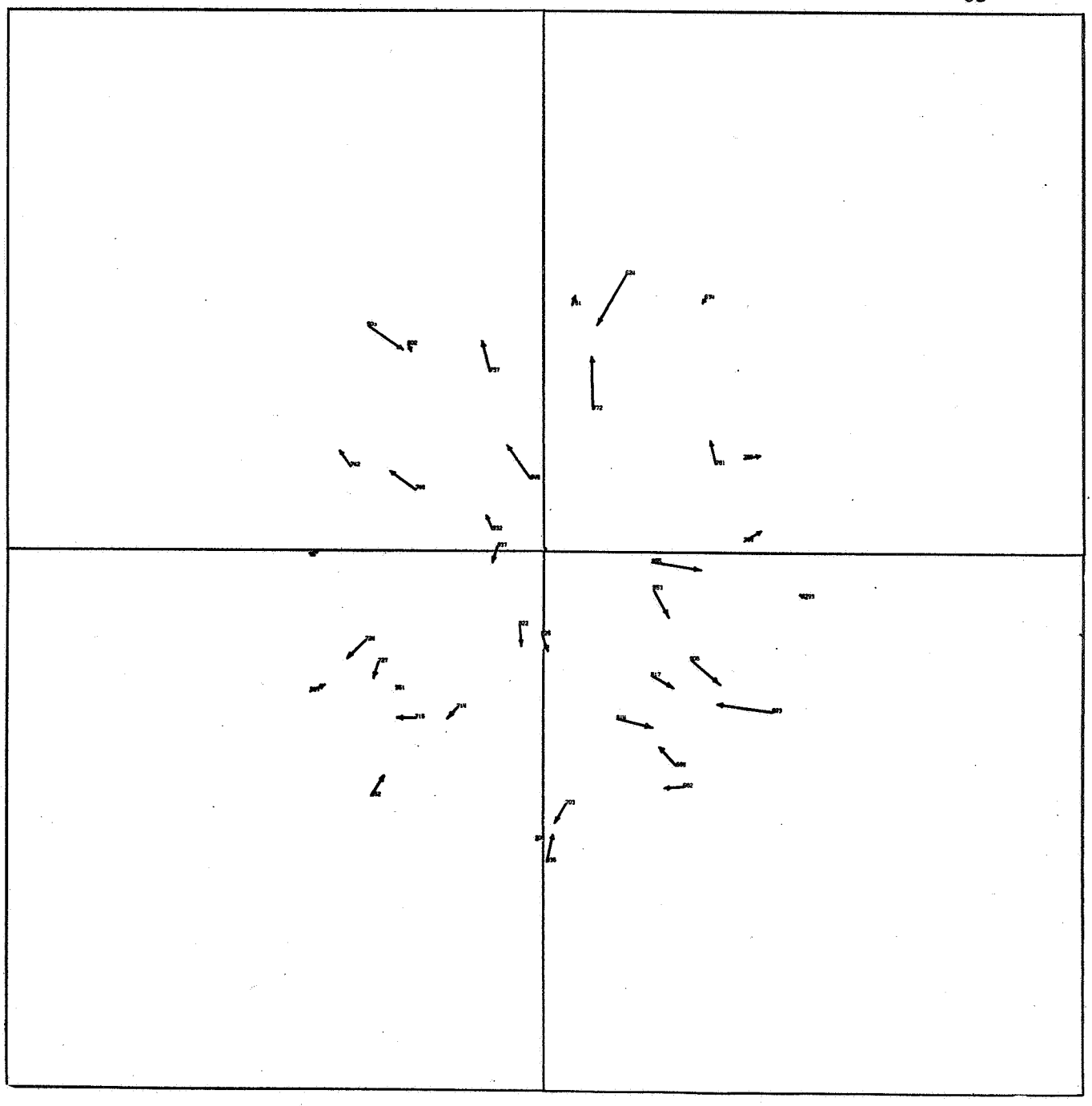

SCALE
0.1 inch = 3 microns = 2 arc seconds

CHART 22: PLATE 2559
TEST 5 RESIDUALS, PROJECTIVE EQUATIONS APPLIED TO STARS
WITHIN 4 CENTIMETERS OF THE PLATE CENTER
Satellite 313 is origin
m_0 = 3.96 microns

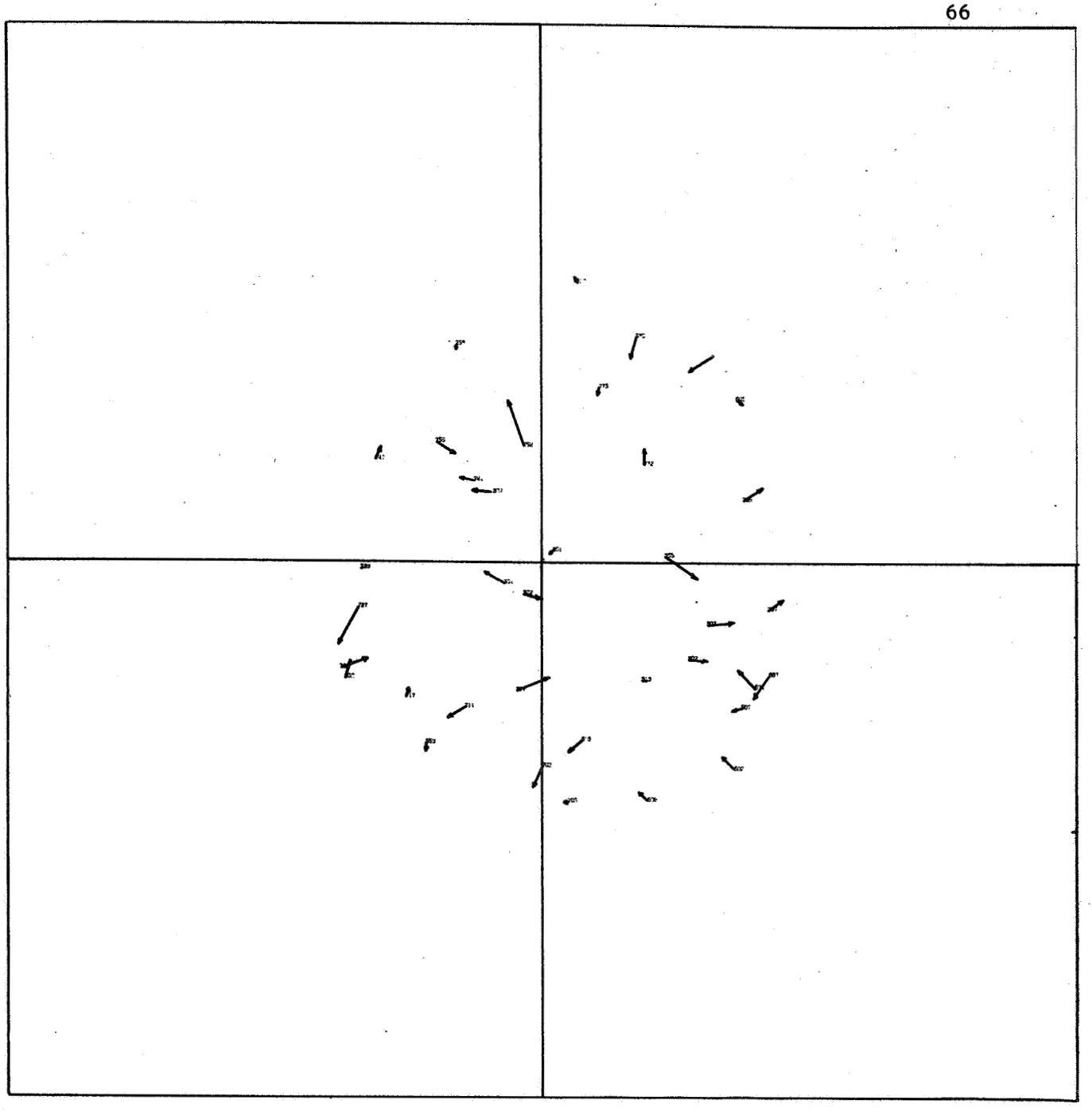

SCALE
0.1 inch = 3 microns = 2 arc seconds

CHART 23: PLATE 5205
TEST 5 RESIDUALS, PROJECTIVE EQUATIONS APPLIED TO STARS
WITHIN 4 CENTIMETERS OF THE PLATE CENTER
Star 851 is origin
m_0 = 3.08 microns

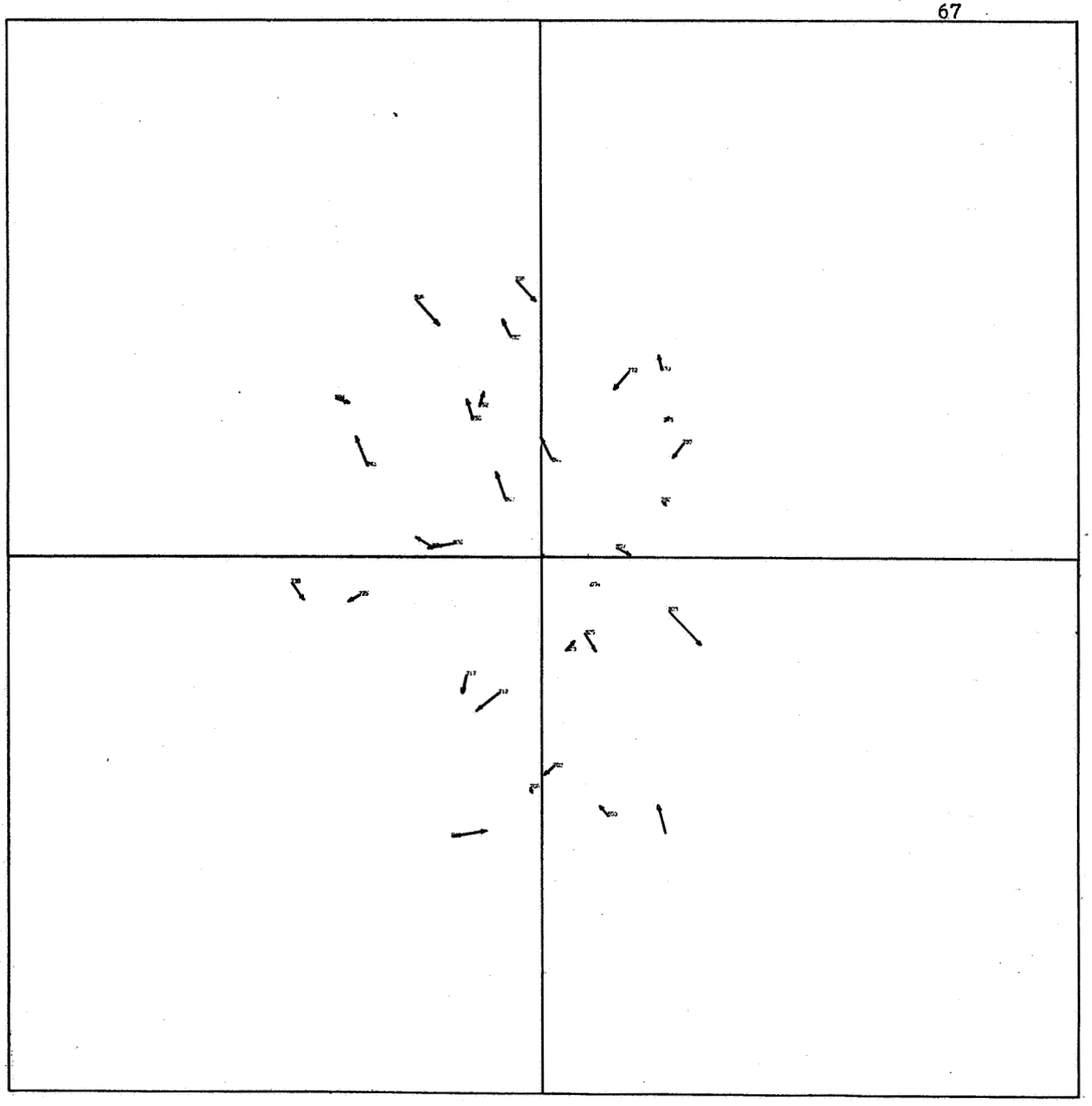

SCALE
0.1 inch = 3 microns = 2 arc seconds

CHART 24: PLATE 6132
TEST 5 RESIDUALS, PROJECTIVE EQUATIONS APPLIED TO STARS
WITHIN 4 CENTIMETERS OF THE PLATE CENTER
Satellite 313 is origin
m_0 = 3.24 microns

4.4.3 Models 2 and 5: The "Long" Turner's Method.--If the denominator is divided into the numerator in the projective equations, a polynomial occurs in ξ and η . Truncation of the polynomial results in Models 2 and 5 which are given by:

Model 2,

$$\begin{aligned} x_B &= A + B\xi + C\eta + D\xi^2 + E\xi\eta + F\eta^2 + G\xi^3 + H\xi^2\eta \\ &\quad + P\xi\eta^2 + Q\eta^3, \\ y_B &= A' + B'\xi + C'\eta + D'\xi^2 + E'\xi\eta + F'\eta^2 + G'\xi^3 \\ &\quad + H'\xi^2\eta + P'\xi\eta^2 + Q'\eta^3; \end{aligned} \tag{4.21}$$

Model 5

$$\begin{aligned} \xi &= A + Bx_B + Cy_B + Dx_B^2 + Ex_By_B + Fy_B^2 + Gx_B^3 \\ &\quad + Hx_B^2y_B + Px_By_B^2 + Qy_B^3, \\ \eta &= A' + B'x_B + C'y_B + D'x_B^2 + E'x_By_B + F'y_B^2 \\ &\quad + G'x_B^3 + H'x_B^2y_B + P'x_By_B^2 + Q'y_B^3. \end{aligned} \tag{4.22}$$

Model 5 is the same as Model 2, only the roles of x_B, y_B and ξ , η have been reversed. Model 2 is used to obtain a plot of the plate coordinate residuals. Model 5 is used to obtain directions for the satellite since this would be impossible using Model 2. Model 5 is the form that would be used in practice although ξ and η must be regarded as the observed quantities unless another adjustment technique is used.

The formulation of these models is attributed to H. H. Turner [Turner, 1893]. Podobed and Smart elaborate on the purpose of including the various linear and higher order terms. The linear part of the transformation (this will comprise Model 3) is required by non-coincidence of

the standard coordinate origin and the plate coordinate origin (selection of the same image for both origins should reduce this), the rotation of the two systems with respect to each other, the angle between the plate coordinate axes not equal to 90 degrees, and scales being different along the plate coordinate axes. These errors are partly a result of the orientation of the plate in the comparator and of the comparator itself [Podobed, 1965, pp. 184, 185], [Smart, 1962, pp. 289-291]. The second order terms are necessary because the optical axis is not perpendicular to the plane of the plate [Podobed, 1965, pp. 184, 185], [Smart, 1962, p. 291]. If the stars have not been updated for annual aberration and refraction as is the usual case in astronomy, the linear plus second order terms also allow for differential aberration and refraction effects. Although not intended in the original formulation, the higher order terms will also absorb some of the lens distortion effects [Berbert, et. al., 1962]. This can be shown by comparing (4.22) to (4.18) and making a term-wise analysis.

How many higher order terms are employed in equations of the form of (4.21) and (4.22) is a function of the angular field and the camera being used. Since the "long" Turner's method is actually an expansion of the projective equations, one might wonder why the projective equations are not used more in practice or used exclusively since any Turner's method is a truncation of this expansion. The answer is in the fact that the projective equations employ only eight unknowns. Therefore, the coefficients in the polynomial that result from the expansion are constrained. But if these constraints are lifted, then equations of the form of (4.21) and (4.22) result having 20 unique unknowns that are free

to absorb effects of lens distortions and any other effects not specifically modeled [Brown, 1966, p. 35]. This point will become apparent in the results obtained with (4.21) and (4.22).

For reduction of the Minitrack astrographic plates (MOTS), NASA developed equations of the form [Berbert, et al., 1962]:

$$\xi = A + Bx_B + Cy_B + Dx_By_B + Ex_B^2 + Fx_B(x_B^2 + y_B^2),$$
$$\eta = A' + B'x_B + C'y_B + D'x_By_B + E'y_B^2 + F'y_B(x_B^2 + y_B^2). \tag{4.23}$$

The field covered was 11 degrees by 14 degrees. Duane Brown shows that additional terms must be added to (4.23) if the astrometric method is to be used for GEOS application [Brown, 1966]. He finally trims his equations to those given as (4.21) and (4.22) with the recommendation that the following steps be taken before application [Brown, 1966, p. 47]:

A. The plate coordinates should be corrected for lens distortions prior to reduction.

B. Stellar coordinates should be corrected for astronomical refreaction.

Several items must be observed at this point: (1) Brown is discussing the Minitrack system and not a BC-4 camera; (2) recommendation B has been followed by the author but not A. However, the author feels that no more terms should be included in (4.22) even if lens distortion corrections are not made prior to reduction. This model has 20 unknowns already and any more make it less economical than the photogrammetric reduction. Moreover, if the plate coordinates are to be corrected for

lens distortions prior to reduction, the projective equations would be a better choice judging from the results obtained in Section 4.4.2.

Charts 25, 26, and 27 show the residual plots when applying (4.21) to the entire plate area. These plots are approaching in randomness and magnitude the residuals of the photogrammetric reduction. The charts also give standard errors of unit weight, which are higher than desired, and the coordinate origins used. Table 5 gives the differences between the ESSA satellite directions and the satellite directions obtained using equation (4.22).

When different images are used as coordinate origins, the residuals and satellite directions differ slightly each time but these differences are insignificant. This was found to be the case when NASA experimented with (4.23). In that examination it was noticed that the origin could be shifted several centimeters and its right ascension and declination varied by more than a degree without affecting the final results [Berbert, et. al., 1962]. This is most likely due to the inclusion of the second order terms.

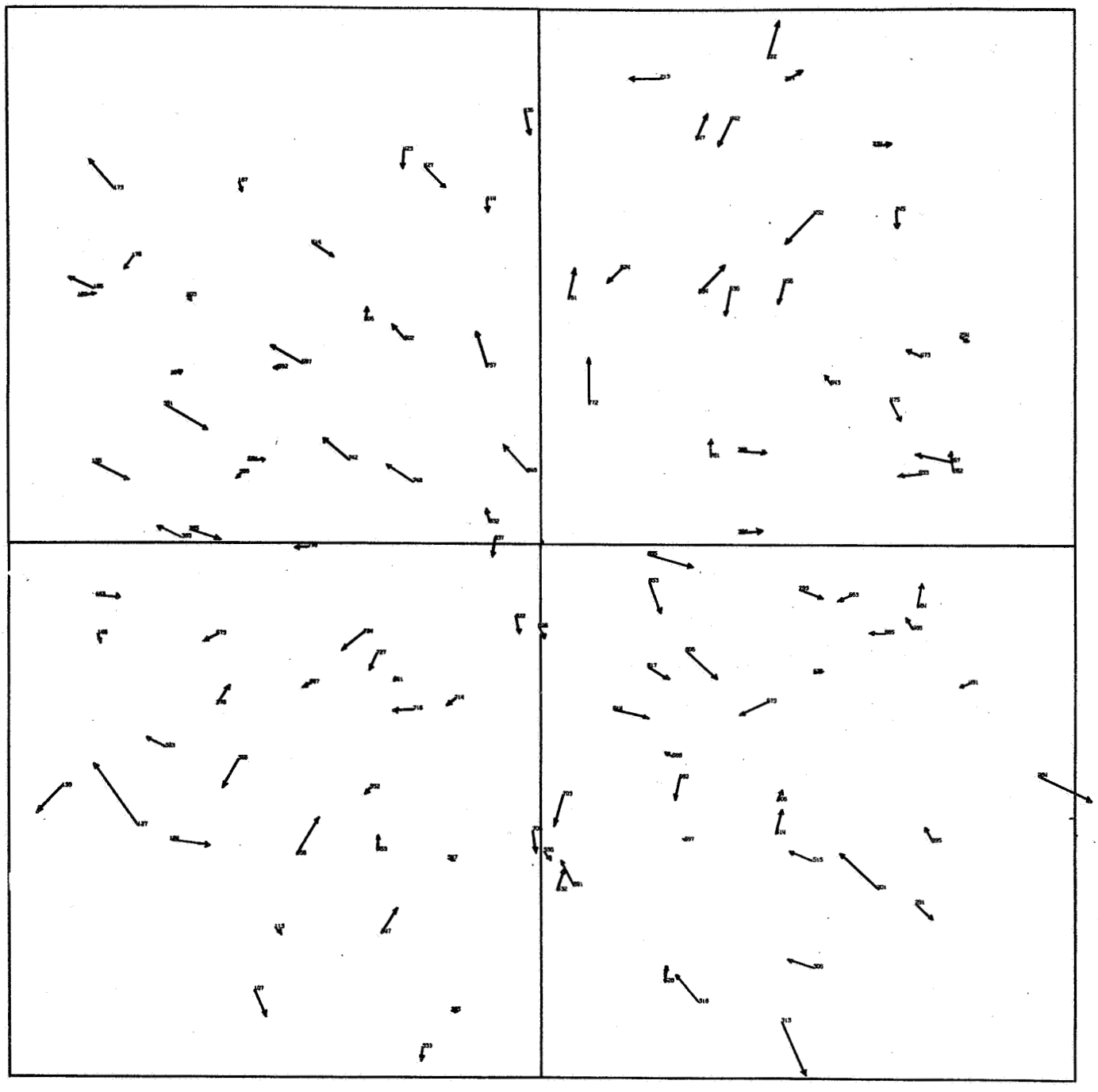

SCALE
0.1 inch = 3 microns = 2 arc seconds

CHART 25: PLATE 2559
RESIDUALS AFTER REDUCTION WITH THE LONG TURNER'S METHOD
Satellite 313 and Star 837 used as origins with
comparable results
m_0 = 3.80 microns

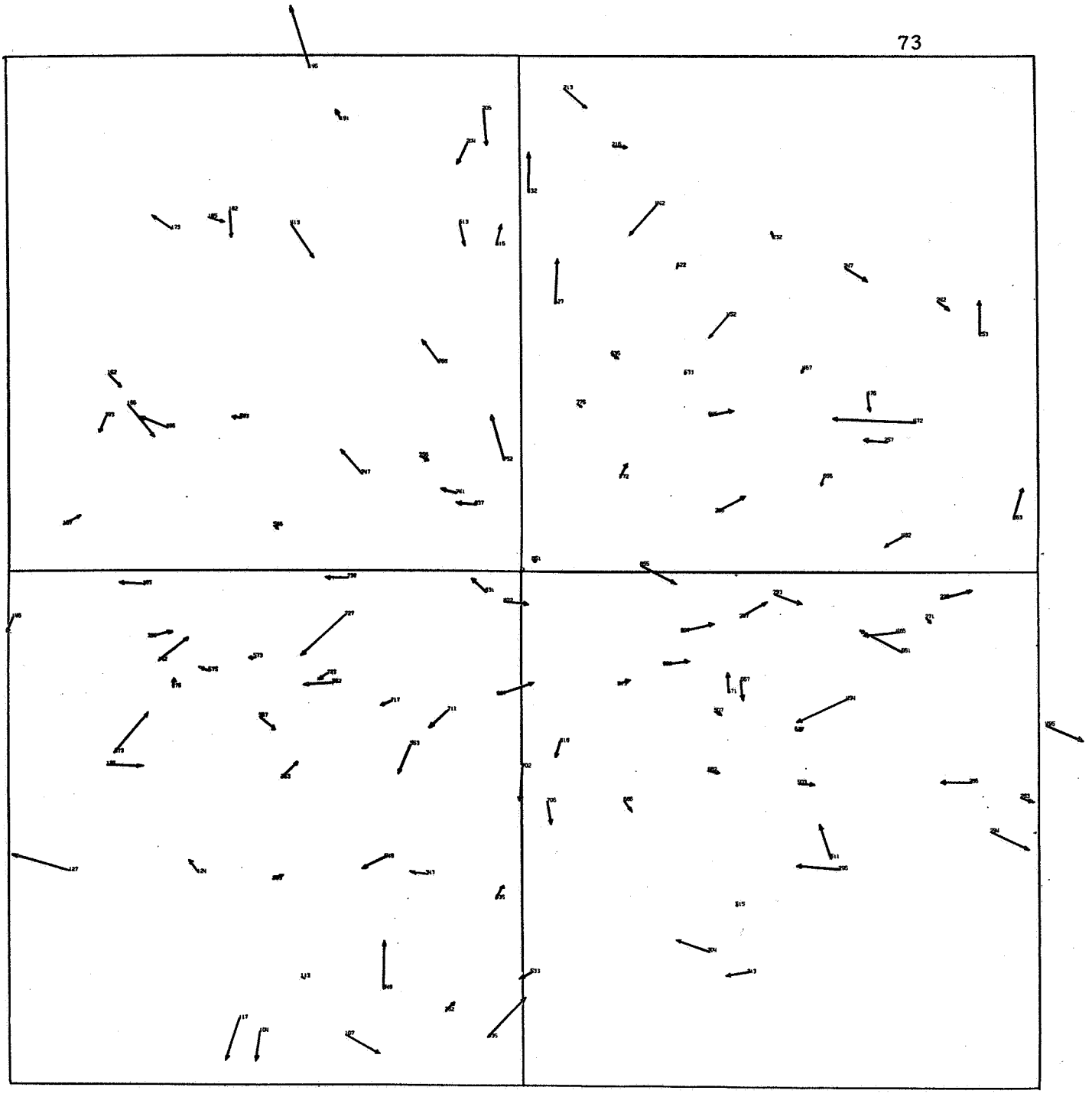

SCALE
0.1 inch = 3 microns = 2 arc seconds

CHART 26: PLATE 5205
RESIDUALS AFTER REDUCTION WITH THE LONG TURNER'S METHOD
Star 851 is origin
m_0 = 4.19 microns

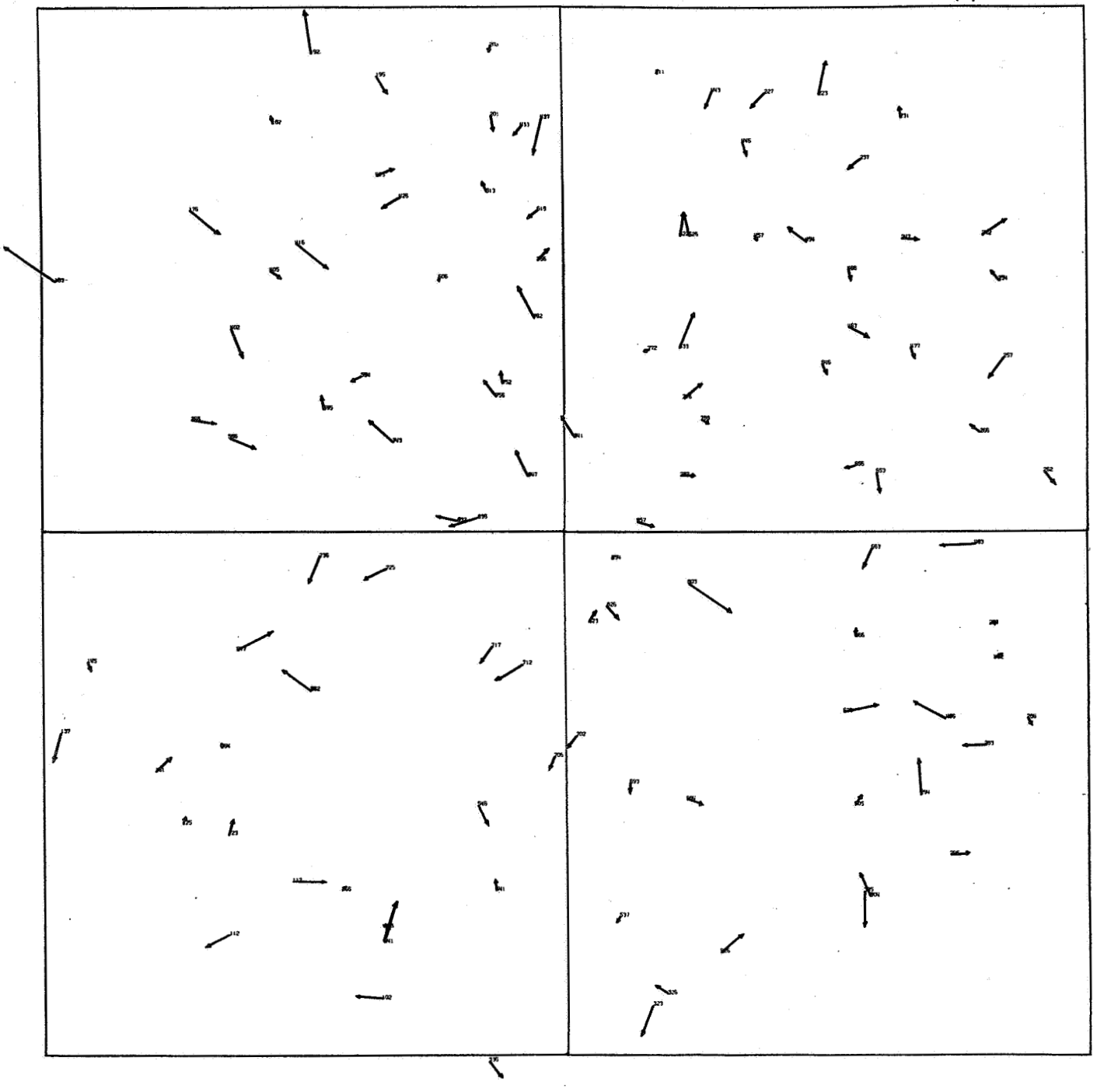

SCALE
0.1 inch = 3 microns = 2 arc seconds

CHART 27: PLATE 6132
RESIDUALS AFTER REDUCTION WITH THE LONG TURNER'S METHOD
Satellite 313 and Star 854 used as origins
with comparable results
m_0 = 3.39 microns

Table 5

ALL PLATES

Differences of Model 5 Interpolated Positions from ESSA Positions for 21 Satellite Images Computed in "Fictitious Observed" Equatorial System

	RA (ESSA-Model 5)			DEC		
No.	2559	5205	6132	2559	5205	6132
	^{s}	^{s}	^{s}	$''$	$''$	$''$
126	0.288	0.070	-0.218	-0.59	-0.54	0.06
143	0.323	0.132	-0.259	-0.67	0.21	-0.04
161	0.347	0.180	-0.290	-0.72	0.86	-0.10
179	0.356	0.208	-0.308	-0.74	1.34	-0.13
201	0.346	0.220	-0.311	-0.70	1.64	-0.10
219	0.320	0.212	-0.298	-0.64	1.68	-0.04
239	0.273	0.193	-0.266	-0.56	1.54	0.04
258	0.215	0.167	-0.224	-0.48	1.26	0.12
281	0.125	0.132	-0.156	-0.38	0.78	0.23
299	0.046	0.101	-0.094	-0.31	0.34	0.30
313	-0.017	0.079	-0.043	-0.26	-0.01	0.35
330	-0.097	0.053	0.022	-0.23	-0.44	0.40
350	-0.187	0.027	0.096	-0.21	-0.90	0.44
368	-0.262	0.006	0.158	-0.22	-1.26	0.45
387	-0.329	-0.009	0.216	-0.25	-1.53	0.46
403	-0.372	-0.019	0.256	-0.30	-1.66	0.45
414	-0.395	-0.023	0.277	-0.33	-1.70	0.45
434	-0.416	-0.025	0.299	-0.40	-1.61	0.45
452	-0.411	-0.020	0.299	-0.45	-1.37	0.48
473	-0.376	-0.008	0.276	-0.50	-0.89	0.53
494	-0.308	0.008	0.225	-0.50	-0.27	0.64
	^{s}	^{s}	^{s}	$''$	$''$	$''$
	0.276	0.090	0.219	0.45	1.04	0.30 *
	-0.025	0.080	-0.016	-0.45	-0.12	0.26 **

*Mean absolute difference
**Mean difference

4.4.4. Model 3: The"Short" Turner's Method.--If the linear terms are retained in equation (4.21) and the higher order terms dropped, Model 3 results, which is given by,

$$x_B = A\xi + B\eta + C,$$
$$y_B = D\xi + E\eta + F. \qquad (4.24)$$

Satellite directions can be computed by,

$$\xi = \frac{By_B - Ex_B + (CE - BF)}{(BD - AE)},$$
$$\eta = \frac{Dx_B - Ay_B + (AF - CD)}{(BD - AE)}. \qquad (4.25)$$

This model has probably been used more than any other by astronomers since Turner first introduced the idea. Its historical application has been limited to areas near the optical axis on very long focal length cameras. (The author's application of (4.24) to the entire plate produces disastrous results not given here.) As discussed in the preceding section, the affine transformation in (4.24) allows for differences in scale in different directions, non-coincidence of the origins of the two coordinate systems, non-perpendicularity of the plate coordinate axes and a rotation of one system with respect to the other. The use of (4.24) implies that the photographic plane is parallel to the tangent plane on the celestial sphere. It is therefore suggested that choice of the point of tangency is critical.

To find the area where (4.24) may be applied with good results, the following empirical approach is taken. Assume that Model 2 is rigorous (the results of the last section allow this assumption). If the

significant terms are kept in (4.21) after the adjustment, the following equations define the transformations on each plate:

Plate 2559

$$\begin{aligned} x_B &= 0.28\xi - 0.11\eta + 0.00087\xi^2 - 0.0029\xi\eta + 0.0011\eta^2, \\ y_B &= 0.11\xi + 0.28\eta + 0.00029\xi^2 - 0.00019\xi\eta - 0.0026\eta^2; \end{aligned} \tag{4.26}$$

Plate 5205

$$\begin{aligned} x_B &= 0.03\xi - 0.049\eta + 0.0020\xi^2 + 0.0012\xi\eta - 0.00028\eta^2, \\ y_B &= 0.049\xi - 0.30\eta + 0.00038\xi^2 + 0.0023\xi\eta + 0.0015\eta^2; \end{aligned} \tag{4.27}$$

Plate 6132

$$\begin{aligned} x_B &= 0.046\xi - 0.30\eta - 0.00019\xi^2 + 0.00089\xi\eta + 0.0010\eta^2, \\ y_B &= 0.30\xi + 0.046\eta - 0.0010\xi^2 - 0.0011\xi\eta - 0.00017\eta^2. \end{aligned} \tag{4.28}$$

In a preliminary adjustment using Model 3 and stars in a confined area of radius about 2.5 centimeters, the following empirical relationships are found (disregarding the translation term):

Plate 2559

$$\begin{aligned} x_B &= 0.28\xi - 0.11\eta, \\ y_B &= 0.11\xi + 0.28\eta; \end{aligned} \tag{4.29}$$

Plate 5205

$$\begin{aligned} x_B &= 0.30\xi - 0.049\eta, \\ y_B &= 0.049\xi - 0.30\eta; \end{aligned} \tag{4.30}$$

Plate 6132

$$\begin{aligned} x_B &= 0.046\xi - 0.30\eta, \\ y_B &= 0.30\xi + 0.046\eta. \end{aligned} \tag{4.31}$$

It is evident that the maximum magnitude of the neglected terms is on the order of 0.0029 $\xi\ \eta$ for Plate 2559, 0.0023 $\xi\ \eta$ for Plate 5205, and 0.0011 $\xi\ \eta$ for Plate 6132. If the error committed in using Model 3 is to be less than 3 microns, the usable area appears to have a radius of about 1.5 centimeters for Plate 2559, 1.7 centimeters for Plate 5205, and 2.2 centimeters for Plate 6132. These figures are arrived at by letting ξ equal η and setting the maximum error terms given above equal to 3 microns. The resulting equations are solved for ξ and η and multiplied by the focal length to get ξ and η in the scale of the photograph. Since ξ equals η, either one times $\sqrt{2}$ gives the radial distance from the origin. By examining (4.26) through (4.28) one can see that it is possible to go out farther from the origin in certain directions but that the above procedure gives the largest radial distance where the error should be minimal in all directions.

Test 1

Certain stars in a reduced area around the plate center are selected on each plate for the reduction. Initially the best origins (Origin 1) available are used. That is, satellite 313 on 2559 and 6132, and star 851 on 5205. Then, star 837 is used as the origin on 2559 and star 854 on 6132 (Origin 2). There is a remarkable difference in results. The reason for this is attributed to the fact that with Model 3, any choice of origin that is obviously more than a differential distance from the true optical center establishes a tangent plane on the celestial sphere that is appreciably not parallel to the photographic plane. The planes theoretically

should be parallel. The radii for the reduced areas are as follows: Plate 2559, 2.8 centimeters; Plate 5205, 2.8 centimeters; Plate 6132, 2.2 centimeters.

The results for Plate 6132 are acceptable (with Origin 1). In fact, it had been predicted for this plate that stars out to 2.2 centimeters could be used without introducing appreciable error in the results. The other two plates exhibit bad results as expected. Charts 28, 29, and 30 show the residuals for Test 1 using the best available origins. Charts 31 and 32 are the result of changing origins on Plates 2559 and 6132. The standard errors of unit weight are also given on the charts.

Test 2

Stars as close as possible to the plate center are selected for the reduction. Charts 33, 34, and 35 show the residual plots. The results for Plate 5205 are not very encouraging. It would seem that in limiting the plate area, the resulting limitation on the number of star images available hampers the ability of the reduction to leave only random errors in the adjusted plate coordinates.

Differences of the satellite directions from those of ESSA are given in Table 6. There is a noticeable systematic difference between the ESSA results and the Model 3 results.

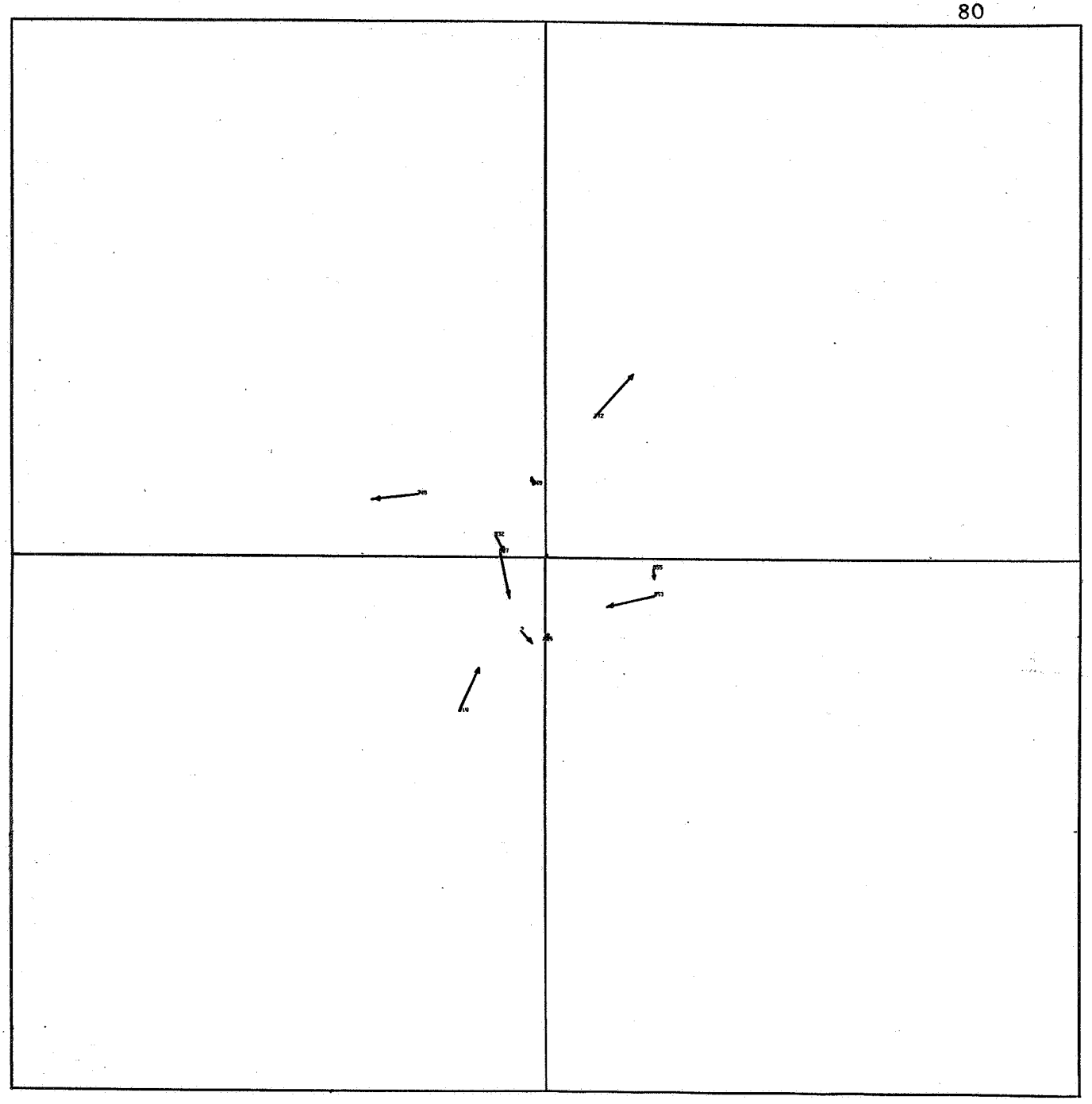

SCALE
0.1 inch = 3 microns = 2 arc seconds

CHART 28: PLATE 2559
TEST 1 RESIDUALS, SHORT TURNER'S METHOD APPLIED TO STARS
WITHIN 2.8 CENTIMETERS OF THE PLATE CENTER
Satellite 313 is origin
m_0 = 5.80 microns

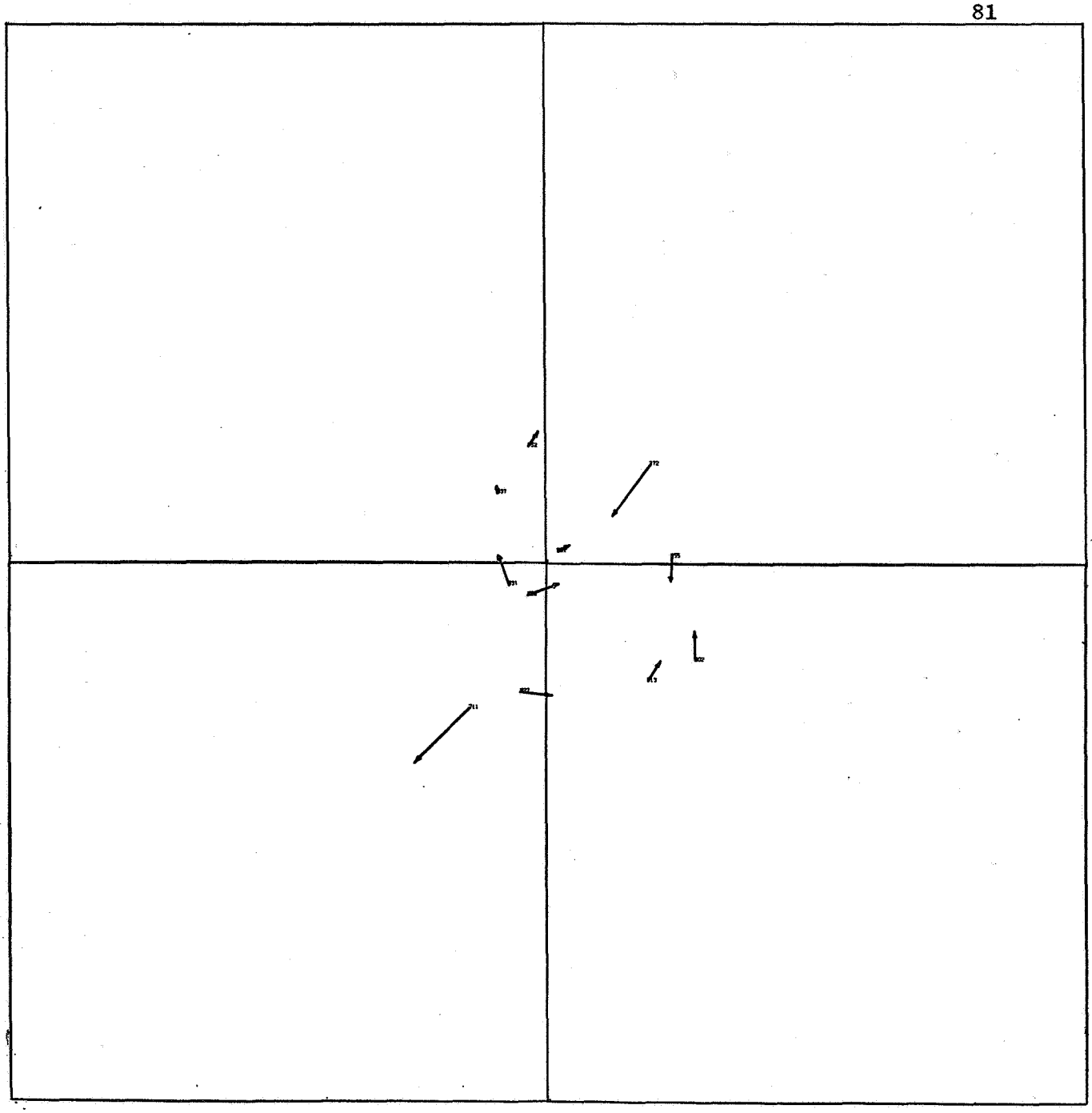

SCALE
0.1 inch = 3 microns = 2 arc seconds

CHART 29: PLATE 5205
TEST 1 RESIDUALS, SHORT TURNER'S METHOD APPLIED TO STARS
WITHIN 2.8 CENTIMETERS OF THE PLATE CENTER
Star 851 is the origin
m_0 = 5.56 microns

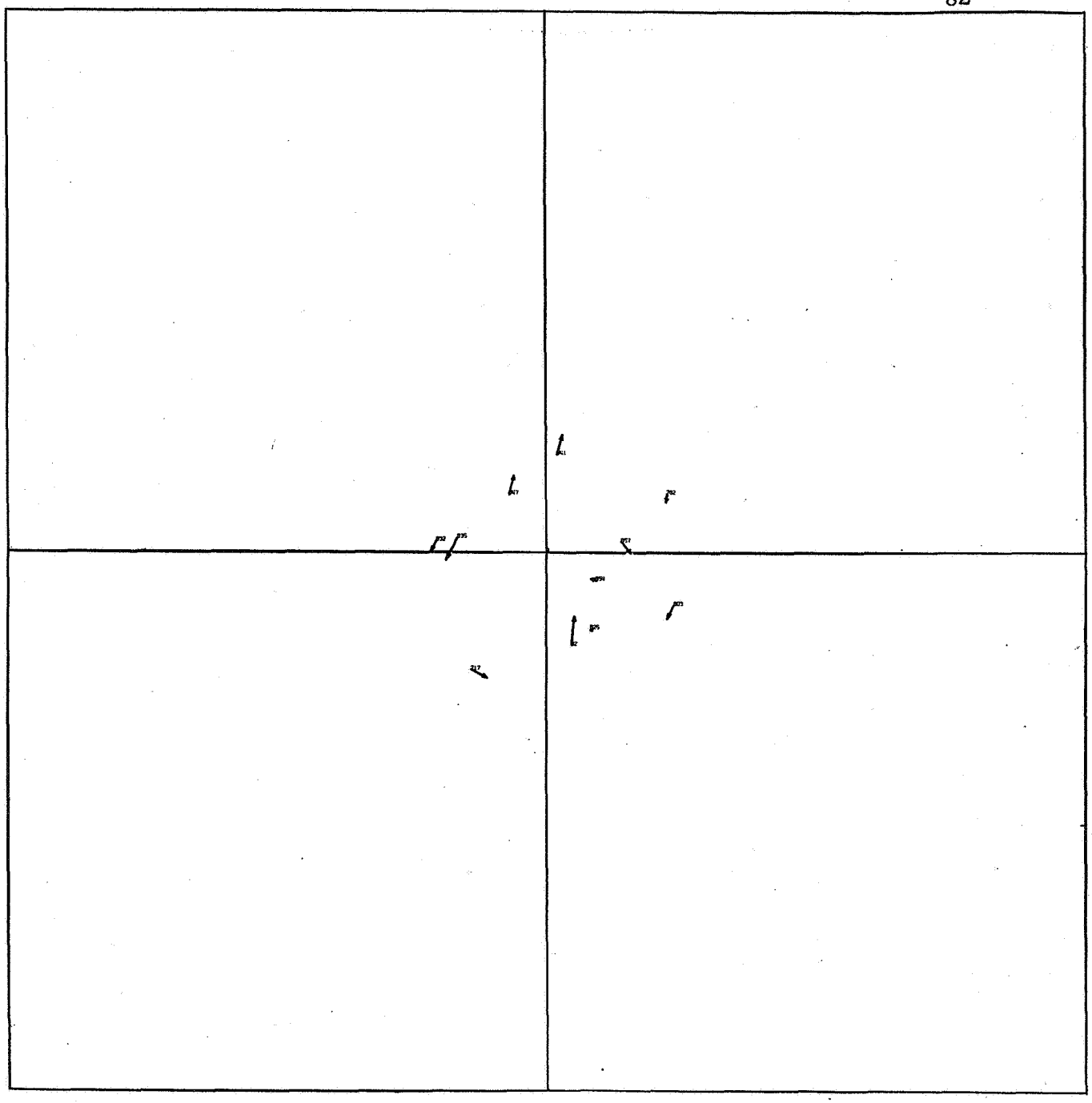

SCALE
0.1 inch = 3 microns = 2 arc seconds

CHART 30: PLATE 6132
TEST 1 RESIDUALS, SHORT TURNER'S METHOD APPLIED TO STARS
WITHIN 2.2 CENTIMETERS OF THE PLATE CENTER
Satellite 313 is origin
m_0 = 2.59 microns

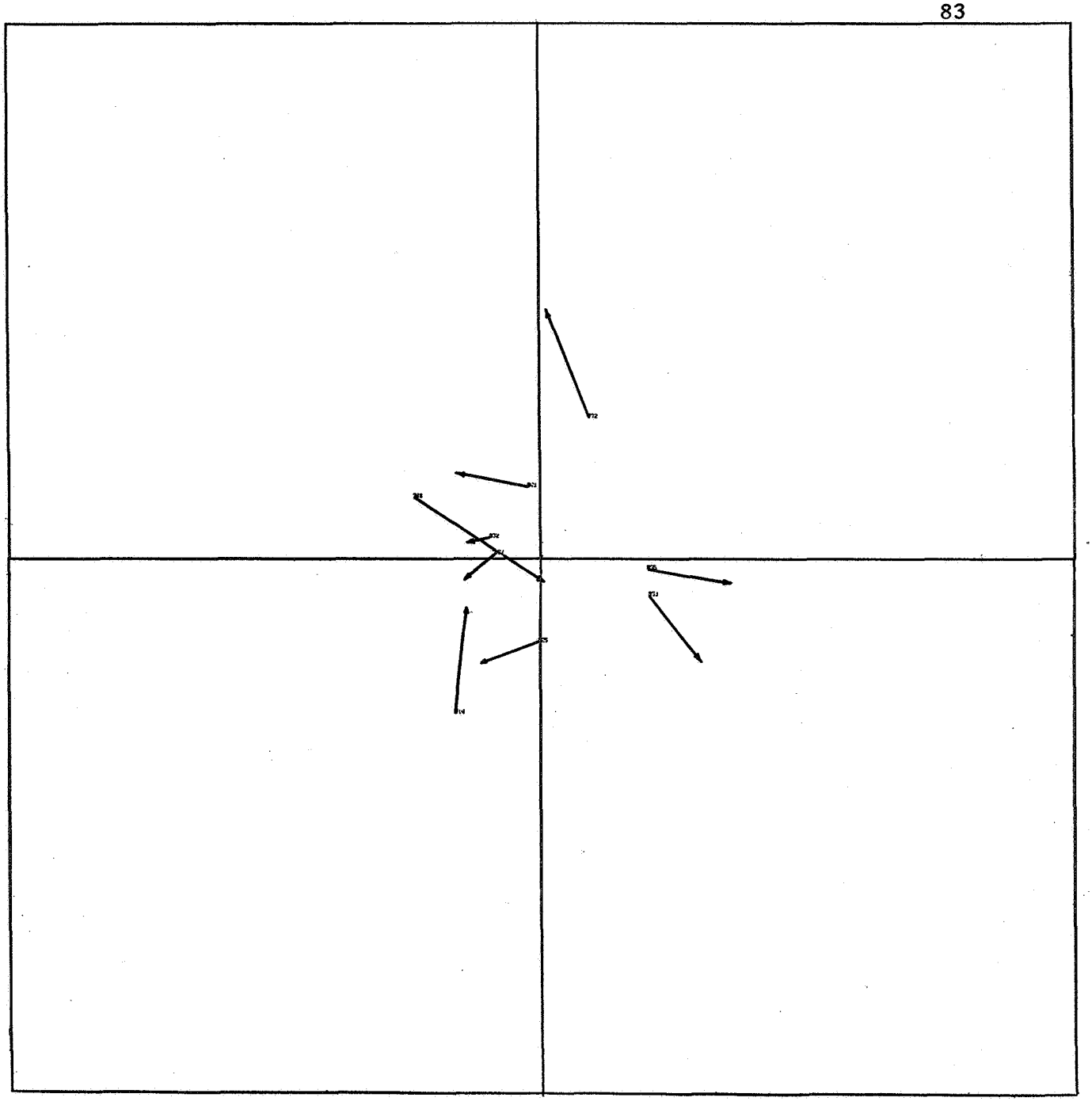

SCALE
0.1 inch = 3 microns = 2 arc seconds

CHART 31: PLATE 2559
TEST 1 RESIDUALS, SHORT TURNER'S METHOD APPLIED TO STARS
WITHIN 2.8 CENTIMETERS OF THE PLATE CENTER
Star 837 is origin
m_0 = 13.93 microns

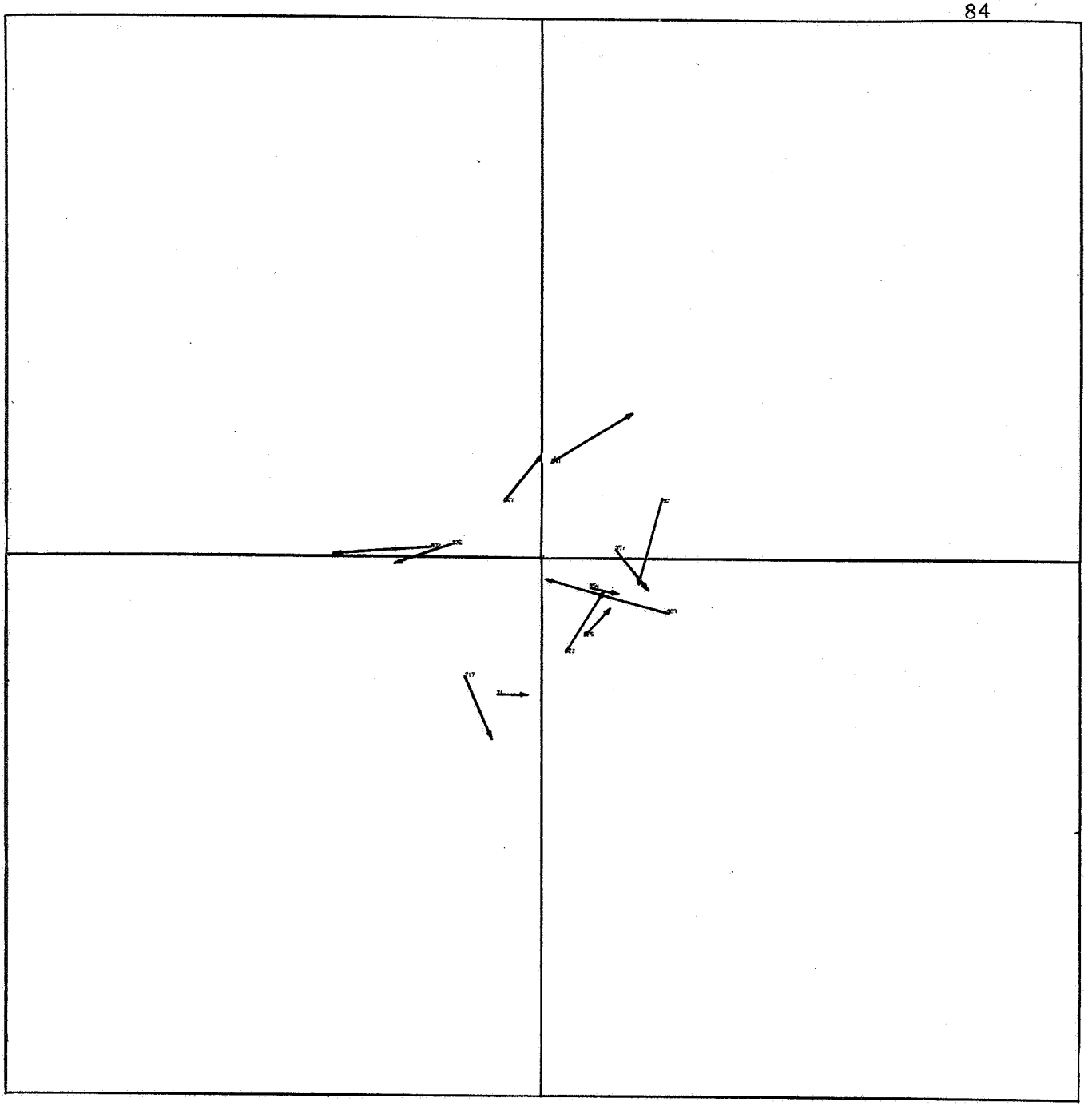

SCALE
0.1 inch = 3 microns = 2 arc seconds

CHART 32: PLATE 6132
TEST 1 RESIDUALS, SHORT TURNER'S METHOD APPLIED TO STARS
WITHIN 2.2 CENTIMETERS OF THE PLATE CENTER
Star 854 is origin
m_0 = 11.19 microns

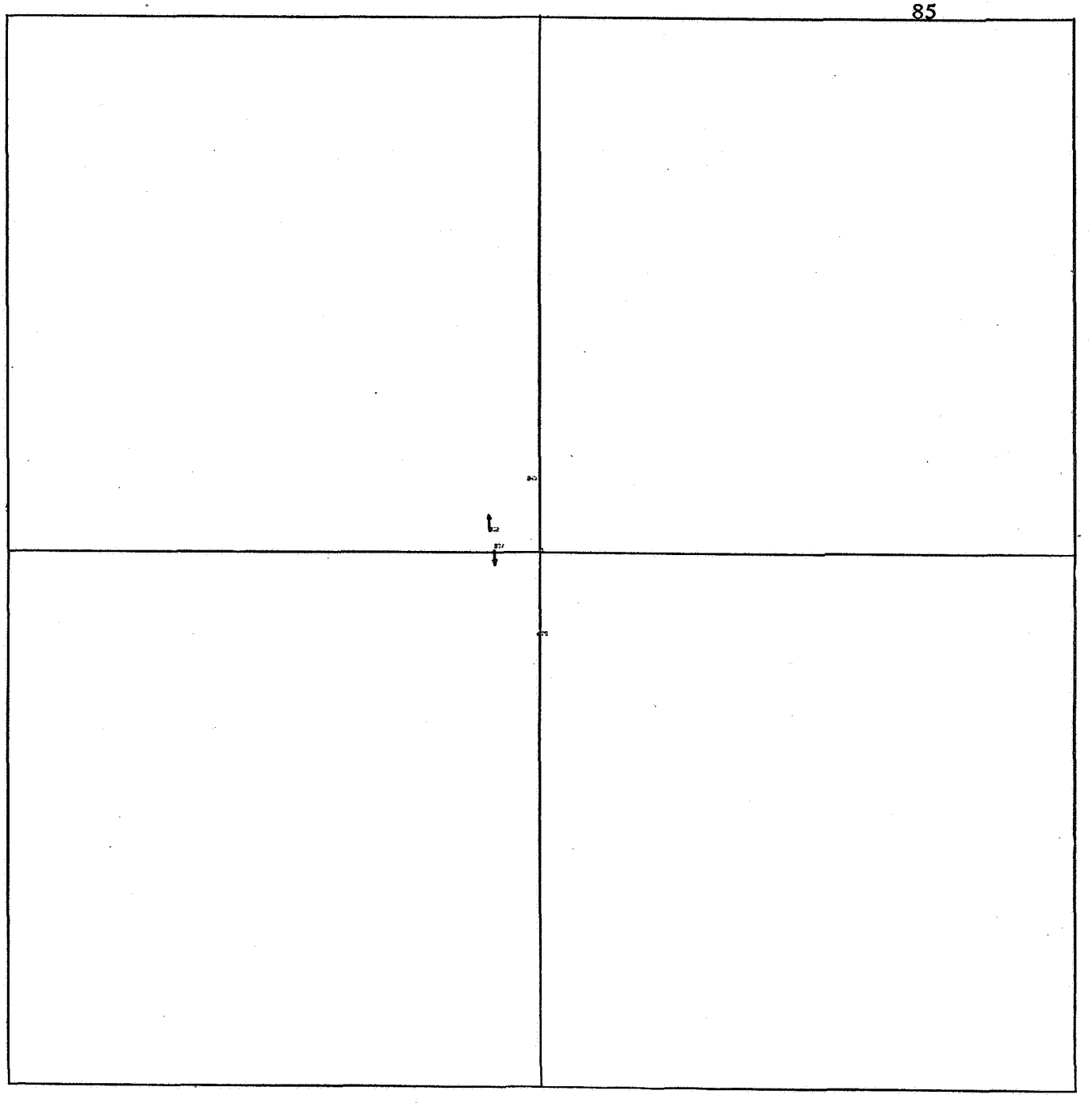

SCALE
0.1 inch = 3 microns = 2 arc seconds

CHART 33: PLATE 2559
TEST 2 RESIDUALS, SHORT TURNER'S METHOD APPLIED TO STARS
AS CLOSE TO PLATE CENTER AS POSSIBLE
Satellite 313 is origin
m_0 = 2.24 microns

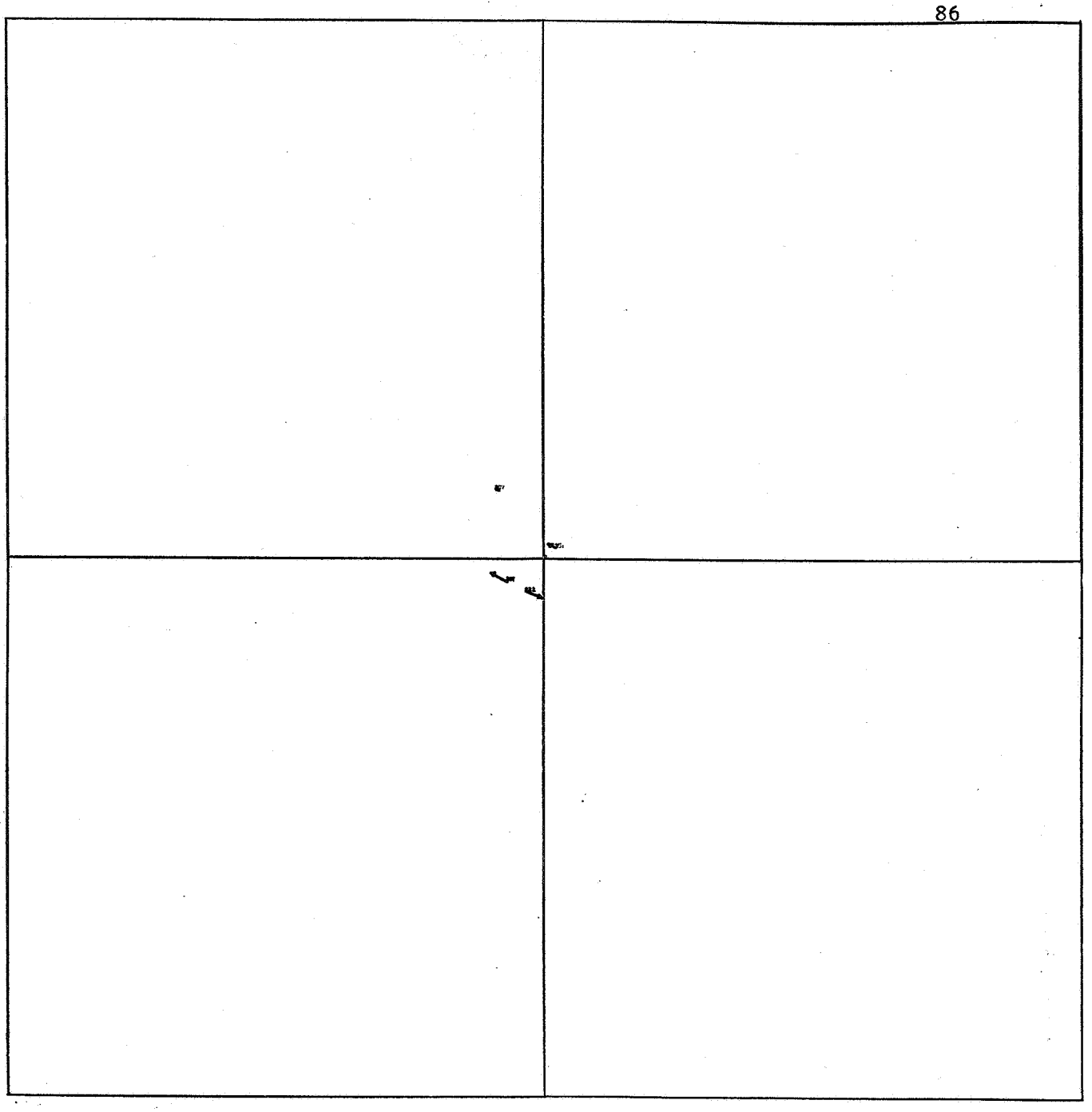

SCALE
0.1 inch = 3 microns = 2 arc seconds

CHART 34: PLATE 5205
TEST 2 RESIDUALS, SHORT TURNER'S METHOD APPLIED TO STARS
AS CLOSE TO PLATE CENTER AS POSSIBLE
Star 851 is origin
m_0 = 3.69 microns

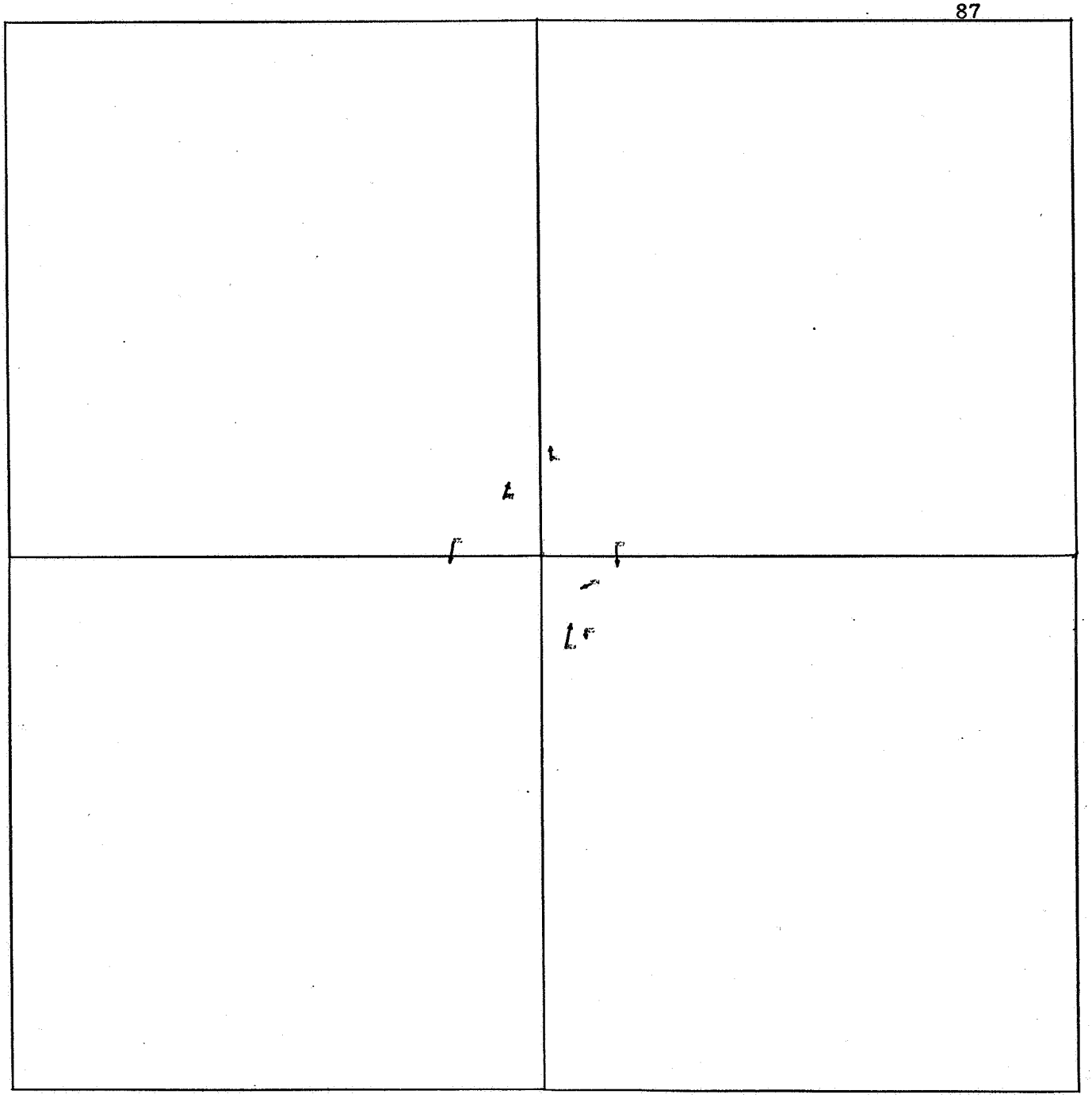

SCALE
0.1 inch = 3 microns = 2 arc seconds

CHART 35: PLATE 6132
TEST 2 RESIDUALS, SHORT TURNER'S METHOD APPLIED TO STARS
AS CLOSE TO PLATE CENTER AS POSSIBLE
Satellite 313 is origin
m_0 = 3.04 microns

Table 6

Differences of Models Interpolated Positions from ESSA Positions for 21 Satellite Images Computed in "Fictitious Observed" Equatorial System

No.	ESSA - Test 1	ESSA - Test 2	PLATE 2559	ESSA - Test 1	ESSA - Test 2
	s			"	
239	-0.149			-0.70	
258	-0.051			-1.24	
281	0.008			-1.80	
299	0.017			-2.18	
	s			"	
313	0.005	-0.119		-2.46	-5.27
330	-0.031	-0.112		-2.80	-5.98
350	-0.093	-0.139		-3.19	-0.67
368	-0.163	-0.193		-3.56	1.60
387	-0.242			-3.95	
403	-0.306			-4.31	
	s	s		"	"
	0.106	0.141		2.62	3.38*
	-0.100	-0.141		-2.62	-2.58**
			PLATE 5205		
258	0.108			-2.08	
281	0.207			0.39	
299	0.224	-0.082		1.27	1.36
313	0.211	-0.108		1.40	0.78
330	0.167	-0.164		0.96	-0.53
350	0.090			-0.28	
368	0.001			-1.95	
	0.144	0.118		1.19	0.89*
	0.144	-0.118		-0.04	0.54**
			PLATE 6132		
239	0.011			-0.30	
258	-0.097			-0.55	
281	-0.162	-0.198		-0.77	-1.15
299	-0.166	-0.217		-0.91	-1.12
313	-0.145	-0.208		-1.01	-1.07
330	-0.094	-0.168		-1.14	-1.02
350	-0.005	-0.097		-1.33	-0.99
368	0.096	-0.008		-1.53	-0.98
387	0.217			-1.81	
	0.110	0.149		1.04	1.06*
	-0.038	-0.149		-1.04	-1.06**

*Mean Absolute difference
**Mean difference

5. CONCLUSIONS

The projective equations cannot be used to reduce the entire area of a BC-4 stellar plate. Unmodeled distortion effects are too great toward the outer edges of the plate. However, if the zenith distance is such that a refraction model can be considered constant, and if lens distortion parameters are known and fairly constant for a given camera, then the projective equations could be used for an entire plate reduction after the measured coordinates are corrected for lens distortion effects and the stellar coordinates corrected to contain the effects of atmospheric refraction. In fact, certain agencies do not calibrate the camera for each exposure. Parameters from a previous adjustment are used and considered constant for a period of time. The behavior of the distortion characteristics of an Astrotar lens over a period of time is not known to this author. However, if it is not necessary to recalibrate the BC-4 camera after each exposure, it appears that the projective equations could be applied using the procedure just described to obtain results equal to those a complete photogrammetric reduction would provide. If no precorrections are made for lens distortions but the stellar coordinates have refraction effects added, then the experimentation shows, at least for three BC-4 cameras, that a confined area no greater than 3 centimeters (6 degrees) in radius from the plate center can be reduced with good results. This area, labelled Model 1, is indicated in Charts 36, 37, and

38. An image as close as possible to the geometrical plate center should be used as the optical center, but no iteration techniques need be applied to obtain the optical center if the projective equations are used.

It is obvious from the results of the experimentation with Model 2, that if enough higher order terms are included in the transformation equations, the reduction results can be made comparable to those obtained photogrammetrically. However, 20 unknowns are already enough to warrant using a complete photogrammetric reduction. Model 2 has possibilities if a reduced plate area is to be used so that several higher order terms can be dropped yet no pre-corrections be made for lens distortions.

Model 3 should be applied with caution under the following conditions.

A. The satellite image(s) for which directions are desired should be located close to the geometrical plate center and completely contained in the field of reference stars used in the reduction.

B. Sufficient star images should be available and equally distributed in all directions around the satellite images. Plate 6132 gives a good example of this. Violation of this shows up in the satellite directions computed for Plates 2559 and 5205.

C. The area of reduction should be no greater than 2 centimeters (4 degrees) in radius if the BC-4 lens distortion characteristics are comparable to those of the camera that exposed Plate 6132 and conditions A and B exist. Generally, if conditions A and B exist within a field 1.5 centimeters (3 degrees) in radius, the reduction should be done in this area.

D. The choice of the point of tangency of the tangent plate should be made with extreme care. Therefore, the geometrical center must be approximated as closely as possible in right ascension and declination. If possible, an iteration technique should be used to obtain the best point of tangency to use as an origin for both the plate and standard coordinate systems.

Charts 36, 37, and 38 also show the area where success should be achieved using Model 3 if the conditions mentioned above exist as for Plate 6132. The field shown is 3 degrees in radius although this could probably be expanded if a good distribution of stars existed. The Model 3 reduction was not ideally applied for Plates 2559 and 5205 because of a lack of condition A and B. Therefore, in confining the reduction to the recommended area given one must still allow for the other conditions to be met.

We must conclude, therefore, that general astrometric techniques are not adequate when used alone to reduce entire plate areas for short focal length ballistic cameras. Distortions involved require specific modeling, such as the photogrammetric method provides, for the reduction to obtain accuracies that present day equipment will provide. However, astrometric techniques can be applied to advantage if done in one of the ways described above depending on the nature of the taking camera and the location of the satellite images with respect to the optical axis.

Figures 1 through 6 show the values given in Tables 2 to 6 plotted for each of the 21 satellite images. The results presented here are as expected. The reductions with higher standard errors of unit weight

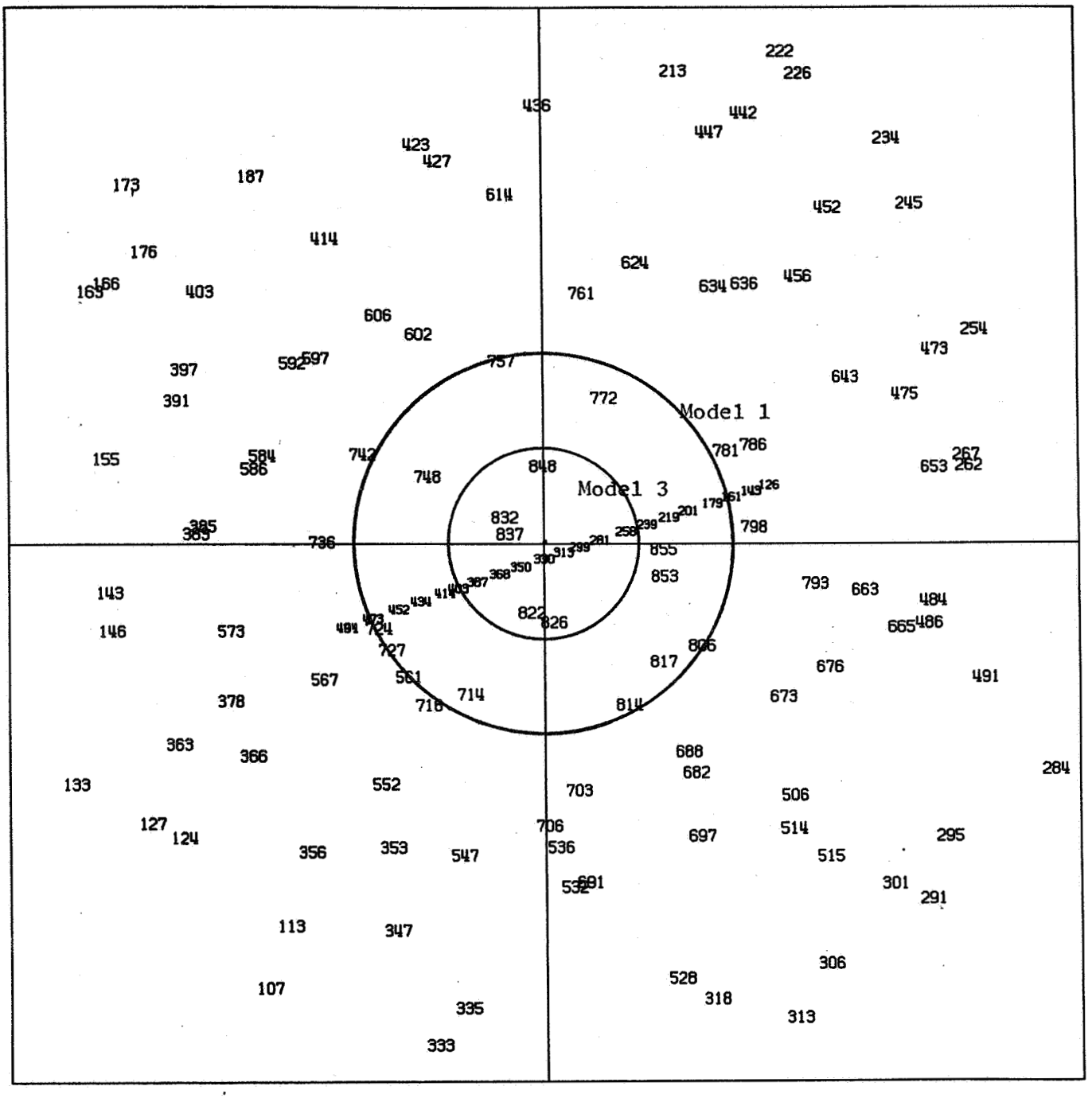

CHART 36: PLATE 2559
REDUCED AREAS TO USE FOR MODELS 1 AND 3 WITHOUT PRE-CORRECTING MEASURED COORDINATES

Model 1: Projective Equations
Model 3: "Short" Turner's Method

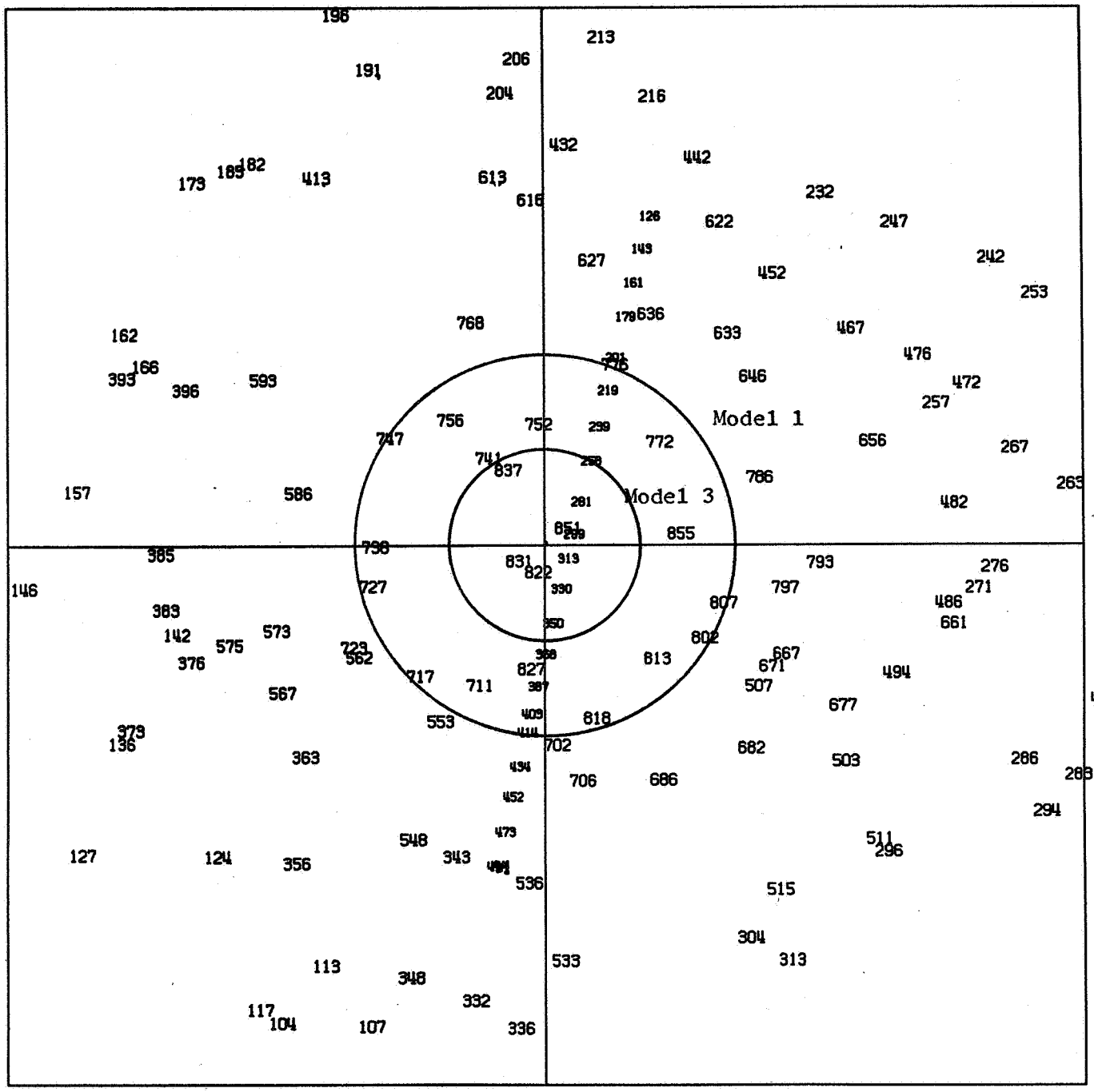

CHART 37: PLATE 5205
REDUCED AREAS TO USE FOR MODELS 1 AND 3 WITHOUT PRE-CORRECTING MEASURED COORDINATES

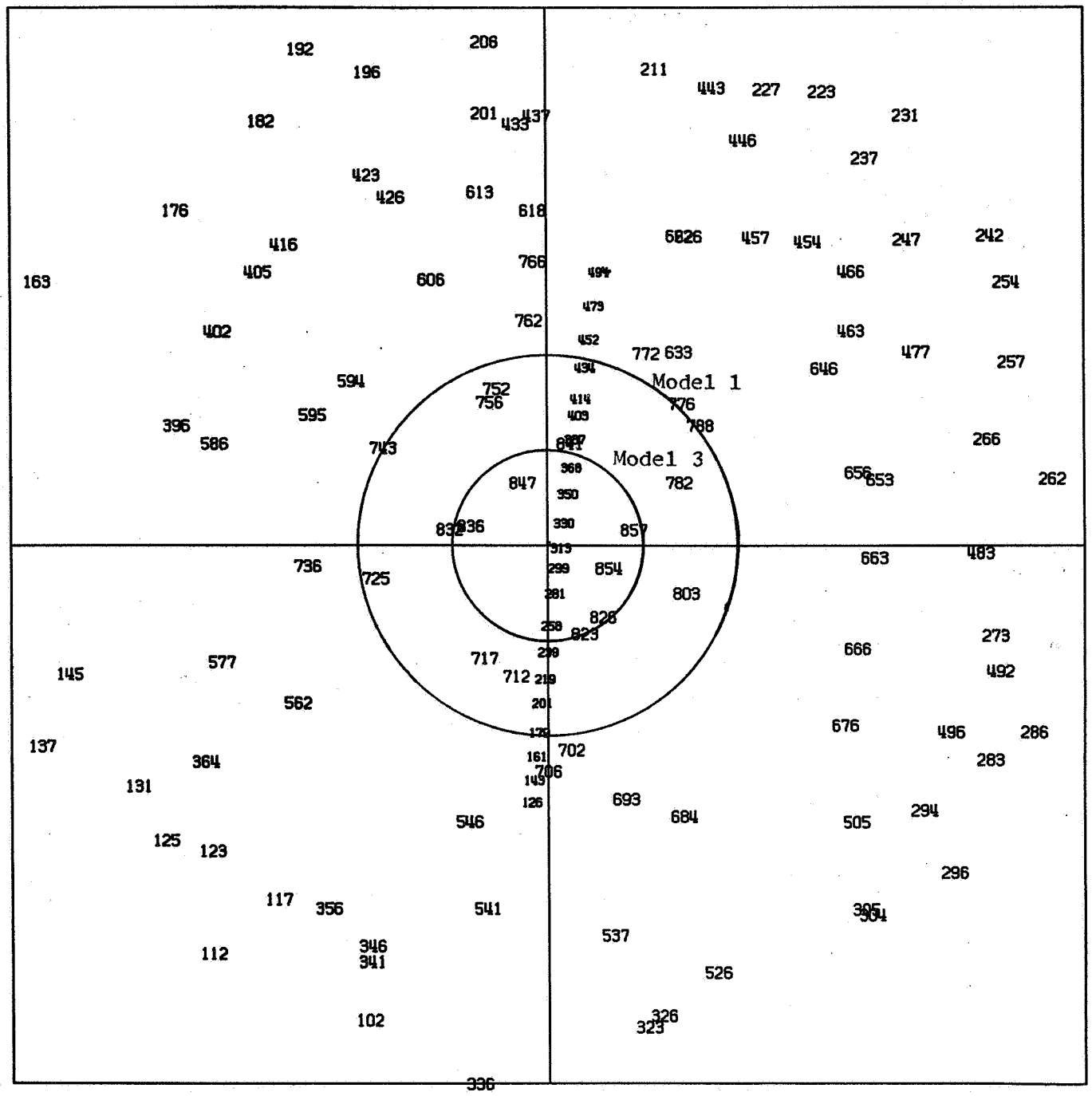

CHART 38: PLATE 6132
REDUCED AREAS TO USE FOR MODELS 1 AND 3 WITHOUT PRE-CORRECTING MEASURED COORDINATES

Table 7

Summary of Standard Errors of Unit Weight for the Astrometric Reductions and the ESSA Photogrammetric Reduction
Numbers given are in microns.

Model No.	Test No.	Description	Plate 2559	Plate 5205	Plate 6132
		ESSA Photogrammetric	2.96	3.17	2.80
1	1	Projective equations applied to entire plate area	10.04	10.03	7.81
1	2	Same as Test 1 but with measured coordinates corrected for decentering distortion	10.05	10.35	7.77
1	3	Same as Test 1 but with measured coordinates corrected for all lens distortions	3.06	3.34	2.62
1	4	Projective equations applied to stars within 3.4 cm. of plate center	2.82	2.96	2.37
1	5	Projective equations applied to stars within 4 cm. of plate center	3.96	3.08	3.24
2		"Long" Turner's for entire plate area	3.80	4.19	3.39
3	1	"Short" Turner's for stars within 2.8 cm. of plate center (2.2 cm. for 6132)	5.80	5.56	2.59
3	2	"Short" Turner's for stars in immediate vicinity of plate center	2.24	3.69	3.04

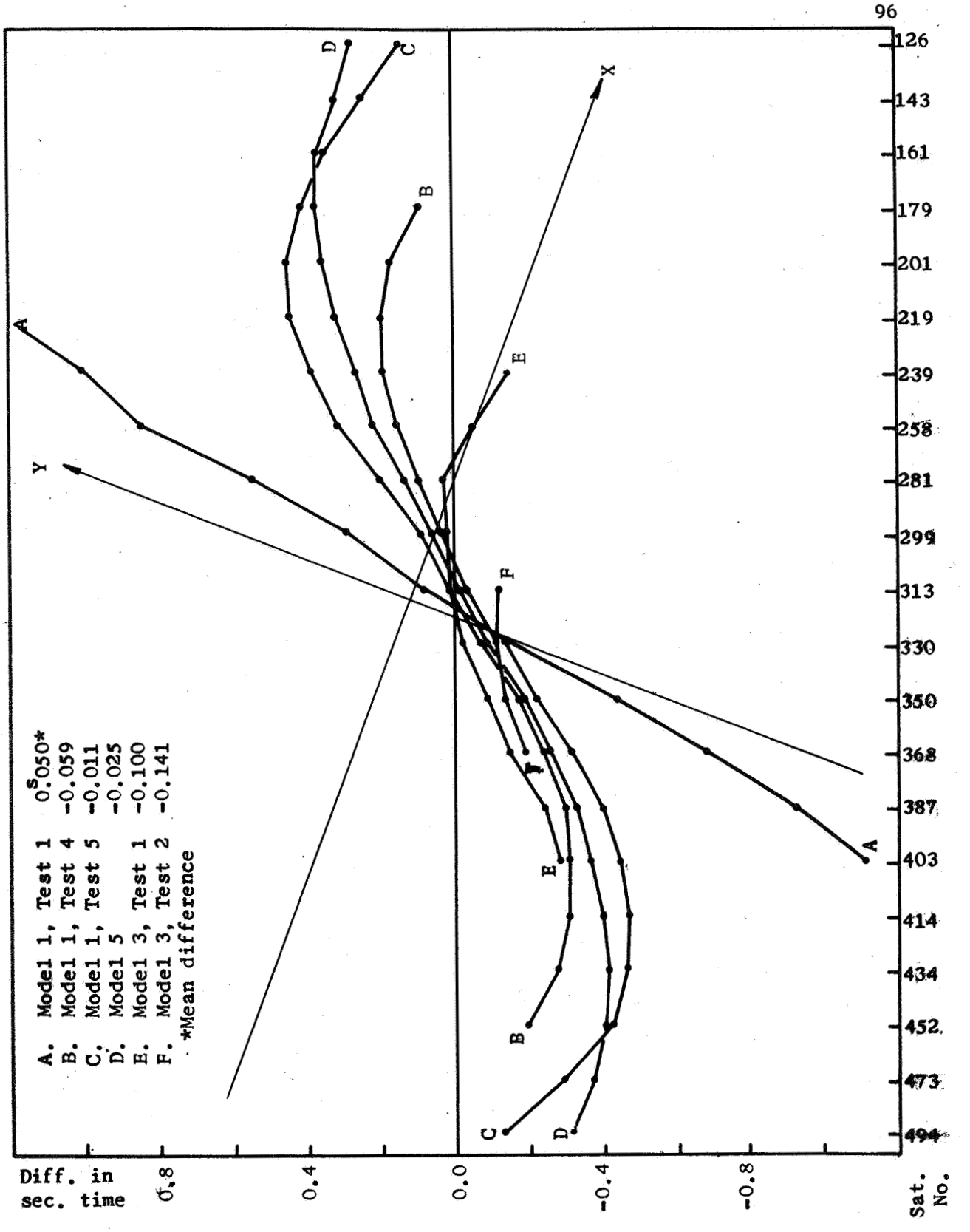

FIGURE 1. PLATE 2559: ESSA RA - ASTRO. RA

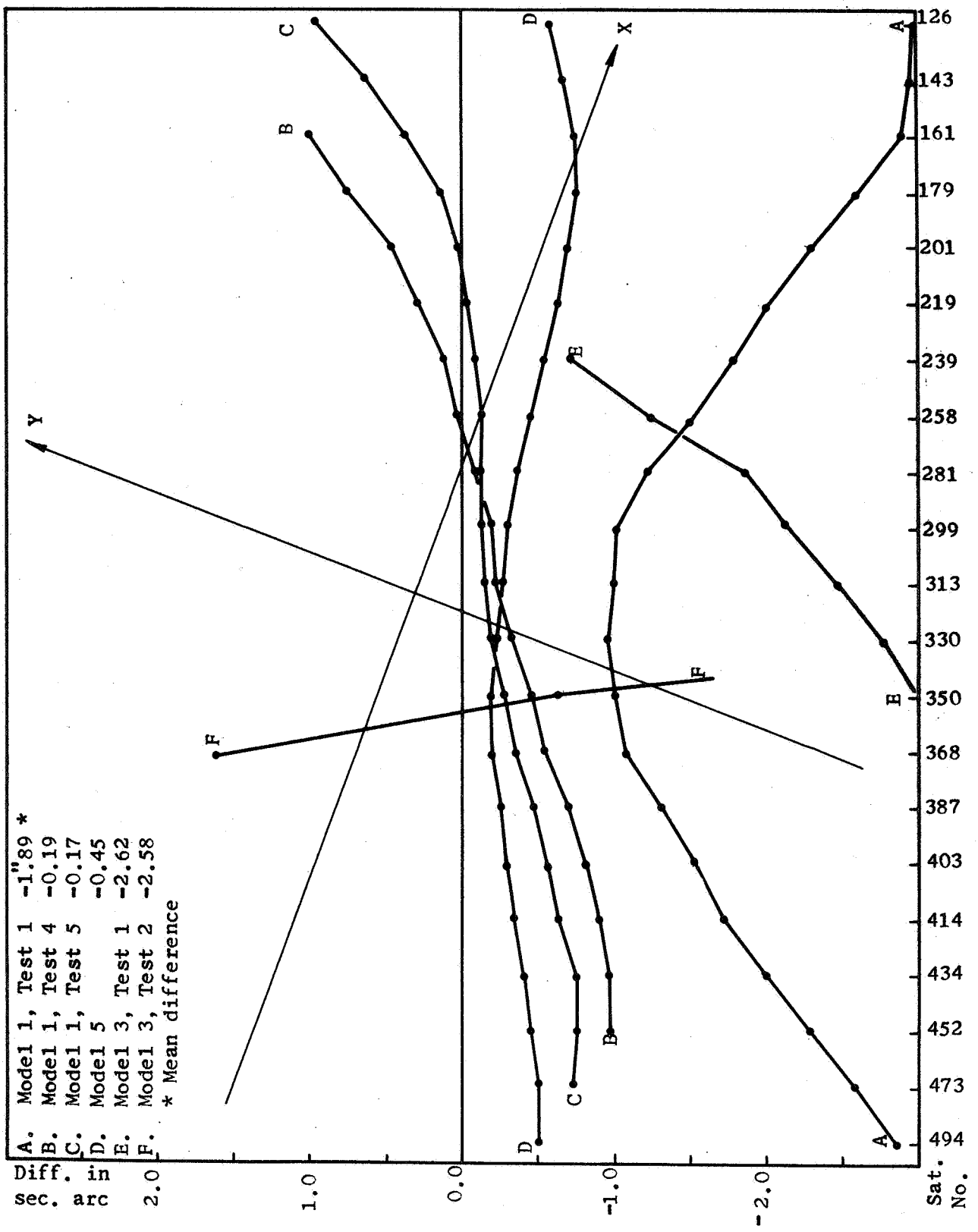

FIGURE 2. PLATE 2559: ESSA DEC - ASTRO DEC

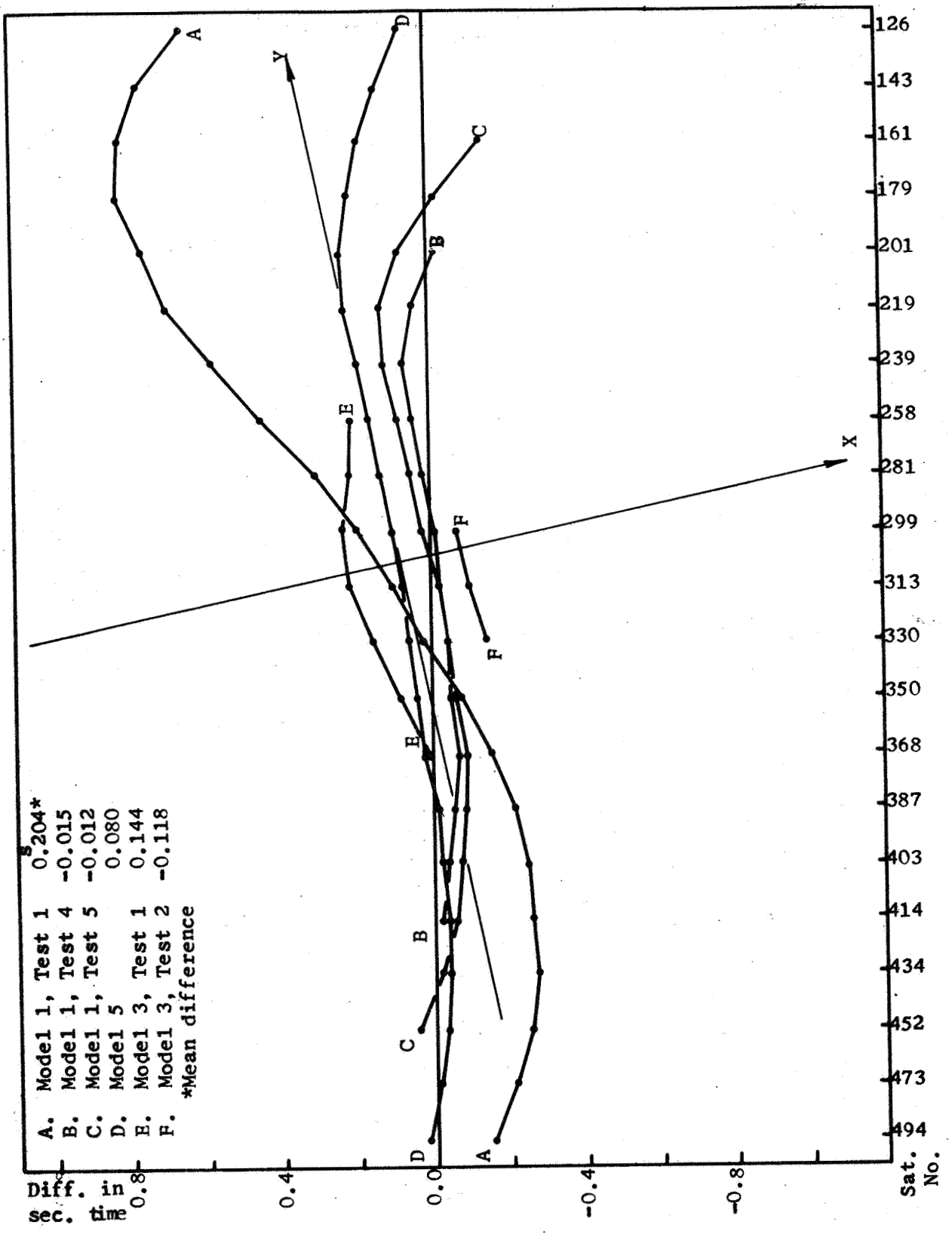

FIGURE 3. PLATE 5205: ESSA RA - ASTRO RA

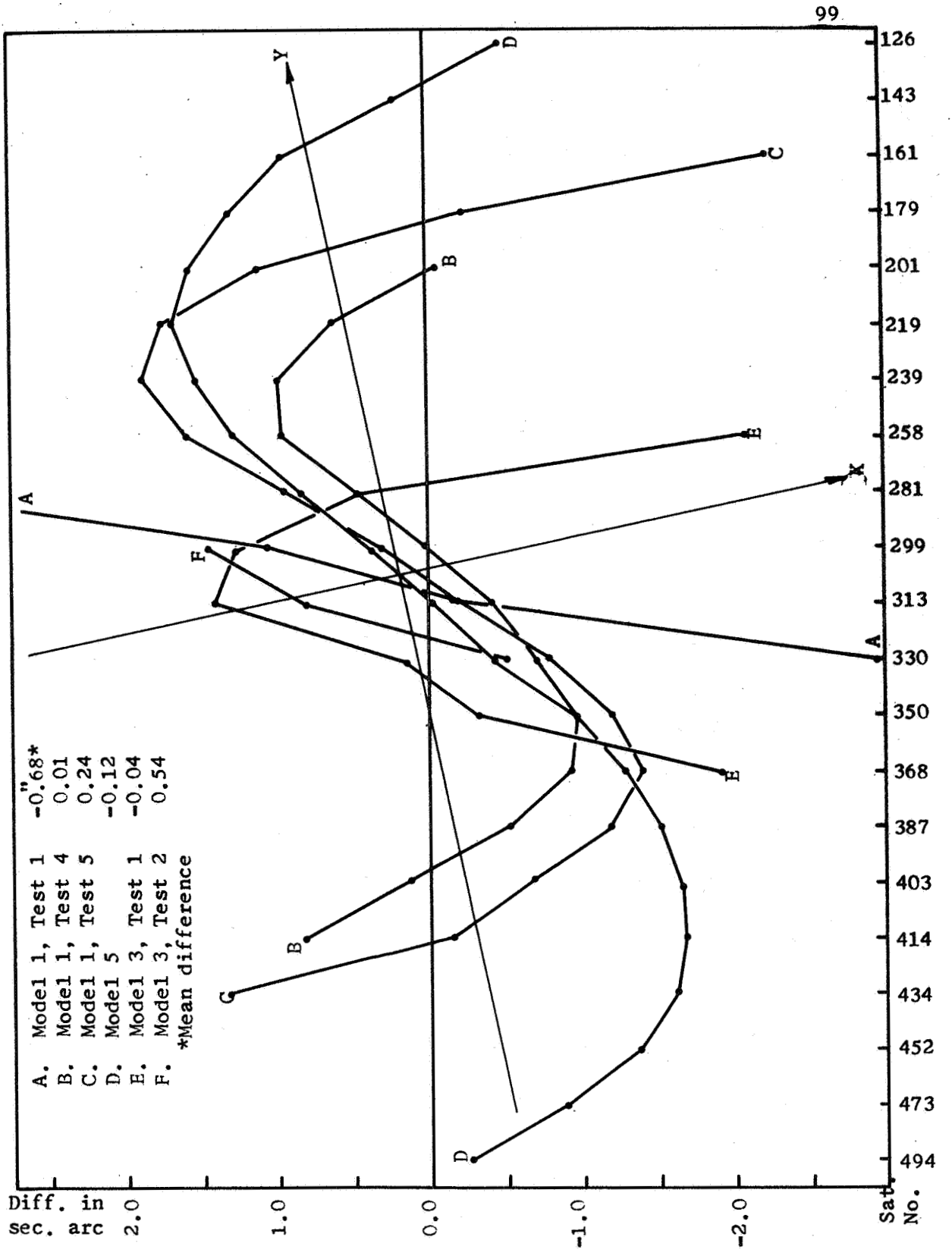

FIGURE 4. PLATE 5205: ESSA DEC - ASTRO. DEC

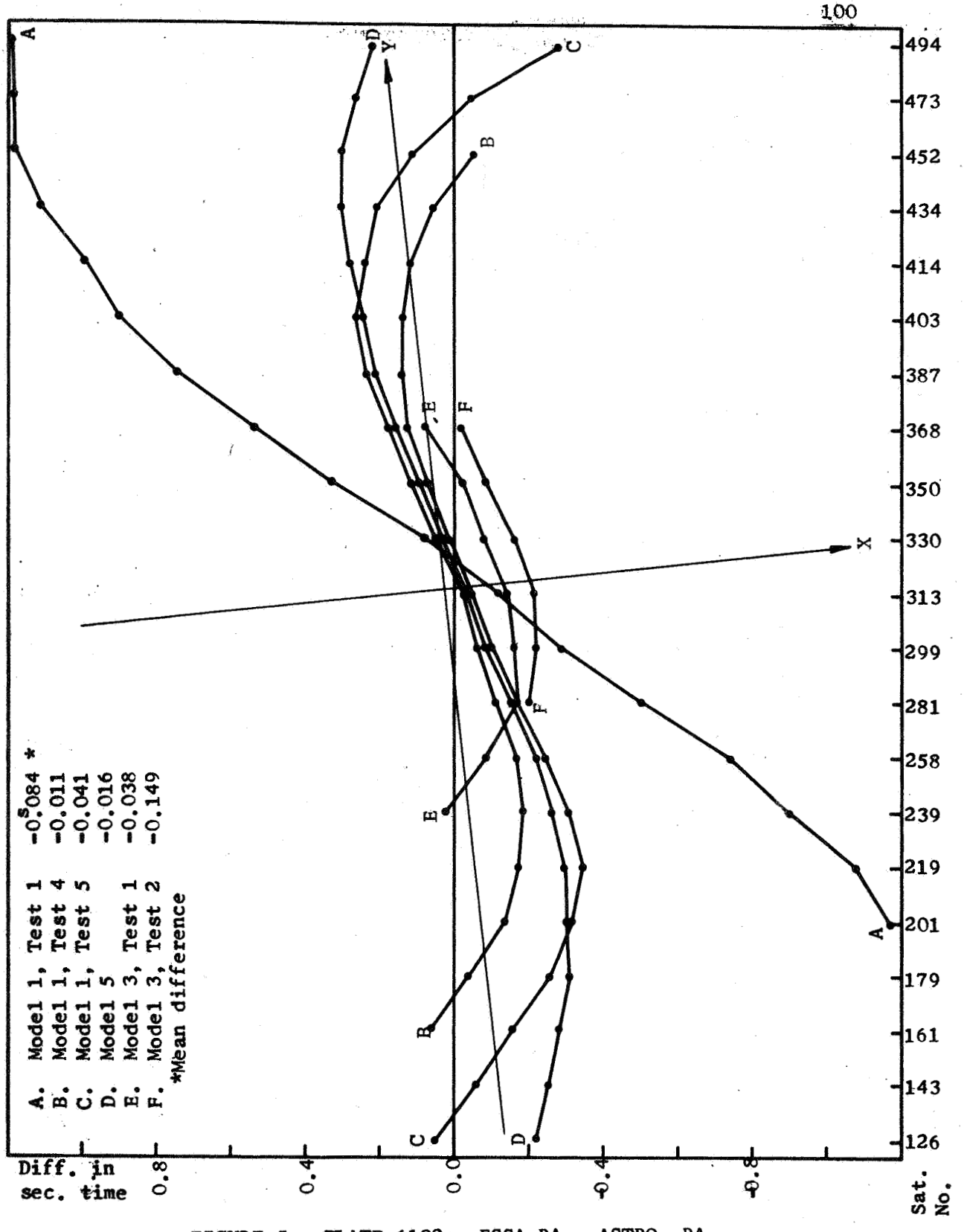

FIGURE 5. PLATE 6132: ESSA RA - ASTRO. RA

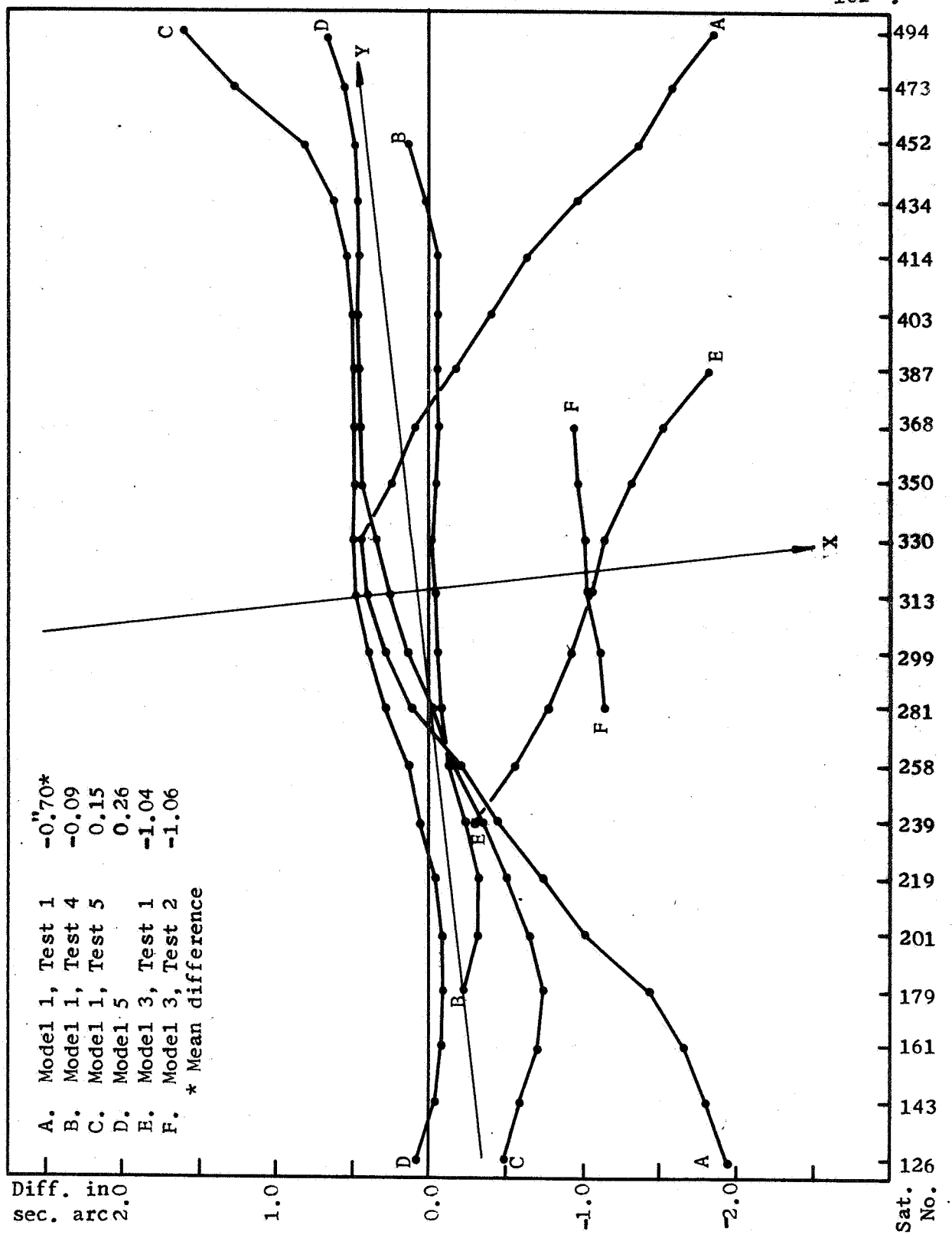

FIGURE 6. PLATE 6132: ESSA DEC - ASTRO. DEC

show larger deviations in computed satellite positions from the ESSA positions. Test 1 for Model 1 is a good example of this. Generally, plots are roughly symmetric about the plate center, illustrating the effect of the particular mathematical structure at a given distance from the plate center.

Table 13 summarizes the standard errors of unit weight for the astrometric reductions.

BIBLIOGRAPHY

Aeronautical Chart and Information Center (1968). Submitted Material for the Reduction of ESSA Measurements for Event 1536, St. Louis, Missouri.

Allen, Robert Shaw (1966). "A Computer Program for Use in Computing a First Order Latitude by the Horrebow-Talcott Method," Master of Science Thesis, The Ohio State University.

American Ephemeris and Nautical Almanac (A.E.N.A.) for the Year 196X, Issued by the Nautical Almanac Office, United States Naval Observatory.

American Society of Photogrammetry (1966). Manual of Photogrammetry, Third Edition, Vol. I, Vol. II, American Society of Photogrammetry, Falls Church, Virginia.

Berbert, J. H., Good, W. E., and Oosterhaut, J. D. (1962). "Reduction of the Minitrack Astrographic Plates," Photographic Science and Engineering, Nov.-Dec.

Brown Associates, Inc. (1966). "Geodetic Data Analysis for Geos A, An Experimental Design," Prepared for National Aeronautics and Space Administration, Goddard Space Flight Center, Greenbelt, Maryland, Contract NAS 4-9860.

Brown, Duane C. (1957). "A Treatment of Analytical Photogrammetry with Emphasis on Ballistic Camera Applications," RCA Data Reduction Technical Report, No. 39, Air Force Missile Test Center, Air Research and Development Command, Patrick AFB, Florida.

Brown, Duane C. (1963). "Notes on the Reduction of Stellar Plates for Determination of Directions of Flashing Light Beacons," The Use of Artificial Satellites in Geodesy (Veis, G. editor) Interscience Publishers, New York, pp. 163-186.

Brown, Duane C. (1964). "An Advanced Reduction and Calibration for Photogrammetric Cameras," Prepared for Air Force Cambridge Research Laboratories, Office of Aerospace Research, United States Air Force, Bedford, Massachusetts, January.

Computer Center of The Ohio State University. SCATRAN Reference Manual and "General Plot Package," Columbus, Ohio, 1965.

Conference on the Construction and Use of Star Catalogues (1966), held held at the University of Maryland, 3-5 October 1966. Reprinted from the Astronomical Journal, Vol. 72, No. 5, pp. 551-630, June, 1967.

Conrady, A. (1919). "Decentered Lens Systems," Monthly Notices of Royal Astronomical Society, Vol. 79, pp. 384-390.

Eichhorn, Heinrich (1962). "Astrometric Investigation of a Baker-Nunn Camera," Van Vleck Observatory, Middletown, Conn., Report on Air Force Contract 19(604)-7330.

Eichhorn, Heinrich (1963). "The Relationship Between Standard Coordinates of Stars and the Measured Coordinates of their Images," Applied Optics, January.

Eichhorn, Heinrich (1963). "Investigations on Photographic Astrometric Technique," Van Vleck Observatory, Middletown, Connecticut, Report on Air Force Contract 19(604)-7330.

Eichhorn, Heinrich and Williams, Carol A. (1963). "On the Systematic Accuracy of Photographic Astrometric Data," Astronomical Journal, Vol. 68, No. 4, pp. 221-231.

Environmental Science Services Administration (1967). Satellite Triangulation Data for Event 1536, 30 November 1965, Rockville, Maryland.

Explanatory Supplement to the Astronomical Ephemeris and the American Ephemeris and Nautical Almanac (1961). Prepared jointly by the Nautical Almanac Offices of the United Kingdom and the United States of America, Her Majesty's Stationery Office, London.

Fallon, Frederick W. (1966). "Star Catalogue Requirements for Sattelite Geodesy," Conference on the Construction and Use of Star Catalogues, pp. 611-616.

Fallon, Frederick W. (1967). "A General Solution to the Optical Satellite Geodesy Problem," Paper presented to the 1967 Convention of the American Society of Photogrammetry and the American Congress on Surveying and Mapping, St. Louis, Missouri, 2-5 October.

Haligowski, Barbara A. and Lukac, Carl F. (1966). "Reduction of Star Coordinates in Photographic Astrometry," Conference on the Construction and Use of Star Catalogues, pp. 617-619.

Hallert, Bertil (1960). Photogrammetry, Basic Principles and General Survey, McGraw-Hill Book Company, Inc., New York.

Haramundanis, K. (1966). "Experience of the SAO in the Construction and Use of Star Catalogues, " Conference on the Construction and Use of Star Catalogues, pp. 588-596.

Hotter, Frank D. (1967). "Preprocessing Optical Satellite Observations," Reports of the Department of Geodetic Science, No. 82, Prepared for National Aeronautics and Space Administration, Washington, D.C., The Ohio State University Research Foundation, April.

Jefferys, W. H. (1963). "On Computational Technique for Photographic Astrometry with Overlapping Plates," Astronomical Journal, Vol. 68, No. 2.

Mueller, Ivan I. (1964). Introduction to Satellite Geodesy, Frederick Ungar Publishing Co., New York.

Mueller, Ivan I. (In Press). Spherical and Practical Astronomy Applied to Geodesy, Ungar Publishing Co., New York.

Mueller, Ivan I., Hotter, F. D., Krakiwsky, E. J., and Pope, A.J. (1967) "Global Satellite Triangulation and Trilateration." Paper presented at XIVth General Assembly of the International Union of Geodesy and Geophysics, Lucerne, Switzerland, September 25 - October 7, 1967, by the Department of Geodetic Science, The Ohio State University.

Murton, William N. II. (1967). General 7094 Plot Caller, Computer Center of The Ohio State University, Columbus, Ohio.

National Aeronautics and Space Administration (1968). Submitted Material for the Reduction of ESSA Measurements for Event 1536, Cambridge, Massachusetts.

Podobed, V. V. (1965). Fundamental Astrometry, English edition edited by Vyssotsky, A. N. University of Chicago Press, Chicago.

Schmid, H. H. (1959). "A General Analytical Solution to the Problem of Photogrammetry," Ballistic Research Laboratory Report, 1065.

Slama, Chester (1967). Private Communication to Dr. Ivan I. Mueller of the Department of Geodetic Science, The Ohio State University.

Smart, W. M. (1962). Text-Book on Spherical Astronomy, Fifth Edition, Cambridge University Press.

Smithsonian Astrophysical Observatory (1968). Submitted Material for the Reduction of ESSA Measurements for Event 1536, Cambridge, Massachusetts.

Stark, Marshall M. (1967). "Refraction and the Determination of Second Order Astronomic Atitudes," Master of Science Thesis, The Ohio State University.

Taylor, Eugene A. (1963). "Optical Tracking System for Space Geodesy." The Use of Artificial Satellites in Geodesy (Veis, G. editor) Interscience Publishers, New York, pp. 187-192.

Turner, H. H. (1893). "Preliminary Notes on the Reduction of Photographic Plates," Monthly Notices of the Royal Astronomical Society, Vol. 54, pp. 11-22.

Uotila, Urho A. (1967). Introduction to Adjustment Computations with Matrices, Department of Geodetic Science, The Ohio State University.

Van de Kamp, Peter (1967). Principles of Astrometry, W. H. Freeman and Co., San Francisco and London.

Veach, James. (1967). Modification of Allen, 1966 for SAO Catalogue Input. Department of Geodetic Science, The Ohio State University, Columbus, Ohio.

Veis, George, editor (1963). The Use of Artificial Satellites for Geodesy, Proceedings of the First International Symposium on the Use of Artificial Satellites for Geodesy, Interscience Publishers, New York.